



# VCU

Virginia Commonwealth University  
VCU Scholars Compass

---

Theses and Dissertations

Graduate School

---

2018

## Metabotropic Glutamate Receptor 2 Activation: Computational Predictions and Experimental Validation

Amr Ellaithy

Follow this and additional works at: <https://scholarscompass.vcu.edu/etd>



Part of the [Molecular and Cellular Neuroscience Commons](#), [Neurosciences Commons](#), and the [Pharmacology Commons](#)

© The Author

---

Downloaded from

<https://scholarscompass.vcu.edu/etd/5319>

This Dissertation is brought to you for free and open access by the Graduate School at VCU Scholars Compass. It has been accepted for inclusion in Theses and Dissertations by an authorized administrator of VCU Scholars Compass. For more information, please contact [libcompass@vcu.edu](mailto:libcompass@vcu.edu).

# **Metabotropic Glutamate Receptor 2 Activation: Computational Predictions and Experimental Validation**

A dissertation submitted in partial fulfillment of the requirements for the degree of  
Doctor of Philosophy at Virginia Commonwealth University  
by

Amr Ellaithy

MB BCh, Bachelor of Medicine, Bachelor of Surgery, Mansoura University, 2013

Director: Diomedes E. Logothetis, Ph.D.  
Professor, Northeastern University

Virginia Commonwealth University  
Richmond, Virginia  
April, 2018

## Acknowledgments

I would like to thank my advisor, Dr. Diomedes E. Logothetis, whose passion is inspiring and whose trust helped me keep going even at times when I doubted myself. I would also like to thank the members of my committee and the neuroscience program director, Dr. John Bigbee, for their time and help throughout my PhD training. A special thanks to Dr. Gonzalez-Maeso and Dr. Selley for their pharmacological expertise and invaluable input to my dissertation research, and to Dr. Louis De Felice, who although no longer with us, continues to inspire by his dedication to the students he served over the course of his career.

This work would not have been possible without the assistance of many past and present members of the Logothetis Lab, but especially: Dr. Jason Younkin for teaching me electrophysiology and for the wonderful times we spent outside the lab, Dr. Yu Xu for providing me with exciting computational models to test, Dr. Takeharu Kwano for his admirable patience and the tremendous amount of time he spent helping with molecular biology, Heikki Vaananen for the breadth of knowledge and exceptional troubleshooting skills, Guoqing Xiang and Junghoon Ha for the long nights we spent together doing experiments and venting about life as graduate students, and Meghan Masotti for trying to help me finish up my experiments in the last few months before my defense.

A great thank you to my friends; Magdy, Tareq, Mario, Jen, Ahmed, Basim, and Ahmed who have been pillars of support whom I am lucky to have in my life.

Last, but most important of all, I would like to thank my parents, Manal Saad and Abdallah Ellaithy, my sister, and my brother for their unconditional love and unwavering support. I dedicate my graduate work to you.

# Table of Contents

|  |             |
|--|-------------|
| <b>Acknowledgments</b> .....   | <b>ii</b>   |
| <b>List of Figures</b> .....   | <b>v</b>    |
| <b>List of Tables</b> .....  | <b>viii</b> |
| <b>List Of Abbreviations</b> .....   | <b>ix</b>   |
| <b>Abstract</b> .....  | <b>xii</b>  |
| <b>Chapter 1 INTRODUCTION</b> .....  | <b>1</b>    |
| <b>1.1 GPCR to G-protein Signaling</b> .....   | <b>1</b>    |
| <b>1.2 GPCR Activation</b> .....   | <b>4</b>    |
| 1.2.1 GPCR Activation Models.....  | 4           |
| 1.2.2 Targetable Sites on GPCRs .....  | 5           |
| <b>1.3 Structural Basis of GPCR–G protein interactions</b> .....   | <b>7</b>    |
| 1.3.1 Conformational Changes Involved in Receptor Activation .....   | 7           |
| 1.3.2 Allosteric coupling between agonist-binding and nucleotide-binding sites in GPCRs.....               | 9           |
| 1.3.3 Receptor-catalyzed nucleotide exchange .....   | 9           |
| 1.3.4 G protein feedback to the agonist-binding site .....   | 11          |
| <b>1.4 Metabotropic Glutamate Receptors</b> .....  | <b>13</b>   |
| 1.4.1 The Glutamatergic System .....   | 13          |
| 1.4.2 Ionotropic Glutamate Receptors.....  | 13          |
| 1.4.3 Metabotropic Glutamate Receptors .....   | 14          |
| <b>1.5. Metabotropic Glutamate Receptor 2 as a Drug Target</b> .....                                       | <b>17</b>   |
| 1.5.1 mGlu2R localization.....   | 17          |
| 1.5.2 Potential applications of mGlu2R agonists/PAMs.....  | 17          |
| <b>1.6 Hypothesis</b> .....  | <b>22</b>   |
| <b>Chapter 2 MATERIALS AND METHODS</b> .....   | <b>39</b>   |
| <b>2.1 Computational Studies</b> .....   | <b>39</b>   |
| 2.1.1 Building an mGlu2R structural model .....  | 39          |
| 2.1.2 Building mGlu2R-Gi protein complex model.....  | 39          |
| 2.1.3 Identifying allosteric modulators binding .....  | 39          |
| 2.1.4 Molecular dynamics (MD) simulations and data analysis.....   | 40          |
| <b>2.2 Molecular Biology</b> .....   | <b>40</b>   |
| <b>2.3 Drugs and Chemicals</b> .....   | <b>41</b>   |
| <b>2.4 Oocyte Preparation and Injection</b> .....  | <b>41</b>   |
| <b>2.6 Statistics</b> .....  | <b>42</b>   |
| <b>Chapter 3 MAPPING THE INTRAMOLECULAR ELECTROSTATIC INTERACTIONS INVOLVED IN mGlu2R ACTIVATION</b> ..... | <b>44</b>   |
| <b>3.1 Introduction</b> .....  | <b>44</b>   |
| <b>3.2 Results</b> .....   | <b>46</b>   |
| 3.2.1 Creating a structural model of mGlu2R.....   | 46          |

|  |            |
|--|------------|
| 3.2.2. Single mutants of the TM3-TM6 salt bridge disrupt while the double mutant rescues receptor activation.....                                      | 46         |
| 3.2.3. Single mutants of the TM6-TM7 salt bridge disrupt receptor activation but the double mutation fails to rescue receptor activation.....          | 47         |
| 3.2.4. Role of TM3-ICL3 electrostatic interactions in receptor activation .....  | 48         |
| <b>3.3. Discussion .....</b>   | <b>49</b>  |
| <b>Chapter 4 MAPPING THE INTERMOLECULAR ELECTROSTATIC INTERACTIONS BETWEEN mGlu2R AND THE G<math>\alpha</math><sub>i</sub> SUBUNIT.....</b>            | <b>63</b>  |
| <b>4.1 Introduction .....</b>  | <b>63</b>  |
| <b>4.2 Results .....</b>   | <b>64</b>  |
| 4.2.1 Structural modeling of mGlu2R with G $\alpha$ <sub>i</sub> .....   | 64         |
| 4.2.2 mGlu2R residues critical for the interaction with G $\alpha$ tend to be located in or adjacent to intracellular loops 2 and 3.....               | 64         |
| 4.2.3 G $\alpha$ residues that seem critical for the interaction with the receptor tend to be facing intracellular loops 2 and 3 of the receptor ..... | 65         |
| 4.2.4 mGlu2R third intracellular loop interaction with G $\alpha$ protein .....  | 65         |
| 4.2.5 mGlu2R second intracellular loop interaction with G $\alpha$ protein.....  | 66         |
| <b>4.3 Discussion .....</b>  | <b>68</b>  |
| <b>Chapter 5 CONCLUDING REMARKS .....</b>  | <b>87</b>  |
| <b>Literature cited.....</b>   | <b>91</b>  |
| <b>Vita .....</b>  | <b>100</b> |

## List of Figures

|  |    |
|--|----|
| FIGURE 1.1. Major Classes of GPCRs with the Typical Binding Regions of Orthosteric Ligands.                  | 23 |
| Figure 1.2. G protein Activation Cycle.  | 24 |
| Figure 1.3. Pertussis Toxin-Mediated Uncoupling of Gai/o Proteins from Their Cognate GPCRs.                  | 26 |
| Figure 1.4. Conformational heterogeneity of GPCRs and associated- signaling.                                 | 27 |
| Figure 1.5. Modes of action of allosteric modulators   | 28 |
| Figure 1.6. PAMs Maintain Temporal and Spatial Patterns of Native Receptor Signaling.                        | 29 |
| Figure 1.7. Outward Rotation of TM6 in Three class A GPCRs Upon Activation.                                  | 30 |
| Figure 1.8. Disruption of the ionic lock in $\beta$ 2AR upon activation.                                     | 31 |
| Figure 1.9. Secondary and tertiary structures of G $\alpha$ .  | 32 |
| Figure 1.10. Glutamate Receptor Categories.  | 34 |
| Figure 1.11. Structural organization of mGluRs.  | 35 |
| Figure 1.12. Classification and sequence homology dendrogram of mGluRs.                                      | 36 |
| Figure 1.13. Subunit Cooperativity in mGluR Activation   | 37 |
| Figure 1.14. Chronic atypical antipsychotic therapy downregulates mGlu <sub>2</sub> R.                       | 38 |
| Figure 2.1 The Xenopus oocyte heterologous expression system.  | 43 |
| Figure 3.1. Structural model of mGlu <sub>2</sub> R TMD.   | 52 |
| Figure 3.2. Monitoring root-mean-square-deviation (RMSD) of the alpha carbons over a 450 nanoseconds MD run. | 53 |

|  |    |
|--|----|
| Figure 3.3. Comparison of the patterns of salt bridges formed between 200 and 450 nanoseconds of MD runs.  | 54 |
| Figure 3.4. Zoomed-in views of the intracellular side of the receptor models in the active and inactive states.  | 55 |
| Figure 3.5. mGlu2R functional assay in <i>Xenopus</i> oocytes.   | 56 |
| Figure 3.6. Effect of charge reversal mutations in the K653-E758 ionic lock between TM3 and TM6.   | 57 |
| Figure 3.7. Effect of charge reversal mutations in the E758-K813 salt bridge between TM6 and TM7.  | 59 |
| Figure 3.8. Effect of charge reversal mutations in the TM3-ICL3 salt bridge.   | 60 |
| Figure 3.9 Conformational changes of mGlu2R upon activation.   | 62 |
| Figure 4.1. Structural model of truncated mGlu2R — G-protein complex.  | 70 |
| Figure 4.2. Schematic cartoon of potential electrostatic interactions within mGlu2R — G-protein complex.   | 71 |
| Figure 4.3. mGlu2R residues potentially critical for the interaction with G $\alpha$ tend to be located in or adjacent to intracellular loops 2 and 3.     | 72 |
| Figure 4.4 G $\alpha$ residues predicted to engage in key electrostatic interactions with mGlu2R.  | 73 |
| Figure 4.5 Effects of mutations in G $\alpha$ residues proposed by computational modeling as candidates for key intermolecular electrostatic interactions. | 74 |
| Figure 4.6 Residues involved in mGlu2R—G $\alpha$ intermolecular electrostatic interactions.   | 75 |
| Figure 4.7 mGlu2R intracellular loop 3 interaction with G $\alpha$ K317 in $\alpha$ 4- $\beta$ 6 linker  | 77 |

|  |    |
|--|----|
| Figure 4.8 Simultaneously destabilizing Gai E33 and D193 interactions with ICL2 restores control levels of activation. | 79 |
| Figure 4.9 Reestablishing the overall mGlu2R R670 — Gai1 E33/D193 Salt Bridge Network.                                 | 81 |
| Figure 4.10 Effects of mutations in mGlu2R ICL2—Gai D193 salt bridge.  | 83 |
| Figure 4.11 Effects of mutations in mGlu2R ICL2—Gai E33 salt bridge.   | 85 |

## List of Tables

|   |    |
|---|----|
| Table 1.1. G Protein Subunits and Their Primary Effectors.  | 25 |
| Table 3.1. Summary of glutamate effects on the TM3-TM6 ionic lock mutants.  | 58 |
| Table 3.2. Summary of glutamate effects on the TM3-ICL3 salt bridge mutants.  | 61 |
| Table 4.1. Summary of the effects of mutations in mGlu2R ICL3—Gai on glutamate responses.                               | 78 |
| Table 4.2. Summary of glutamate responses in single and double mutants of Gai* residues interacting with receptor ICL2. | 80 |
| Table 4.3. Summary of the effect of reestablishing the salt bridge network for residue R670 in ICL2 of mGlu2R.          | 82 |
| Table 4.4. Summary of the effects of mutations in mGlu2R ICL2—Gai D193 on glutamate responses.                          | 84 |
| Table 4.5. Summary of the effects of mutations in mGlu2R ICL2—Gai E33 on glutamate responses.                           | 86 |

## List Of Abbreviations

| <b>Abbreviation</b> | <b>Full name</b>  |
|---------------------|---|
| 5-HT <sub>2A</sub>  | Serotonin 2A Receptor   |
| AC                  | Adenylyl cyclase  |
| ADP                 | Adenosine diphosphate   |
| AHD                 | Alpha helical domain  |
| AMPA                | $\alpha$ -amino-3-hydroxy-5-methyl-4-isoxazole propionic acid |
| BINA                | Biphenyl-indanone A   |
| cAMP                | Cyclic adenosine monophosphate                                |
| CNS                 | Central nervous system  |
| CRD                 | Cysteine-rich domain  |
| DOB                 | 2,5-dimethoxy-4-bromoamphetamine                              |
| EC <sub>50</sub>    | Half maximal effective concentration                          |
| ECD                 | Extracellular domain  |
| E <sub>max</sub>    | maximum response achievable                                   |
| FISH                | Fluorescence in situ hybridization                            |
| FRET                | Flourescence resonance energy transfer                        |
| G $\alpha$          | G protein alpha subunit                                       |
| GABA                | Gamma-aminobutyric acid                                       |
| G $\beta\gamma$     | G protein beta gamma dimer                                    |
| GDP                 | Guanine diphosphate   |
| GFP                 | Green fluorescent protein                                     |
| GIRK                | G protein-coupled inwardly rectifying potassium channel       |

|        |  |
|--------|--|
| GIRK4* | G protein-coupled inwardly rectifying potassium channel 4* |
| GPCR   | G protein-coupled receptor                                 |
| GTP    | Guanine triphosphate                                       |
| HDAC2  | Histone deacetylase 2                                      |
| ICL    | Intracellular loop   |
| KO     | Knockout   |
| LBD    | Ligand binding domain                                      |
| LSD    | Lysergic acid diethylamide                                 |
| MD     | Molecular dynamics   |
| mGluR  | Metabotropic glutamate receptor                            |
| mGlu2R | Metabotropic glutamate receptor 2                          |
| mGlu3R | Metabotropic glutamate receptor 3                          |
| NAM    | Negative allosteric modulator                              |
| NMDA   | N-Methyl-D-aspartic acid                                   |
| PAM    | Positive allosteric modulator                              |
| PCP    | Phencyclidine  |
| pEC50  | The negative logarithm of the EC50 value                   |
| PTX    | Pertussis toxin  |
| RHD    | Ras homology domain  |
| RMSD   | root-mean-square-deviation                                 |
| TEVC   | Two electrode voltage clamp                                |
| TM     | Transmembrane  |
| TMD    | Transmembrane domain                                       |

VGLUT

vesicular glutamate transporters

VTA

Ventral tegmental area

WT

Wildtype

# Abstract

## **METABOTROPIC GLUTAMATE RECEPTOR 2 ACTIVATION: COMPUTATIONAL PREDICTIONS AND EXPERIMENTAL VALIDATION**

By Amr Ellaithy, MB BCh

A dissertation submitted in partial fulfillment of the requirements for the degree of Doctor of Philosophy at Virginia Commonwealth University.

Virginia Commonwealth University, 2018

Director: Diomedes E. Logothetis, Ph.D.  
Professor, Northeastern University

G protein-coupled receptors (GPCRs) are the largest family of signaling proteins in animals and represent the largest family of druggable targets in the human genome. Therefore, it is of no surprise that the molecular mechanisms of GPCR activation and signal transduction have attracted close attention for the past few decades. Several stabilizing interactions within the GPCR transmembrane (TM) domain helices regulate receptor activation. An example is a salt bridge between 2 highly conserved amino acids at the bottom of TM3 and TM6 that has been characterized for a large number of GPCRs. Through structural modeling and molecular dynamics (MD) simulations, we predicted several electrostatic interactions to be involved in metabotropic glutamate receptor 2 (mGlu2R) activation. To experimentally test these predictions, we employed a charge reversal mutagenesis approach to disrupt predicted receptor electrostatic intramolecular interactions as well as intermolecular interactions between the receptor and G proteins. Using two electrode voltage clamp in *Xenopus laevis* oocytes

expressing mutant receptors and G-proteins, we revealed novel electrostatic interactions, mostly located around intracellular loops 2 and 3 of mGlu2R, that are critical for both receptor and G-protein activation. These studies contribute to elucidating the molecular determinants of mGluRs activation and conformational coupling to G-proteins, and can likely be extended to include other classes of GPCRs.

# Chapter 1 INTRODUCTION

## 1.1 GPCR to G-protein Signaling

G protein-coupled receptors (GPCRs) are the largest family of signaling proteins in animals, and represent the largest family of druggable targets in the human genome (Wacker, Stevens, and Roth 2017). Many disorders have been linked to mutations and polymorphisms in GPCRs. Therefore, the molecular mechanisms of GPCR activation and signal transduction have attracted close attention for the last half century.

The general structure of all GPCRs is the same: an extracellular amino terminus, a seven-transmembrane helical domain (TMD), an intracellular carboxy terminus, and 6 loops (3 extracellular and 3 intracellular) connecting the TMD helices. GPCRs vary in the length of N-terminal domain, intracellular loops, and C-terminus (**Fig. 1.1**).

In simplest terms, GPCRs serve as signal transducers. They transduce extracellular signals, whether induced by hormones, neurotransmitters, photons, odorants, tastants, or other small molecules, into intracellular signaling events (Lefkowitz 2007). This common theme unifies the cellular function of the hundreds of GPCRs involved in numerous physiological processes.

As with GPCRs, heterotrimeric guanine nucleotide-binding proteins (G-proteins) represent another essential family of signaling proteins that has been highly conserved over evolution. Each G-protein heterotrimer consists of  $G\alpha$ ,  $G\beta$ , and  $G\gamma$  subunits. Each subunit has distinctive isoforms including 16  $G\alpha$ , 5  $G\beta$ , and 13  $G\gamma$  isoforms in humans that assemble in distinct combinations, which contribute to the specificity with regards to both GPCRs and effector systems (Milligan and Kostenis 2006). G-proteins function to

transduce signals from this vast array of receptors to protein effectors such as ion channels and enzymes, thus regulating the levels of intracellular second messengers. In the absence of ligand, the affinity of the G-protein to the GPCR is low, and the  $G\alpha$  subunit of the heterotrimer, which contains the nucleotide binding site, is bound to guanine diphosphate (GDP) forming the inactive heterotrimer (**Fig. 1.2**). Ligand-induced receptor activation promotes the engagement of the GDP-bound heterotrimer and accelerates GDP dissociation, the rate-limiting step in G-protein activation. The resulting nucleotide-free receptor–G-protein complex has a very short lifetime because the high intracellular GTP concentration facilitates rapid GTP binding to the nucleotide-binding site of  $G\alpha$ . The GTP-bound  $G\alpha$  undergoes conformational changes that result in the dissociation from  $G\beta\gamma$  subunits. Both elements of the G-protein can regulate the activity of effector proteins such as adenylyl cyclases (ACs), phospholipases, and ion channels (**Table 1.1**). The cycle is terminated by hydrolysis of GTP to GDP either via the intrinsic GTPase activity of the  $G\alpha$  subunit or accelerated by GTPase-activating proteins, the largest family of which are the regulators of G-protein signaling (RGS) proteins. This leads to the reassociation of the  $G\alpha$  and  $G\beta\gamma$  subunits into the inactive heterotrimer complex (Milligan and Kostenis 2006).

G proteins can be generally grouped into 4 families:  $G_{\alpha s}$ ,  $G_{\alpha i}$ ,  $G_{\alpha q}$ , and  $G_{\alpha 12}$  (**Table 1.1**). Traditionally, G protein-mediated responses have been classified into pertussis toxin (PTX)-sensitive and PTX-insensitive responses, because of the ability of this bacterial toxin to selectively inactivate G proteins of the  $G_i$  family (**Fig. 1.3**). This property is widely exploited to test for the involvement of  $G_i$  in cellular responses. At the molecular level, PTX ADP-ribosylates the  $G_{\alpha i}$  subunit functionally uncoupling  $G_i$

proteins from GPCRs, and thereby, preventing their activation (Vauquelin and Von Mentzer 2008).

## 1.2 GPCR Activation

### 1.2.1 GPCR Activation Models

GPCRs were first described to exist in two distinct conformations, active and inactive, akin to the open and closed states of an ion channel. This binary “on-off switch” idea was the basis for the classical ternary complex model of GPCR-driven signaling (De Lean, Stadel, and Lefkowitz 1980). This view considered the activation of a receptor by an agonist to produce a ternary complex with the G protein, thus activating the G protein to initiate a cellular response. However, a number of biophysical studies have shown that GPCRs are dynamic proteins that can sample multiple conformations (Manglik et al. 2015; Yao et al. 2009). Accumulating evidence has supported an alternative multi-state model where GPCRs can adopt multiple conformational states that exist in an equilibrium dependent on the bound ligand and the interacting cognate G protein (Gurevich and Gurevich 2017; Samama et al. 1993; Ghanouni et al. 2001). This conformational equilibrium cannot be shifted to a single inactive or active conformation, which explains the reported constitutive activity of many GPCRs (Seifert and Wenzel-Seifert 2002; Costa and Herz 1989). Depending on its intrinsic efficacy, a ligand can shift the equilibrium to increase the proportion of receptors in active conformational states in the case of agonists, or to stabilize receptors in more inactive conformations in the case of inverse agonists (**Fig. 1.4**). Moreover, different intracellular signaling proteins might prefer distinct receptor conformations, adding more complexity to the multitude of cellular effects a ligand-bound receptor can initiate. The ability of ligands to stabilize some unique conformational states activating certain cellular pathways and not others has been termed “biased signaling”, functional selectivity”, and “stimulus

trafficking” (Urban et al. 2007; Conn, Christopoulos, and Lindsley 2009). Biased signaling provides a potential opportunity to selectively target signaling pathways critical for therapeutic efficacy and exclude other pathways associated with adverse effects.

### ***1.2.2 Targetable Sites on GPCRs***

GPCRs have been classically targeted through their endogenous ligand (orthosteric)-binding site. This approach has often failed to yield highly selective orthosteric compounds. This can be explained by the fact that orthosteric sites are often highly conserved between subtypes of a single GPCR subfamily which renders the development of subtype-selective orthosteric ligands challenging.

An alternative relatively recent approach has been to target allosteric sites — sites that are spatially distinct from, but conformationally linked to, the orthosteric site (**Fig. 1.5.A**). Allosteric modulators can modify the action of the orthosteric ligand by modulating its affinity and/or efficacy (**Fig. 1.5.B**), either in a positive (in case of positive allosteric modulators, PAMs) or a negative direction (in case of negative allosteric modulators, NAMs) (Ellaithy et al. 2015). This phenomenon is referred to as ‘cooperativity’ (Conn, Christopoulos, and Lindsley 2009). PAMs enhance the response to an agonist and cause a leftward (and often an upward) shift in the concentration–response curve for the orthosteric agonist. Interestingly, a PAM can behave either as a pure PAM, eliciting no detectable response in the absence of the orthosteric agonist, or as an ago-PAM that can directly activate a receptor. NAMs noncompetitively antagonize agonists and cause a rightward (and often downward) shift in the agonist concentration-response curves (**Fig. 1.5.B**). Neutral allosteric ligands occupy the allosteric site without affecting the

agonist responses; yet, they can block the effects of both PAMs and NAMs (Christopoulos et al. 2014).

PAMs have an advantage over synthetic orthosteric agonists in their ability to maintain the temporal and spatial fidelity of receptor signaling (**Fig. 1.6**) because their effects are dependent on the presence of the endogenous ligand. Unlike synthetic orthosteric agonists, PAMs will not continuously activate the receptor, thus receptor desensitization and/or downregulation is less likely to occur. Moreover, an allosteric drug is more likely to fine-tune physiological responses with less risk of toxicity since no effect is expected at saturating concentrations above that determined by cooperativity (Christopoulos 2014). This saturability phenomenon is referred to as the 'ceiling level' of the allosteric effect.

## 1.3 Structural Basis of GPCR–G protein interactions

The idea that different GPCRs have common molecular activation mechanisms allowing diverse extracellular stimuli to utilize shared downstream signaling molecules was proposed in the late 1980s based on the structural homology of GPCRs (Strader, Sigal, and Dixon 1989). However, GPCRs are inherently challenging proteins for structural studies largely due to their conformational plasticity, and until recently, high-resolution structures that allow mechanistic understanding of receptor activation have been impossible to obtain. This has changed over the past decade thanks to advances in structural biology that allowed unprecedented detailed examination of the mechanisms underlying receptor activation (Manglik and Kruse 2017).

### *1.3.1 Conformational Changes Involved in Receptor Activation*

Several conserved structural rearrangements, referred to as “molecular switches”, regulate receptor activation. Such conformational changes are best appreciated through comparing crystal structures of the same receptor in active and inactive states.

#### *1.3.1.1 Outward Movement of TM6*

The most prominent change seen in all GPCRs examined so far is a movement of the intracellular end of TM6 away from the middle axis of the TMD (**Fig. 1.7**) (Farrens et al. 1996; Altenbach et al. 2008). This creates a cavity on the cytoplasmic face of the receptor that can accommodate the G $\alpha$  C-terminus (Manglik and Kruse 2017).

#### *1.3.1.2 The Ionic Lock*

The “ionic lock” is a common feature of many GPCRs where Arg3.50 in the highly conserved D(E)RY motif at the intracellular end of TM3 serves to stabilize the receptor

in an inactive state through a salt bridge to Glu6.30 (**Fig. 1.8**). This interaction holds the cytoplasmic ends of TM3 and TM6 in close vicinity, thus constraining the receptor in an inactive state (Palczewski et al. 2000; Wang et al. 2018; Rasmussen et al. 2007; Vogel et al. 2008). Breakage of this lock has been postulated to be a critical step in receptor activation since disruption of the ionic lock through mutations increases the constitutive receptor activity (Shapiro et al. 2002; Ballesteros et al. 2001; Rasmussen et al. 1999; Scheer et al. 1997; Scheer et al. 1996; Alewijnse et al. 2000).

### *1.3.1.3 The NPxxY motif*

Another important sequence motif that shows significant rearrangements upon activation is the NPxxY motif located near the intracellular end of TM7. The sequence contains a highly conserved tyrosine (Tyr7.53) which, on activation, changes its rotamer conformation and points towards the core of the TMD allowing the formation of a hydrogen bond between the NPxxY motif and the highly conserved Tyr 5.58 in TM5. This interaction stabilizes the receptor active conformation in a manner analogous to how the ionic lock interaction stabilizes the inactive conformation (Manglik and Kruse 2017).

Most of the previously mentioned structural rearrangements have been characterized in class A GPCRs, but more evidence is revealing other families of GPCRs are utilizing several of the same mechanisms. The outward motion of TM6 has been shown in the crystal structures of activated class B GPCRs (Liang et al. 2017; Zhang et al. 2017; Jazayeri et al. 2017), and the ionic lock has been revealed in the inactive crystal structures of the class C GPCRs metabotropic glutamate receptors mGlu1R and mGlu5R (Doré et al. 2014; Wu et al. 2014). The remarkable degree of conservation of

these structural rearrangements even among distantly related receptors with little primary sequence homology suggests a common evolutionary origin for the activation mechanisms in most GPCRs (Manglik and Kruse 2017).

### ***1.3.2 Allosteric coupling between agonist-binding and nucleotide-binding sites in GPCRs***

Structural studies have revealed that full agonists alone, even those with picomolar affinity, do not completely stabilize a fully active receptor conformation as further receptor activation, including a greater outward movement of TM6, is observed upon addition of the heterotrimeric Gs protein or the Gs-mimetic nanobody Nb80 (Rasmussen et al. 2011; Yao et al. 2009; Nygaard et al. 2013; Manglik et al. 2015; Sounier et al. 2015; Isogai et al. 2016). This suggests that the allosteric coupling between agonist-binding and nucleotide-binding sites is loose, that is, agonist binding is not necessarily translated into a fully active receptor conformation. Rather, agonist binding serves to enhance the probability of sampling intermediate active states that are conducive to interaction with the G protein. After achieving a G protein-interacting conformation and engaging GDP-bound G protein, the receptor functions to accelerate GDP dissociation from G $\alpha$  by allosterically disrupting the nucleotide-binding site (Mahoney and Sunahara 2016).

### ***1.3.3 Receptor-catalyzed nucleotide exchange***

Earlier than for GPCRs, crystal structures for G proteins have been determined in their active (GTP $\gamma$ S-bound), transition (GDP·AlF $_4$ -bound), and inactive (GDP-bound) states (Noel, Hamm, and Sigler 1993; Sunahara et al. 1997; Coleman et al. 1994; Mixon et al. 1995; Lambright et al. 1996; Lambright et al. 1994; Sondek et al. 1994). These

structures revealed that the nucleotide is buried at the interface between the 2 domains of G $\alpha$  subunit, the Ras-homology domain (RHD) and the  $\alpha$ -helical domain (AHD) (**Fig. 1.9**), and suggested a requirement for domain separation for nucleotide entry or exit from its binding pocket.

While domain separation is required for nucleotide release, it has been revealed that GDP remains bound to the RHD upon separation of the two domains or even when the entire AHD has been deleted (Dror et al. 2015). This suggests that GDP dissociation needs to be triggered through other receptor-mediated conformational changes within the RHD that are transmitted to the nucleotide-binding site to promote nucleotide release (Hilger, Masureel, and Kobilka 2018).

Numerous studies have identified several receptor contact sites on G-protein (**Fig. 1.9A**) (Oldham and Hamm 2008). Those are specific parts of G $\alpha$  N terminus ( $\alpha$ N), C terminus ( $\alpha$ C),  $\alpha$ 3– $\beta$ 5 loop, and  $\alpha$ 4– $\beta$ 6 loop. The reorientation places the nucleotide  $\sim$ 30 Å from the sites of nearest receptor contact, posing the question of how receptors cause GDP release from this distance (Oldham and Hamm 2008).

Two potential allosteric connections have been suggested for propagation of conformational changes from the activated receptor to the nucleotide-binding pocket (Mahoney and Sunahara 2016):

**G $\alpha$  C-terminus:** Comparison of the interactions formed by the C-terminal  $\alpha$ 5 helix of G $\alpha$  in GDP-bound structures (Scheerer et al. 2008; Choe et al. 2011; Standfuss et al. 2011) and in the  $\beta$ 2AR-bound nucleotide-free state (Rasmussen et al. 2011) shows that upon receptor binding, the distal C-terminus rotates approximately 60° and translates 5 Å up to embed into the cavity opened by the outward rotation of receptor's TM6, leading to

several rearrangements within the  $G\alpha$  RHD (Mahoney and Sunahara 2016). The most important rearrangement is that of  $\beta 6$ - $\alpha 5$  loop, which directly contacts the purine base through the conserved TCAT motif (**Fig. 1.9A**), resulting in a decrease in the affinity of the bound nucleotide (Dror et al. 2015).

***G $\alpha$  N-terminus:*** The N-terminal helix ( $\alpha N$ ) of  $G\alpha$  subunits is followed by the  $\beta 1$ -strand, which in turn is followed by the  $\beta 1$ - $\alpha 1$  loop — also known as the P-loop — a highly conserved structural feature of both small molecular weight and heterotrimeric G proteins that coordinates the  $\alpha$ - and  $\beta$ -phosphates of GDP. Interaction of the  $\alpha N$  with ICL2 of the activated receptor (Rasmussen et al. 2011) perturbs the P-loop-GDP interaction triggering nucleotide release from G-protein (Chung et al. 2011).

The role of  $\alpha N$  also helps explain the involvement of  $G\beta\gamma$  in nucleotide exchange. In the heterotrimer,  $G\beta\gamma$  helps to position the  $\alpha N$  in a conformation that engages ICL2 of the receptor allowing for receptor-catalyzed nucleotide release, without actually making contact with the receptor (Mahoney and Sunahara 2016).

The process of GDP dissociation may require the cooperative engagement of both N- and C- termini by the receptor (Mahoney and Sunahara 2016). The crystal structure of  $A_{2A}R$ -mini  $G\alpha_s$  complex that lacked the N-terminus-ICL2 interaction and remained GDP-bound supports this idea (Carpenter et al. 2016). Which  $G\alpha$  terminus engages the receptor first remains to be determined.

#### ***1.3.4 G protein feedback to the agonist-binding site***

It has been shown that the ligand-binding affinity of the receptor is enhanced when engaged by G protein or nanobodies that behave as G protein mimics (e.g. Nb80) (Rasmussen et al. 2011; Huang, Manglik, et al. 2015; Kruse et al. 2013). Several GPCR

crystal structures reveal conformational changes in the extracellular loops the result in the formation of a lid-like structure above the ligand binding site (Isogai et al. 2016; DeVree et al. 2016). This active closed conformation of the receptor hinders ligand dissociation, which explains the G protein-mediated effects on enhancing agonist binding affinity (Mahoney and Sunahara 2016).

## 1.4 Metabotropic Glutamate Receptors

### 1.4.1 The Glutamatergic System

Glutamate is the major excitatory neurotransmitter in the mammalian central nervous system (CNS). It plays key roles in physiological processes including learning and memory, as well as pathological contexts such as excitotoxic neuronal injury which follows CNS trauma or ischemia. Therefore, tight control of glutamatergic neurotransmission is necessary to maintain optimal neuronal function and prevent excessive activation of the system. To help achieve that, multiple levels of regulation have evolved (Sanacora et al. 2008).

In the brain, glutamate can be either synthesized *de novo* from glucose via the tricarboxylic acid cycle or recycled through the glutamate/glutamine cycle. Glutamate is transported into synaptic vesicles by vesicular glutamate transporters (VGLUTs) where it is stored at high concentrations until being released in a  $\text{Ca}^{2+}$ -dependent manner into the synaptic cleft by exocytosis (Sanacora et al. 2008).

### 1.4.2 Ionotropic Glutamate Receptors

There are two major categories of glutamatergic receptors in the CNS: ionotropic and metabotropic (**Fig. 1.10**). Ionotropic glutamate receptors are ligand-gated ion channels that open upon binding of an agonist. There are three subgroups:

**AMPA receptors.** AMPA ( $\alpha$ -amino-3-hydroxy-5-methyl-4-isoxazole propionic acid) receptors mediate the fast rapidly desensitizing excitatory current at most synapses which constitutes the initial response to glutamate in the synapse. They allow the inward flow of  $\text{Na}^+$  and the outward flow of  $\text{K}^+$  resulting in depolarization of the neuronal membrane (Sanacora et al. 2008).

**Kainate receptors.** Like AMPA receptors, Kainate receptors are ion channels that allow  $\text{Na}^+$  influx and  $\text{K}^+$  efflux mediating fast excitatory neurotransmission, but they appear to have a different distribution from AMPA receptors (Sanacora et al. 2008).

**NMDA receptors.** N-Methyl-D-aspartic acid (NMDA) receptors are also glutamate ion channels that also have glycine or D-serine as coagonists. A distinguishing feature of NMDA receptors is their voltage-sensitive block by  $\text{Mg}^{2+}$ .  $\text{Mg}^{2+}$  blocks conductance of NMDA channels under basal conditions, but the blockade is overcome by partial depolarization of the resting membrane potential. Once  $\text{Mg}^{2+}$  block is overcome, NMDA receptors mediate the influx of not only  $\text{Na}^+$  but of  $\text{Ca}^{2+}$  as well. The resulting intracellular  $\text{Ca}^{2+}$  increase activates multiple enzyme cascades that are involved in physiological processes such as long-term potentiation, as well as pathophysiological conditions such as excitotoxicity associated with CNS injury (Sanacora et al. 2008).

### ***1.4.3 Metabotropic Glutamate Receptors***

Metabotropic glutamate receptors (mGluRs) belong to class C GPCRs, distinguished by their large extracellular bilobed ligand-binding domain (LBD) and a cysteine-rich domain (CRD) that links the LBD to the TMD (**Fig. 1.11**). Another distinguishing feature of class C GPCRs is constitutive homo- or heterodimerization at the cell surface (Kniazeff et al. 2011; Romano, Yang, and O'Malley 1996; Doumazane et al. 2011). The eight mGluR subtypes identified so far are classified into three groups (**Fig. 1.12**) based on sequence homology, G-protein coupling, and pharmacology (Nakanishi 1992). Group I mGluRs (mGlu1R and mGlu5R) are predominantly coupled to  $G_{q/11}$  and activate the phospholipase C enzyme. Group II mGluRs (mGlu2R and mGlu3R) and group III

(mGlu4R, mGlu6R, mGlu7R, and mGlu8R) are coupled to  $G_{i/o}$  proteins that inhibit adenylyl cyclase activity (Ellaithy et al. 2015).

#### ***1.4.3.1 Molecular Determinants of mGluR Dimerization***

In full-length mGluRs, dimerization has been shown to be required for glutamate-induced activation (El Moustaine et al. 2012). Dimerization of mGluRs was long thought to be mainly stabilized by intersubunit disulfide bridges involving the extracellular domains (Romano, Yang, and O'Malley 1996; Kunishima et al. 2000; Ray and Hauschild 2000). Recent evidence from single-molecule subunit imaging, which relies on counting photobleaching steps in GFP-tagged receptors, indicates that mGluR dimerization is primarily mediated via hydrophobic LBD interactions, with modest contributions from an intersubunit disulfide bridge and the TMD. Mutations that disrupt disulfide bridging compromises dimerization without eliminating it, unlike mutations in the hydrophobic dimerization interface of the LBD that result in complete monomerization (Levitz et al. 2016).

#### ***1.4.3.2 Subunit Cooperativity in mGluR Activation***

Whether agonist binding to only one versus to both subunits in a dimer is required for receptor activation was for long subject to debate. For example, one study suggested that activation does not occur until two ligands bind (Kammermeier and Yun 2005), whereas another suggested that glutamate binding to one subunit can activate mGluRs but that binding to both subunits activates more efficiently (Kniazeff et al. 2004). These studies faced the technical difficulty of confining ligand binding to one subunit by introducing mutations that lower glutamate affinity in the second subunit. However, there remained a

concern that these mutations might have altered activation in unforeseen ways. A recent paper circumvented this challenge through selective liganding with photoswitchable tethered agonists covalently linked to one or both subunits of mGlu2R homodimers, and revealed that receptor activation is highly cooperative (Levitz et al. 2016). Although agonist binding to one subunit does activate the receptor, binding to both subunits yields 5x more activation, indicating high cooperativity (**Fig. 1.13**).

## **1.5. Metabotropic Glutamate Receptor 2 as a Drug Target**

### ***1.5.1 mGlu2R localization***

mGlu2R is widely expressed in the brain, with generally similar distribution patterns in human and rodent brains. Areas where mGlu2R is particularly expressed include the prefrontal cortex, hippocampus, striatum, thalamus, and amygdala (Ghose et al. 2009; Marek 2010). In addition, mGlu2Rs are primarily located presynaptically outside of the active zone on pre-terminal regions of axons where they can be activated by excessive synaptic glutamate, hence allowing them to function as autoreceptors inhibiting further glutamate release and modulating synaptic transmission (Schoepp 2001).

### ***1.5.2 Potential applications of mGlu2R agonists/PAMs***

Due to its wide expression in the brain, heteromerization with other GPCRs (see below), and modulatory effect on various neurocircuits, mGlu2R has attracted considerable attention as a potential therapeutic target, with schizophrenia being the most explored clinical application to date. Other potential applications include epilepsy (Metcalf et al. 2017), cerebral ischemia (Motolese et al. 2015; Mastroiacovo et al. 2017), neurodegeneration (Richards et al. 2010; Kim et al. 2010), depression (Matrisciano et al. 2008; Fell et al. 2011; Witkin et al. 2016), anxiety (Tizzano, Griffey, and Schoepp 2002), cognition (Griebel et al. 2016), substance use disorders (Johnson and Lovinger 2015; Yang et al. 2017), smoking cessation (Kenny, Gasparini, and Markou 2003), and chronic pain (Jones et al. 2005; Carlton, Du, and Zhou 2009).

#### ***1.5.2.1 mGlu2R and Schizophrenia***

Schizophrenia is a chronic debilitating syndrome that affects approximately 1% of the general population. Symptoms are often variable but generally can be categorized into

positive (e.g., hallucinations, delusions, and disorganized speech and behavior), negative (e.g., social withdrawal, lack of motivation, flat affect), and cognitive (e.g., impairments in learning, memory, attention, and executive functions). These symptoms are typically associated with social and/or occupational dysfunction (Ellaithy et al. 2015).

Two classes of antipsychotic drugs are currently available for the treatment of schizophrenia. The first generation, or typical, antipsychotics such as haloperidol and chlorpromazine are high-affinity dopamine D2 antagonists. Because of their widespread blockade of dopamine, they are associated with adverse effects such as hyperprolactinemia and extrapyramidal symptoms. The second generation, or atypical, antipsychotics such as clozapine and olanzapine have less affinity for D2 receptors and higher affinity for the serotonin 2A receptor (5-HT<sub>2A</sub>). Although not associated with extrapyramidal symptoms, they are associated with weight gain and metabolic abnormalities such as dyslipidemia and impaired glucose tolerance (Ellaithy et al. 2015).

The past two decades have witnessed a rise in the 'NMDA receptor hypofunction' hypothesis for pathogenesis of schizophrenia, whereby defective NMDA receptors on cortical  $\gamma$ -amino- butyric acid (GABA) interneurons render these interneurons less effective in inhibiting glutamate neurons that project to the ventral tegmental area (VTA). This disinhibition results in excessive glutamatergic stimulation of the dopamine mesolimbic pathway, a key pathway, the hyperfunctioning of which has long been viewed to underlie schizophrenia (Schwartz, Sachdeva, and Stahl 2012). Hence, a variety of presynaptic, postsynaptic, and regulatory proteins involved in glutamatergic signaling have been proposed as potential therapeutic targets. One such target was

mGlu2R which is expressed in several areas implicated in the pathophysiology of schizophrenia such as the prefrontal cortex, hippocampus, striatum, thalamus, and amygdala (Ghose et al. 2009; Marek 2010). Several studies have reported dysregulation in mGlu2R expression levels in the brains of schizophrenic individuals (Bullock et al. 2008; Kordi-Tamandani, Dahmardeh, and Torkamanzehi 2013; González-Maeso et al. 2008; Ghose et al. 2008; Gupta et al. 2005).

mGlu2/3R agonists were shown to reverse the pro-psychotic-like effects of phencyclidine and psychedelic 5-HT<sub>2A</sub> receptor agonists in rodents (Moghaddam and Adams 1998; Cartmell, Monn, and Schoepp 1999; Moreno et al. 2012). Due to the lack of subtype-selective orthosteric ligands, knockout (KO) mice and Glu2R-selective PAMs were employed to determine whether the antipsychotic-like effects of mGlu2/3R agonists are mediated via mGlu2R, mGlu3R, or both. Both approaches revealed that these effects are predominantly mGlu2R-mediated. For example, the inhibitory effects of mGlu2/3R agonists on PCP- and amphetamine-evoked hyperlocomotor activity are absent in mGlu2R-KO but not in mGlu3R-KO mice.

Not only does mGlu2R seem to be the target for group II mGluR antipsychotics, but it has also been found to crosstalk with the 5-HT<sub>2A</sub> receptor, a key target for 2nd generation antipsychotics. For example, the pharmacological and behavioral effects induced by hallucinogenic 5-HT<sub>2A</sub> agonists are abolished in mGlu2R-KO mice (Moreno et al. 2011). On the other hand, the locomotor activity induced by the mGlu2/3R antagonist LY341495 is attenuated in 5-HT<sub>2A</sub>-KO mice (González-Maeso et al. 2008). Similarly, the antipsychotic-like behavioral effects of LY379268 are absent in 5-HT<sub>2A</sub>-KO mice, whereas the 5-HT<sub>2A</sub>-dependent behavioral effects of clozapine are absent in

mGlu2R-KO mice (Fribourg et al. 2011). Chronic treatment with the hallucinogenic 5-HT2A agonist 2,5-dimethoxy-4-bromoamphetamine (DOB) in mice attenuates the behavioral effects of the mGlu2/3R agonist LY379268 (Benneyworth, Smith, and Sanders-Bush 2008), whereas chronic treatment by LY341495 decreases 5-HT2A binding and the hallucinogenic effects of lysergic acid diethylamide (LSD) (Moreno et al. 2013).

In heterologous expression systems, co-expression of mGlu2R with 5-HT2A potentiates glutamate-induced mGlu2R-coupled Gi signaling and attenuates serotonin-induced 5-HT2A-coupled Gq signaling. Moreover, drugs that stabilize the active or inactive conformation in one receptor induce the opposite conformation of the partner receptor (Fribourg et al. 2011; Baki et al. 2016).

Neuroanatomical approaches such as fluorescent in situ hybridization (FISH) and immunohistochemistry revealed an overlapping cortical distribution of mGlu2R and 5-HT2A (González-Maeso et al. 2008; Fribourg et al. 2011). Using electron microscopy, both receptors were observed in close sub-cellular proximity (Moreno et al. 2012). In addition, 5-HT2A and mGlu2 receptors can be co-immunoprecipitated from plasma membrane preparations of mouse (Fribourg et al. 2011) and human (González-Maeso et al. 2008) frontal cortex. Taken together, these data suggest that 5-HT2A and mGlu2 participate in a GPCR heteromeric complex with unique signaling properties.

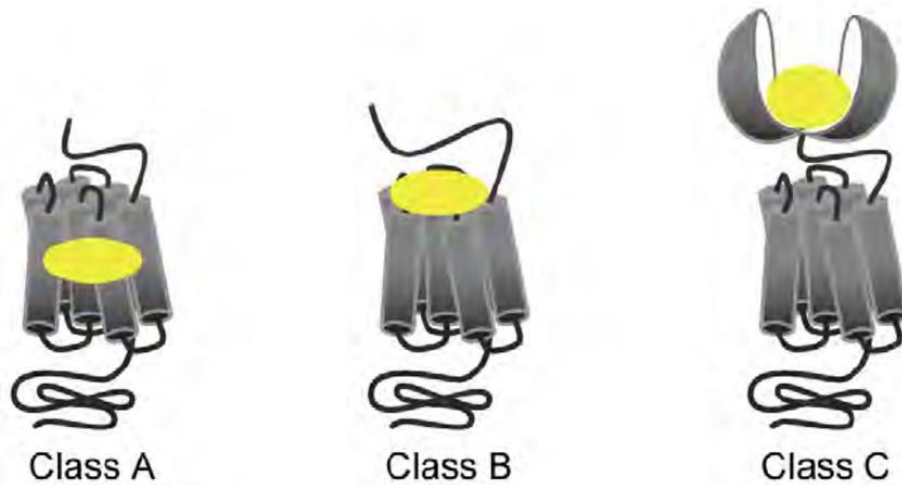
Clinical trials with pomaglmetad methionil (LY2140023 monohydrate; a prodrug of the mGlu2/3R agonist LY404039) revealed significant efficacy against positive and negative symptoms of schizophrenia compared to placebo. Although the efficacy was not as significant as for olanzapine, pomaglmetad was safe and well-tolerated and,

importantly, was neither associated with extrapyramidal symptoms nor with metabolic abnormalities, which are often problematic with the currently available antipsychotics (Patil et al. 2007). Subsequent phases of clinical trials showed either inconclusive results (Kinon et al. 2011) or results that did not separate from placebo (Hopkins 2013). Interestingly, recent preclinical evidence revealed that the therapeutic effects of pomaglometad depend on previous exposure to antipsychotic drugs. In mouse models, atypical antipsychotics, such as clozapine and risperidone, but not typical ones, such as haloperidol, induce repressive histone modifications at the promoter region of the mGlu2 (*Grm2*) gene in the frontal cortex (Kurita et al. 2012) (**Fig. 1.14**). The translational significance of these preclinical findings has been validated recently in a post-hoc analysis; schizophrenia patients previously treated with atypical antipsychotics did not show a significant therapeutic response to pomaglometad, whereas those who were treated with haloperidol did (Kinon et al. 2015).

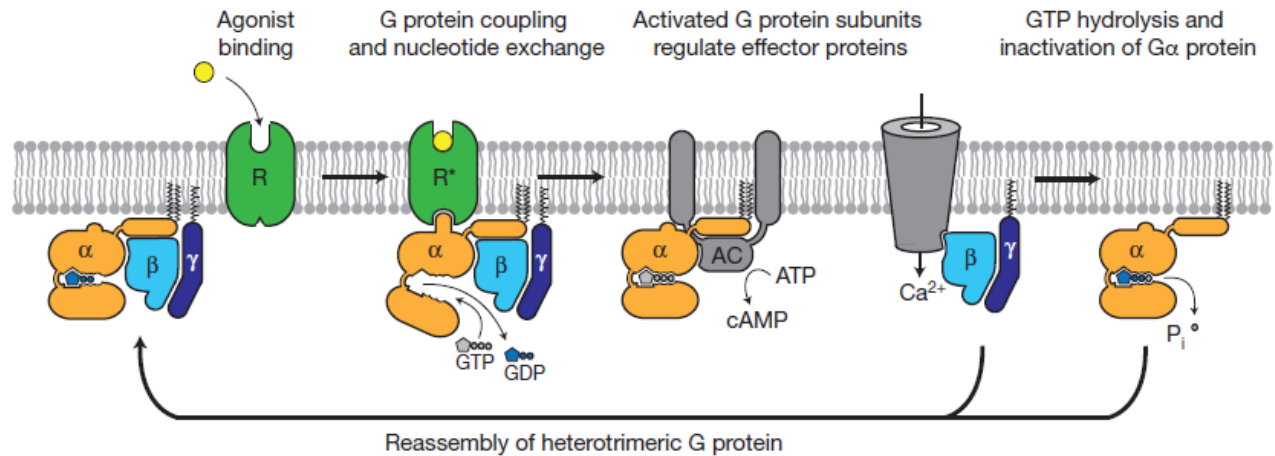
Two mGlu2R PAMs are also in clinical trials. ADX71149 from Addex and Janssen, showed the first successful clinical proof-of-concept and demonstrated safety and tolerability. Patients with residual negative symptoms were identified as the subpopulation most likely to benefit from ADX71149 (Therapeutics 2012). The second compound, AZD8529 from AstraZeneca, failed to separate from placebo in a Phase IIa study, unlike the active control risperidone (Litman et al. 2016). However, it is worth mentioning that these studies did not stratify patients according to their previous antipsychotic treatment history.

## 1.6 Hypothesis

Despite their physiological and pharmaceutical importance, much remains to be discovered about the molecular determinants of GPCR activation and coupling to G-protein. We hypothesize that several electrostatic interactions play key roles in mGlu2R activation and signaling. A large number of potential mGlu2R intramolecular as well as mGlu2R—G $\alpha$  intermolecular electrostatic interactions were suggested by structural modeling and molecular dynamics (MD) simulations. We set out to test the significance of those interactions using charge reversal mutagenesis with functional testing in *Xenopus laevis* oocytes expressing mutant receptors and G-proteins,



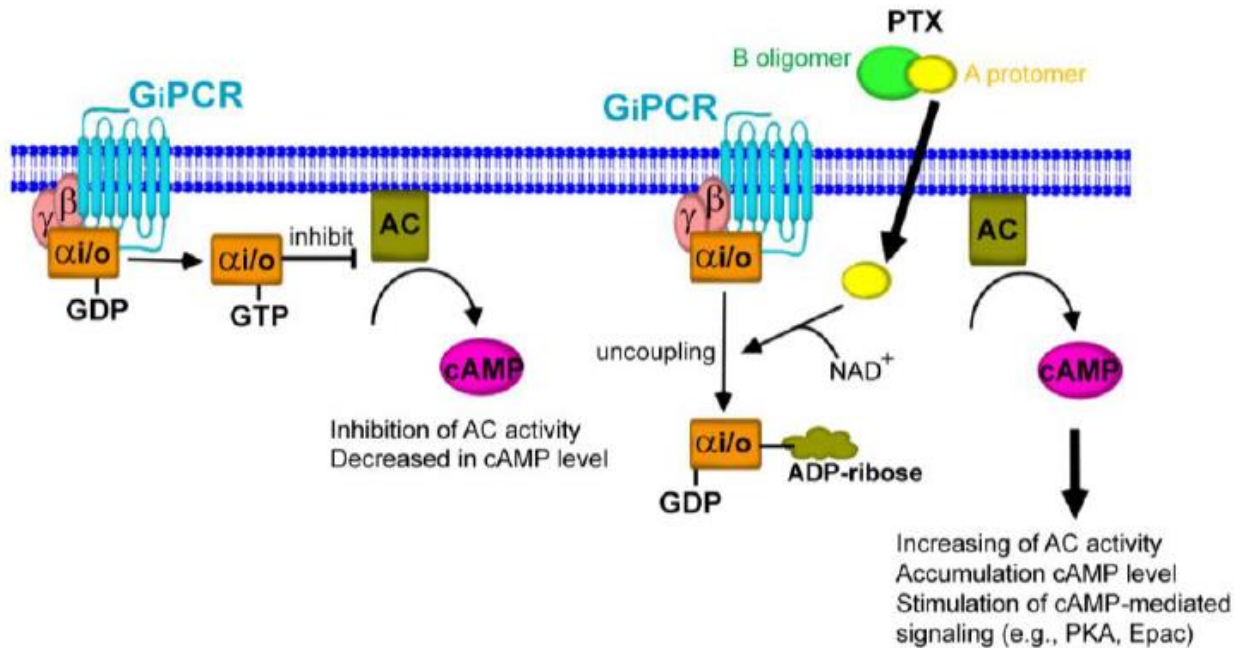
**Figure 1.1 Major Classes of GPCRs with the Typical Binding Regions of Orthosteric Ligands.** Class A (rhodopsin-like) GPCRs have a short extracellular N-terminus and an intracellular C terminus of variable length. Small ligands, such as biogenic amines, bind to a hydrophilic pocket within the transmembrane domain (TMD). Class B (Secretin family) agonist peptides simultaneously bind to the large extracellular N-terminal domain and the pocket between helices occupied in class A GPCRs by their small molecule ligands. Class C GPCRs differ from the others in that the N-terminus, in which the orthosteric binding site is located, is very long. (Stewart et al. 2012).



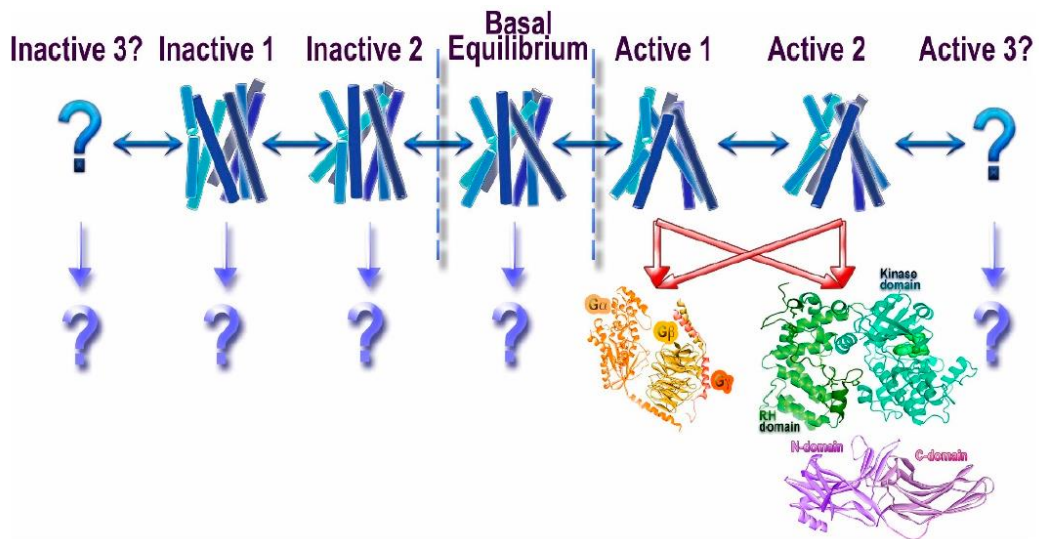
**Figure 1.2 G protein Activation Cycle.** Ligand binding to the GPCR induces a conformational change in the receptor that is transduced to the  $\text{G}\alpha$  subunit increasing its affinity for GTP and promoting the exchange of GDP for GTP. The activated GTP-bound  $\text{G}\alpha$  subunit dissociates from the  $\text{G}\beta\gamma$  subunits, whereupon both elements of the G-protein can regulate the activity of effector proteins. The cycle is terminated by hydrolysis of GTP to GDP, leading to the reassociation of the  $\text{G}\alpha$  and  $\text{G}\beta\gamma$  subunits into the inactive heterotrimer complex (Rasmussen et al. 2011).

**Table 1.1. G Protein Subunits and Their Primary Effectors.** (Hermans 2003)

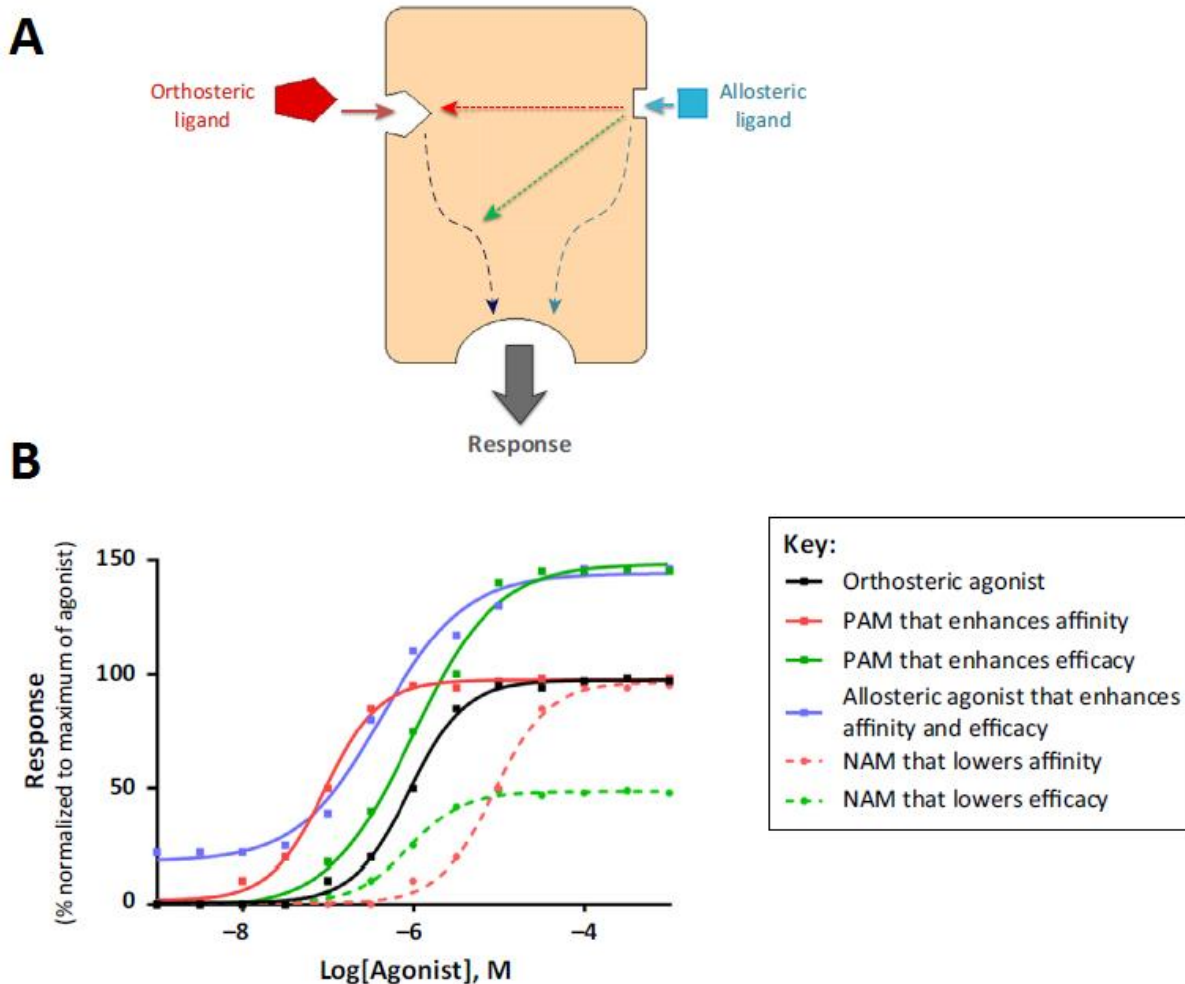
| Subunit         | Family  | Main subtypes  | Primary effector   |
|-----------------|---|--|--|
| $\alpha$        | $\alpha_s$  | $G\alpha_s, G\alpha_{olf}$                               | Adenylate cyclase $\uparrow$   |
|                 | $\alpha_{i/o}$  | $G\alpha_{i-1}, G\alpha_{i-2}, G\alpha_{i-3}$            | Adenylate cyclase $\downarrow$   |
|                 |   | $G\alpha_{oA}, G\alpha_{oB}$                             | $K^+$ channels $\uparrow$  |
|                 |   | $G\alpha_{t1}, G\alpha_{t2}$                             | $Ca^{2+}$ channels $\downarrow$  |
|                 |   | $G\alpha_z$  | Cyclic GMP phosphodiesterase $\uparrow$  |
| $\alpha_{q/11}$ | $G\alpha_q, G\alpha_{11}, G\alpha_{14}, G\alpha_{15}, G\alpha_{16}$ | Phospholipase C $\uparrow$                               |  |
| $\beta$         | $\alpha_{12}$   | $G\alpha_{12}, G\alpha_{13}$                             | ?  |
|                 | $\beta_{1-5}$ (6?)  | Different assemblies of $\beta$ - and $\gamma$ -subunits | Adenylate cyclase $\uparrow/\downarrow$<br>Phospholipases $\uparrow$<br>Phosphatidylinositol 3-kinase $\uparrow$               |
| $\gamma$        | $\gamma_{1-11}$ (12?)   |  | Protein kinase C $\uparrow$<br>Protein kinase D $\uparrow$<br>GPCR kinases $\uparrow$<br>$Ca^{2+}, K^+$ (and $Na^+$ ) channels |



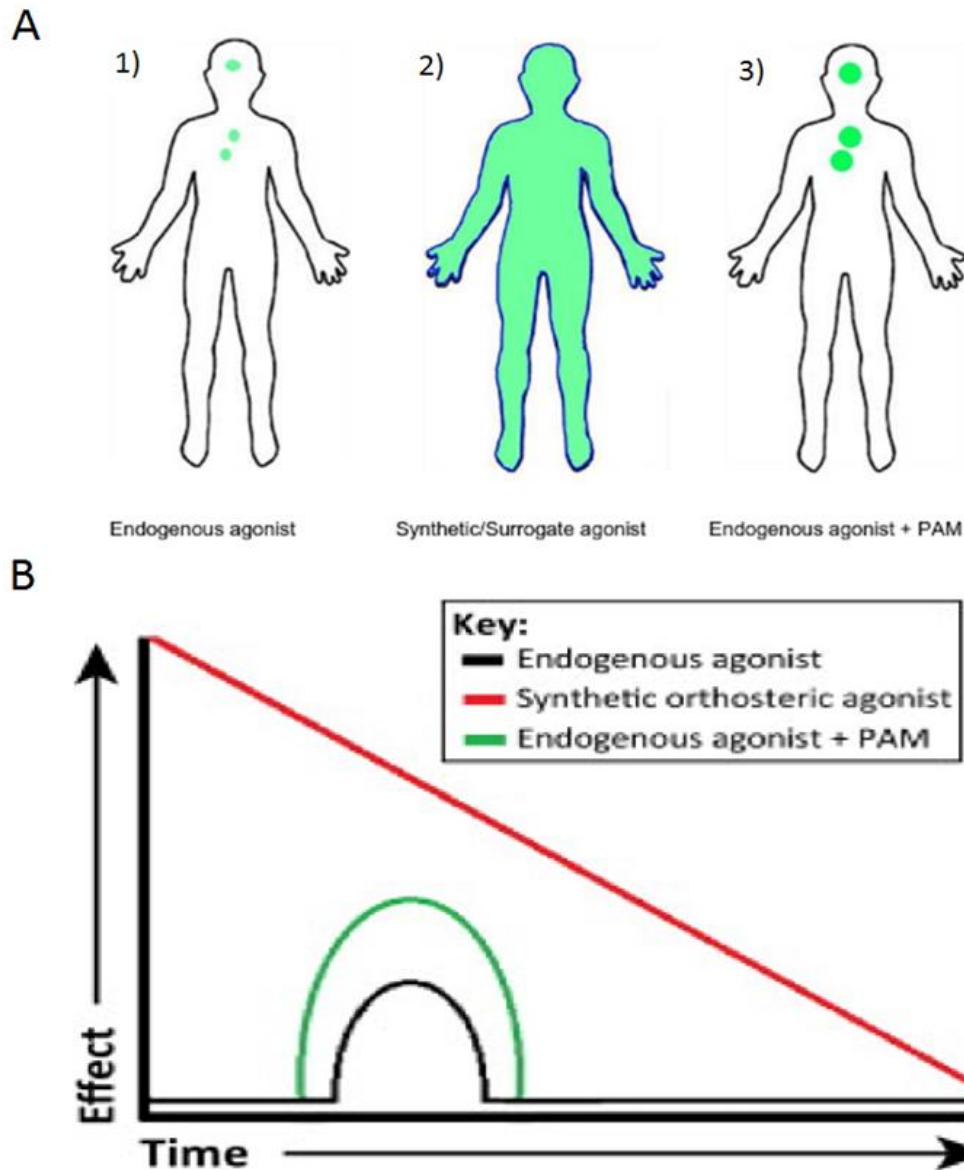
**Figure 1.3 Pertussis Toxin-Mediated Uncoupling of Gai/o Proteins from Their Cognate GPCRs.** When the A-protomer of PTX penetrates into the host cells, the Gai/o is ADP-ribosylated by the B-protomer resulting in inactivation of Gai/o. Inhibition of the inhibitory effect of Gai/o on adenylyl cyclase activity results in the elevation of intracellular cAMP levels, leading to activation of the cAMP-mediated signaling pathway (Vauquelin and Von Mentzer 2008).



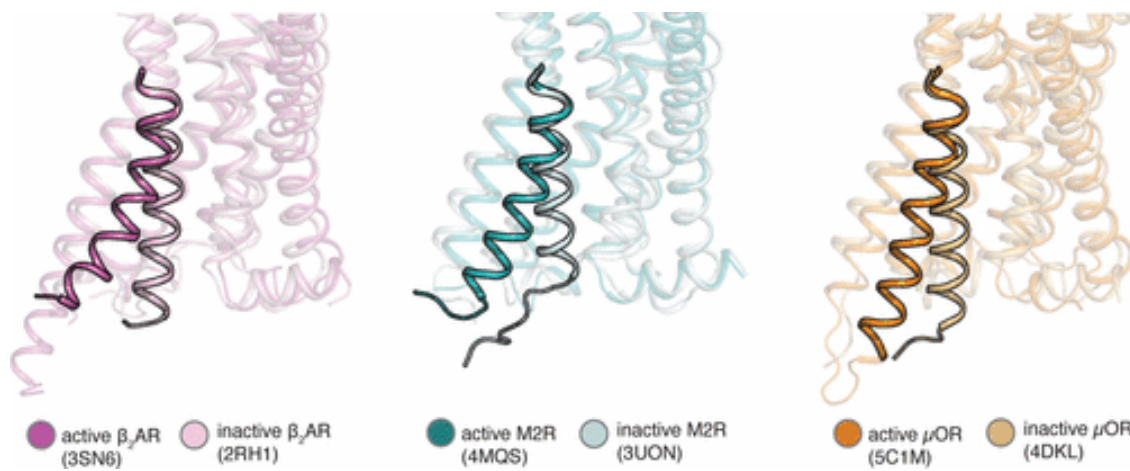
**Figure 1.4 Conformational heterogeneity of GPCRs and associated- signaling.** Unliganded GPCRs exist in an equilibrium between multiple conformations (basal equilibrium). Agonists partially shift the equilibrium towards active conformations, whereas inverse agonists shift the equilibrium in the opposite direction. The different active conformations might be associated with variable degrees of activation of the same signaling pathway, or even associated with different signaling pathways (biased signaling) (Gurevich and Gurevich 2017).



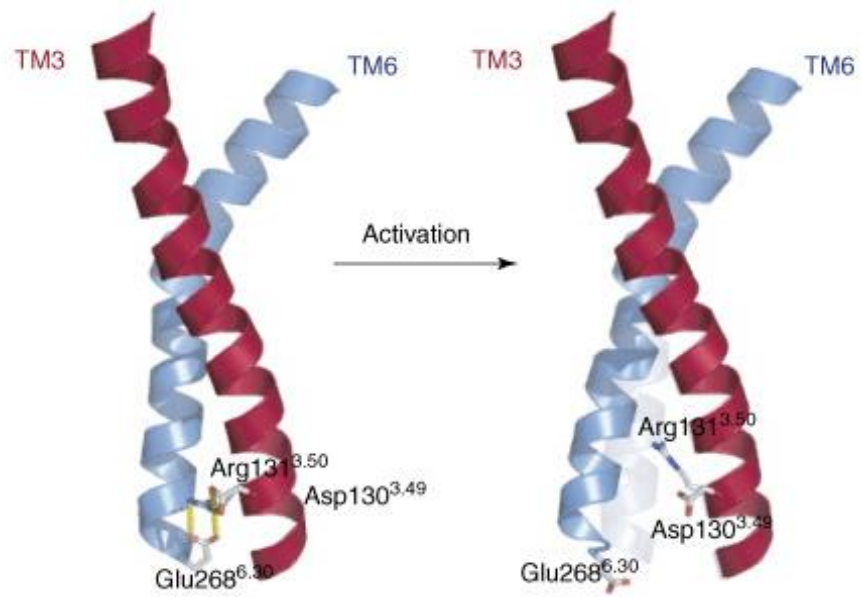
**Figure 1.5 Modes of action of allosteric modulators.** **A**, An allosteric ligand binds to a site distinct from the orthosteric binding site and modulates the affinity (red) and/or efficacy (green) of the orthosteric ligand. Some allosteric ligands are capable of directly eliciting a response on their own (blue). **B**, Schematic representation of the various potential effects mediated by different allosteric ligands on the functional response of an orthosteric agonist. The first (solid red) is a positive allosteric modulator (PAM) that purely enhances orthosteric agonist affinity, as evidenced by an increase in potency (lower  $EC_{50}$ ) and leftward shift of the concentration-response curve compared to the orthosteric agonist alone (solid black). The second (solid green) is a PAM that purely enhances agonist efficacy, as evidenced by an increase in  $E_{max}$  and upward shift in its concentration-response curve. The third (blue) demonstrates an allosteric agonist that modulates both the affinity and efficacy. The fourth (dashed red) is a negative allosteric modulator (NAM) that decreases the orthosteric agonist affinity, and thereby shifts its concentration-response curve to the right. The fifth (dashed green) is a NAM that decreases the orthosteric agonist efficacy and causes a downward shift in the concentration-response curve (Ellaithy et al. 2015).



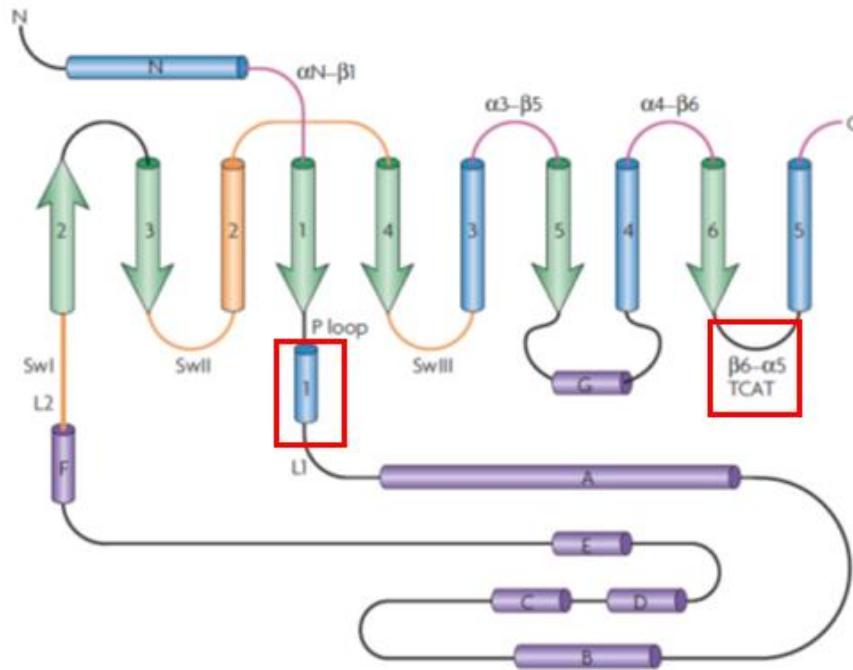
**Figure 1.6 PAMs Maintain Temporal and Spatial Patterns of Native Receptor Signaling.** **A**, 1)Endogenous agonist is released at locations where its effects are required. 2)Synthetic agonist is widely distributed and, thus can activate receptors throughout the body in locations where the signaling effects are not needed. 3)PAMs enhance the effects of endogenous agonists while still maintaining the spatial pattern of endogenous signaling (Burford, Traynor, and Alt 2015). **B**, A synthetic orthosteric agonist often produces a bigger effect than the endogenous agonist; however, its effects may decline with time as a result of receptor desensitization and/or downregulation. On the contrary, a PAM maintains the temporal pattern of endogenous signaling, and thus is less likely to cause receptor desensitization and/or downregulation (Ellaithy et al. 2015).



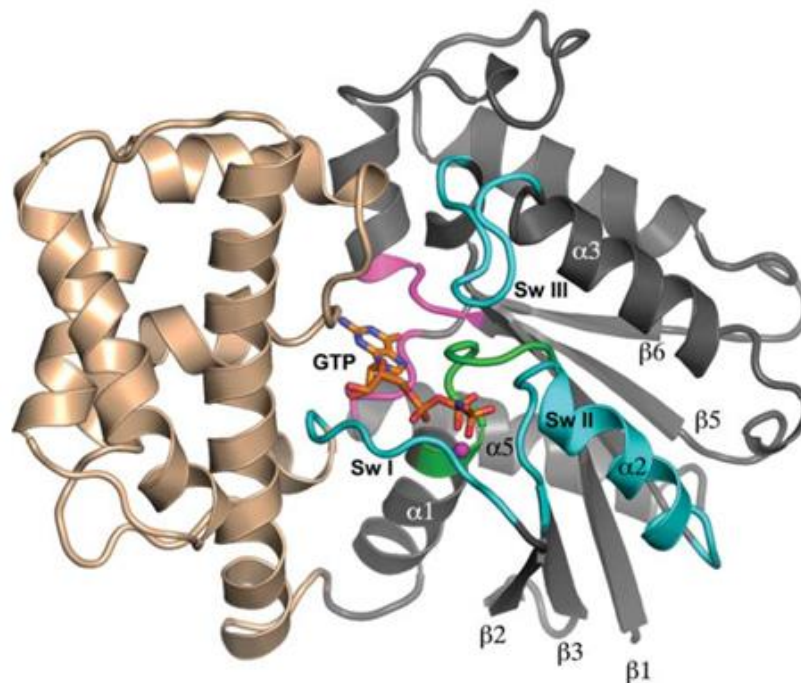
**Figure 1.7 Outward Rotation of TM6 in Three class A GPCRs Upon Activation.** Three class A GPCRs (beta-2 adrenergic, Muscarinic-2, and Mu-opioid receptors) captured in their crystallographic inactive and active conformations exhibit similar outward rotation of the intracellular end of TM6 (highlighted) upon activation, creating a G protein binding cavity on the cytoplasmic side (Latorraca, Venkatakrisnan, and Dror 2016).



**Figure 1.8** Disruption of the ionic lock in  $\beta$ 2AR upon activation. (Kobilka and Deupi 2007).

**A**

Nature Reviews | Molecular Cell Biology

**B**

**Alpha Helical Domain (AHD)    Ras Homology Domain (RHD)**

**Figure 1.9 Secondary and tertiary structures of G $\alpha$ .** A, Diagram of the secondary structure of G $\alpha$  with  $\alpha$ -helices represented as cylinders and  $\beta$ -sheets as arrows. Alpha

helical domain (AHD) is comprised of seven lettered  $\alpha$ -helices (purple). Linkers 1 and 2 (L1 and L2) connect the AHD with the Ras homology domain (RHD). The switch regions (orange) and receptor contact sites (pink) are highlighted. Regions involved in nucleotide binding are surrounded by red rectangles. Those are the TCAT motif in the  $\beta 6$ - $\alpha 5$  loop opposite the receptor-binding C terminus on the  $\alpha 5$  helix, and the phosphate-binding (P) loop connecting the  $\beta 1$  sheet to the  $\alpha 1$  helix (Oldham and Hamm 2008). B, AHD is colored light brown and RHD is colored gray. Switch regions are colored in cyan. The P-loop is colored green, and loop regions involved in recognition and binding of GDP are colored in pink (Sprang 2016).

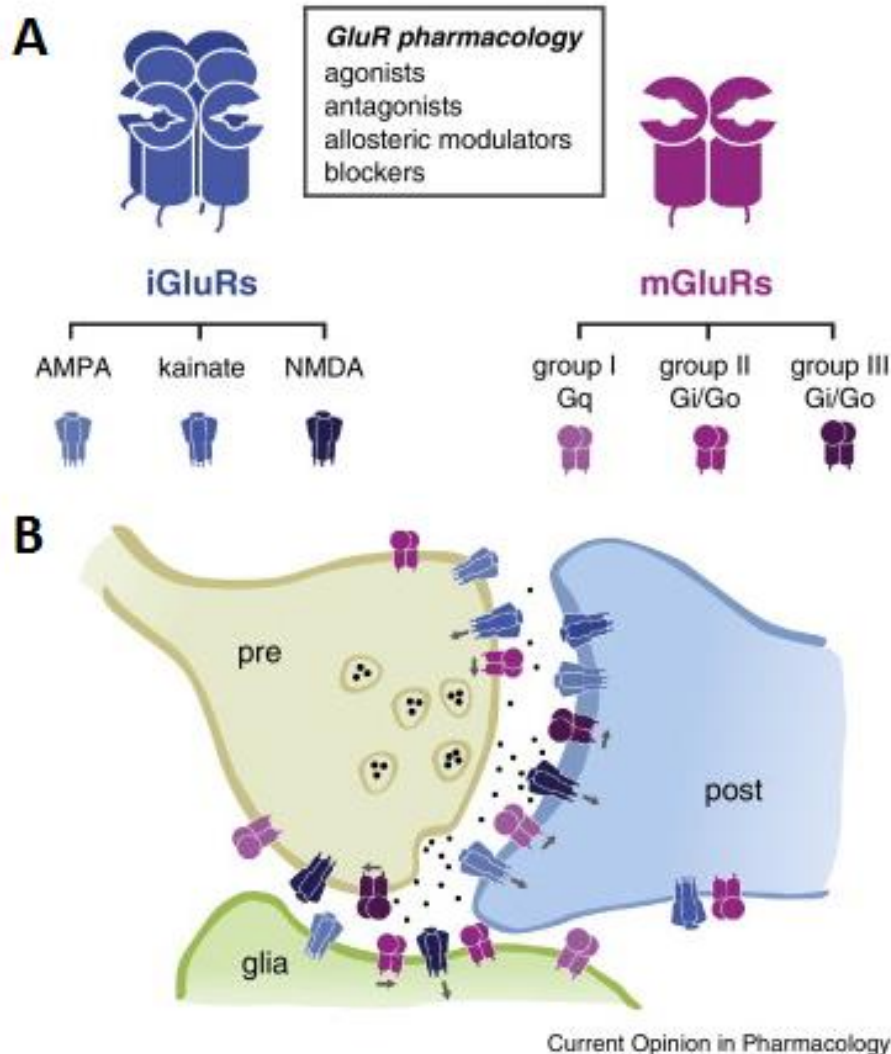


**Figure 1.10 Glutamate Receptor Categories.** **A**, Ionotropic glutamate receptors (iGluRs) are tetrameric ion channels (left) while metabotropic glutamate receptors (mGluRs) are dimeric GPCRs (right). Subunit heteromerization within different subfamilies further increases the functional diversity of iGluRs and mGluRs. **(b)** iGluRs and mGluRs are located both pre- and post-synaptically, where they are involved in different pathways of signal transmission, control of neurotransmitter release, and synaptic plasticity. In addition, mGluRs are located in extrasynaptic locations and glial cells, highlighting their regulatory functions (Reiner, Levitz, and Isacoff 2015).

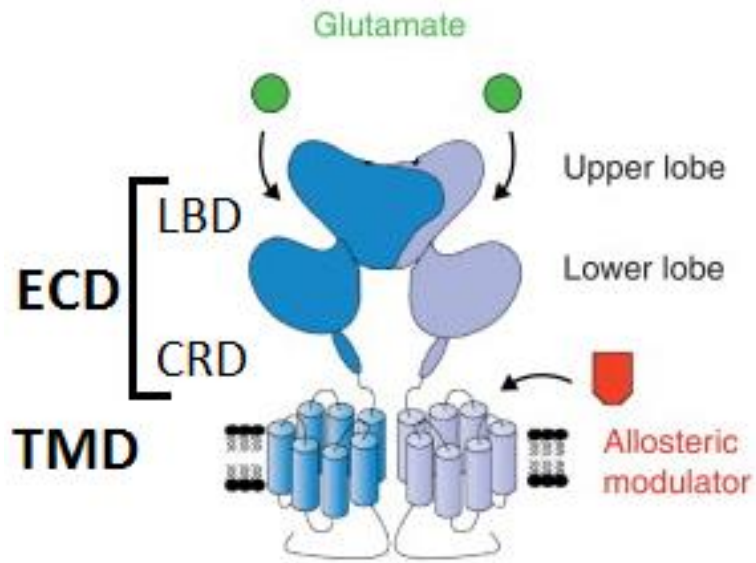


**Figure 1.11 Structural organization of mGluRs.** Cartoon illustrating a full-length mGluR dimer. The large extracellular domain (ECD) consists of a bilobed ligand-binding domain (LBD), which contains the orthosteric i.e. glutamate binding site, and a cysteine-rich domain (CRD, which connects the LBD to the transmembrane domain (TMD). The TMD in turn contains the binding site(s) for allosteric ligands (Rondard and Pin 2015).

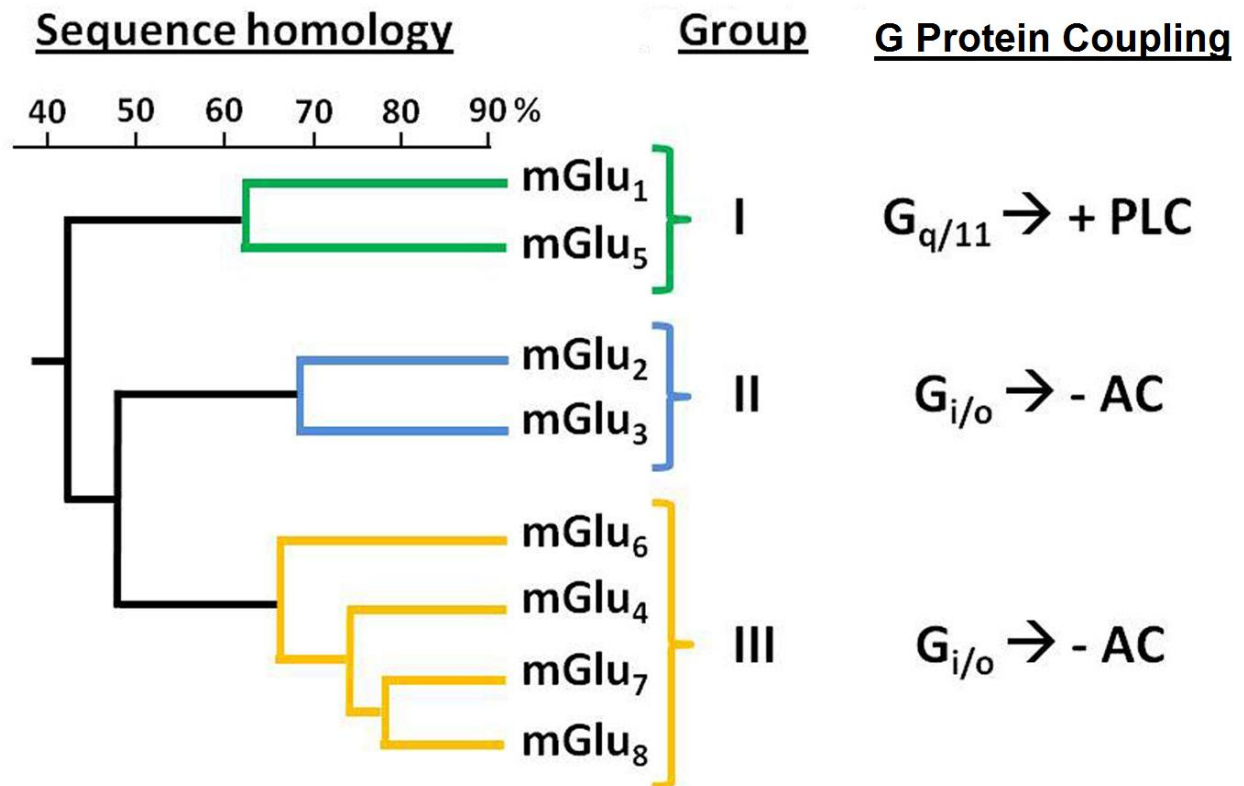


**Figure 1.12 Classification and sequence homology dendrogram of mGluRs.** (Muguruza, Meana, and Callado 2016).



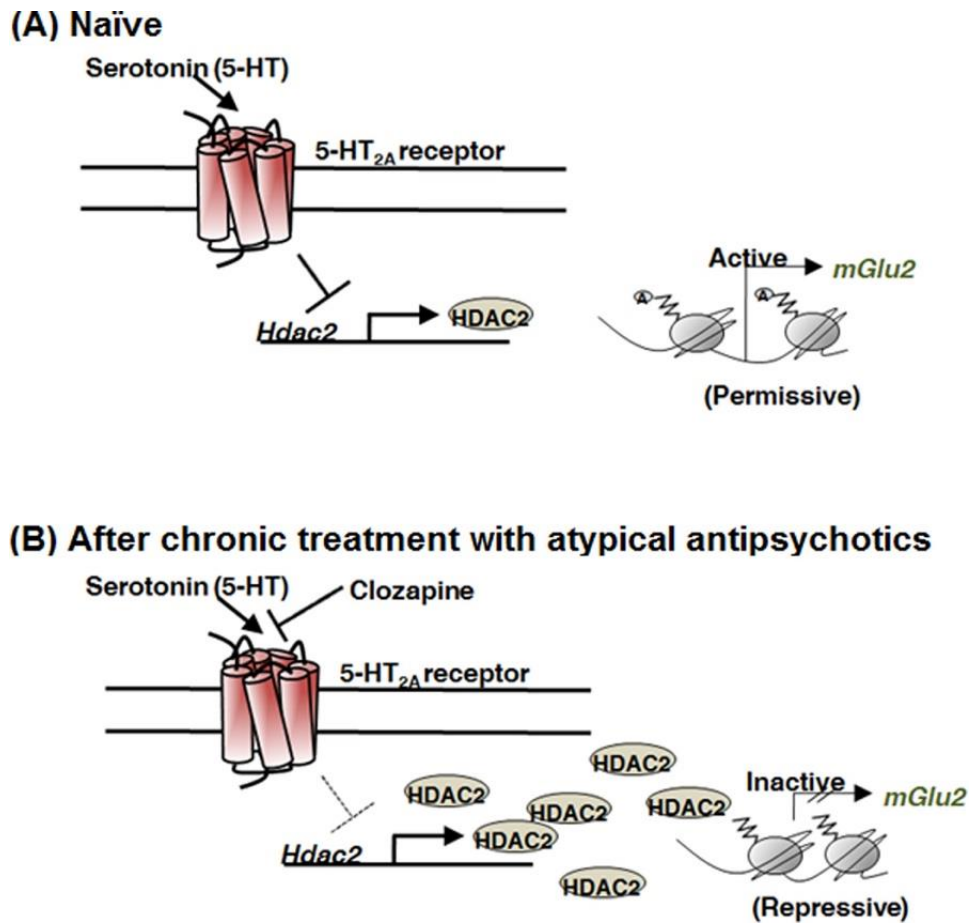


**Figure 1.14 Chronic atypical antipsychotic therapy downregulates mGlu<sub>2</sub>R.** Schematic model of the effect of chronic atypical antipsychotic treatment to the epigenetic status of the *mGlu<sub>2</sub>R* (*Grm2*) gene. **A**, Serotonin-induced activation of 5-HT<sub>2A</sub> receptor represses *HDAC2* gene promoter activity in mouse and in human frontal cortex. **B**, Atypical antipsychotic drugs, such as clozapine, reverse the 5-HT<sub>2A</sub> receptor-dependent repression of *HDAC2*, an effect that is associated with increased *HDAC2* promoter activity and repressive histone modifications at the *mGlu<sub>2</sub>R* promoter (Ellaithy et al. 2015).

## Chapter 2 MATERIALS AND METHODS

### 2.1 Computational Studies

All computational studies were contributed by Dr. Yu Xu.

#### ***2.1.1 Building an mGlu2R structural model***

A model of the mGlu2R truncated TM domain in the inactive state was constructed based on the mGlu5R crystal structure (PDB: 4OO9). The MODELLER program was used to generate an initial homology mGlu2R TM model. The Discovery Studio (DS) 3.5 was used to further refine the model structure via energy minimization.

#### ***2.1.2 Building mGlu2R-Gi protein complex model.***

Based on the  $\beta$ -2 adrenergic receptor-Gs protein complex (PDB:3SN6), a model of the mGlu2R-Gi protein complex was constructed. The truncated TMD mGlu2R model was used to replace the beta2 adrenergic receptor by Discovery Studio (DS) 3.5. The Gas domain was also replaced by the Gai crystal structure bound to GDP (PDB:4N0E). Previous research has shown that a Phe residue in ICL3 of mGluRs forms critical interactions with G alpha (Francesconi and Duvoisin 1998). Hence, we manually aligned the system to reduce the distance between mGlu2R F756 and Gai W258 by 3Å. The whole system was then refined by energy minimization.

#### ***2.1.3 Identifying allosteric modulators binding***

To accurately reproduce the geometry of the small ligand molecules, their structures were optimized by Gaussian 09. We then used AutoDock 4.2 to dock the PAM biphenyl-indanone A (BINA) and the NAM Ro 64-5229 to the truncated mGlu2R model. The docking box (size: 18.75×18.75×18.75Å) was set around the extracellular side of the

receptor TM domain. By empirical free energy scoring, we selected 100 top docking configurations for each allosteric modulator.

#### ***2.1.4 Molecular dynamics (MD) simulations and data analysis***

GROMACS v4.5.3 was used to conduct the simulation. The topology files of small molecules were calculated using the PRODRG web-server. The TMD structures of mGlu2R were immersed in an explicit phosphatidylcholine bilayer using the VMD package and solvated with SPC water molecules with 150 mM NaCl. Energy minimization and position-restrained MD runs were performed. The complexes were subjected to a 450 ns for truncated mGlu2R alone and 100ns for the truncated mGlu2R with Gai protein, runs that were deemed long enough to reach steady-state.

The SIMULAID program was used to analyze/cluster structures, and to calculate interaction networks, including hydrogen bonds, salt bridges and hydrophobic contacts.

## **2.2 Molecular Biology**

The following cDNAs used in the *Xenopus* oocyte heterologous expression system were subcloned into the pXOOM oocyte expression vector: human mGlu2R, all human mGlu2R mutants included in this study, pertussis toxin (PTX) subunit B, human Gai1 C351A (Gai1\*), and human Gai1\* mutants. The pGEMHE vector was used for human GIRK4-S143T (GIRK4\*). Linearized and purified (Pure Link PCR Purification kit, Thermo Fisher Scientific) plasmids were transcribed *in vitro* using an mMACHINE mMACHINE T7 Transcription kit (Thermo Fisher Scientific). Point mutations were introduced by Dr. Takeharu Kawano using standard Pfu-based mutagenesis techniques

according to the QuikChange protocol (Agilent Technologies), and verified by sequencing (Genewiz).

## 2.3 Drugs and Chemicals

L-glutamic acid was purchased from Sigma.

## 2.4 Oocyte Preparation and Injection

Oocytes from *Xenopus laevis* were surgically removed and subjected to collagenase treatment according to standard protocols (**Fig. 2.1**) (Logothetis et al. 1992; Hatcher-Solis et al. 2014). Oocytes were then washed and incubated at 18 °C in an OR2 solution with 2 mM Ca<sup>2+</sup> and Penicillin/ Streptomycin antibiotics. Oocytes at stage V or VI of maturation were selected for microinjection of 1 ng of each cRNA, suspended in equal volumes (50 nL) of DEPC treated water. Injected oocytes were incubated for approximately 48 hours at 18 °C to allow for optimal protein expression.

## 2.5 Two-Electrode Voltage-Clamp Recording and Analysis

Whole-cell currents were measured by conventional two-electrode voltage clamp (TEVC) with a GeneClamp 500 amplifier (Axon Instruments, Union City, CA). A high-potassium (HK) solution was used to superfuse cRNA-injected oocytes expressing the appropriate proteins to obtain a reversal potential for potassium ( $E_K$ ) of zero. The HK contained in millimolar (96 KCl, 1NaCl, 1 MgCl<sub>2</sub>, 5 KOH/HEPES, pH 7.4).

Inwardly rectifying potassium currents through GIRK4\* were obtained by clamping the cells at a voltage ramp from -80 to +80 mV. Basal GIRK4\* currents were defined as the difference between inward currents obtained at -80 mV in HK and those obtained in the presence of 3mM BaCl<sub>2</sub> in HK solution. Glutamate-induced currents were measured

respectively and normalized to basal current to compensate for size variability in oocytes.

## **2.6 Statistics**

All data were expressed as mean  $\pm$  standard error of the mean (SEM), unless otherwise indicated. Error bars in each figure represent SEM. For curve fitting, the following equation from Prism 6 software was used:  $Y = \text{Bottom} + (\text{Top} - \text{Bottom}) / (1 + 10^{((\text{LogEC50} - X) * \text{HillSlope}))}$ . Statistical significance between 2 groups was assessed using student's t-test. When multiple groups were analyzed, a one-way ANOVA followed by Tukey's posthoc test was used (Prism 6). For all statistical analyses, significance was determined using  $p < 0.05$ . Unless otherwise noted, all experiments were performed in at least two separate batches of oocytes.

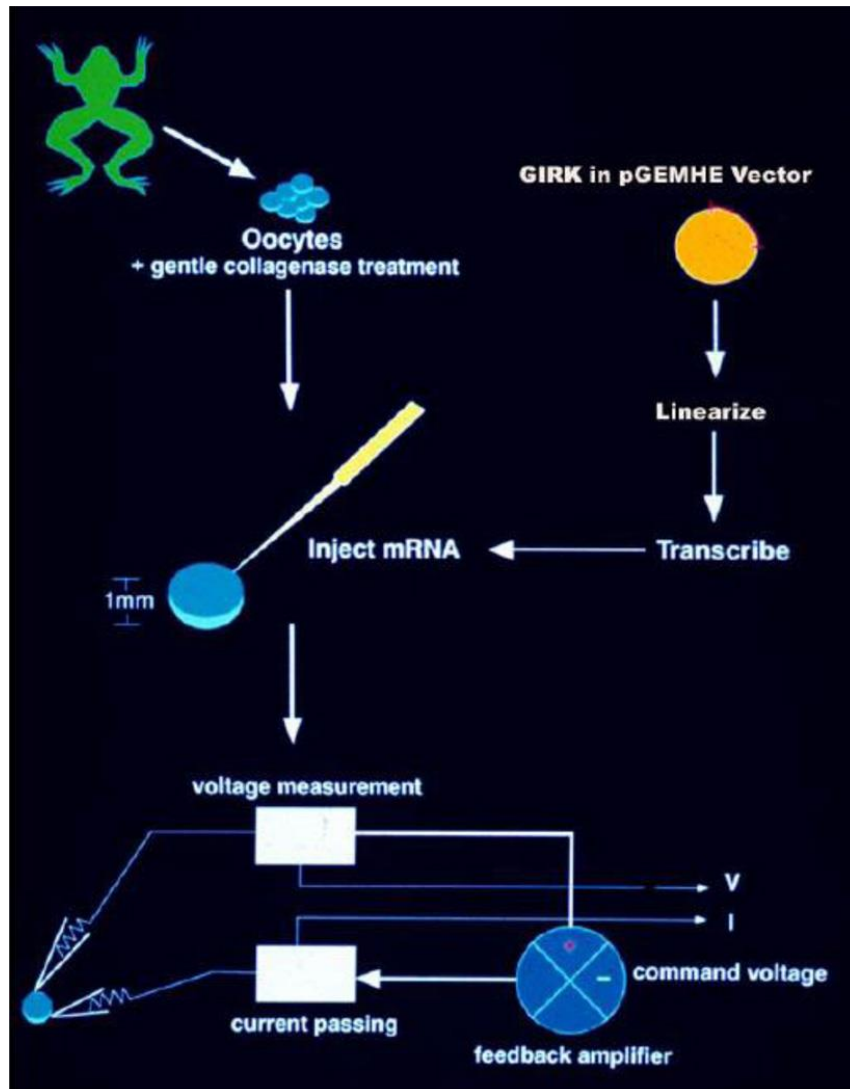


**Figure 2.1 The *Xenopus* oocyte heterologous expression system.** Oocytes are isolated from *Xenopus laevis* frogs through a small abdominal incision and are subjected to mild collagenase treatment to detach them from the surrounding follicular cells. *In vitro* transcribed cRNA from a *Xenopus* vector (e.g. pXOOM) coding for the ion channel of interest (e.g. GIRK) is injected into the isolated oocytes. Two-electrode voltage clamp (TEVC) is utilized to record whole-cell currents, typically 2-3 days post-injection (Hatcher-Solis et al. 2014).

# Chapter 3 MAPPING THE INTRAMOLECULAR ELECTROSTATIC INTERACTIONS INVOLVED IN mGlu2R ACTIVATION

## 3.1 Introduction

Most GPCRs crystallized to date belong to the class A GPCRs, with no single full-length class C structure yet available. Moreover, the available crystal structures of truncated mGluR TMDs are bound by negative allosteric modulators (NAMs), and thus, represent receptor inactive states (Doré et al. 2014; Wu et al. 2014). Apart from the TM3-TM6 ionic lock, very little data are available on the electrostatic interactions governing receptor activation.

In this study, we embarked on an effort to characterize key intramolecular electrostatic interactions underlying the transition from the inactive to the active mGlu2R state, using an approach combining computational modeling, charge reversal mutagenesis, and functional testing using electrophysiology. Our preliminary computational predictions strongly suggested the presence of the TM3-TM6 ionic lock between K653 and E758. In addition, our predictions also led us to hypothesize that, upon breakage of the TM3-TM6 ionic lock during activation, another intramolecular electrostatic interaction is established between K653 in TM3 and E754 in ICL3.

In order to test this hypothesis, we employed our well-established assay of GPCR Gi activity (**Fig. 3.1**) (Fribourg et al. 2011; Hatcher-Solis et al. 2014). *Xenopus laevis* oocytes can be utilized as a heterologous system to express mGlu<sub>2</sub>R, together with G-protein Inwardly Rectifier Potassium 4 star (GIRK4\*) channel which can serve as a reporter for receptor Gi signaling. Two days following cRNA injection, two-electrode voltage-clamp (TEVC) recordings can be performed using a voltage-ramp protocol from

-80 mV to +80 mV. Recordings are performed in High  $K^+$  aqueous solution that is perfused into the chamber and allows for administration of glutamate to study receptor activation. Glutamate-induced activation of mGlu2R results in liberation of the beta gamma subunits ( $G\beta\gamma$ ) from the G protein heterotrimer.  $G\beta\gamma$  can then bind to a cleft formed by cytosolic loops of adjacent subunits of GIRK4\*, potentiating its current (Mahajan et al. 2013), offering a quantitative readout for receptor function.

## 3.2 Results

### 3.2.1 *Creating a structural model of mGlu2R*

Using the available crystal structure of mGlu5R TMD (Doré et al. 2014), a monomeric truncated model of mGlu2R was created (**Fig. 3.1**). 450 nanoseconds molecular dynamics (MD) simulations were performed on both unliganded-receptor and receptor bound to either biphenyl-indanone A (BINA; an mGlu2R PAM) or Ro 64-5229 (an mGlu2R NAM) (**Fig. 3.2**). When the system was deemed stable after the first 200 nanoseconds, 500 snapshots were taken during the remainder of the MD run at a rate of 2 per ns. During this window, the frequency of formation of three prominent salt bridges that stood out were monitored: K653-E758 (TM3-TM6), K653-E754 (TM3-ICL3), and E758-K813 (TM6-TM7) (**Fig. 3.3**). A pattern of salt bridge formation was noticed, whereby the unliganded and NAM systems were comparable and in contrast with the PAM system. The two salt bridges K653-E758 and E758-K813 are stabilized in the receptor alone or 64-5229 (inactive) systems but broken in the BINA (active) system. It is worth mentioning that the first of those two pairs correspond to the TM3-TM6 ionic lock i.e. K3.50-E6.35. The opposite pattern is observed for the salt bridge K653-E754 which it is established upon activation (**Fig. 3.4**). To test these predictions, we resorted to our well established TEVC functional assay in oocytes to test the effects of mutations that reverse the charges of residues involved in these potential intramolecular electrostatic interactions.

### 3.2.2. *Single mutants of the TM3-TM6 salt bridge disrupt while the double mutant rescues receptor activation*

We tested the Gi responses of both the single mutants K653E and E758K as well as the double mutant K653E-E758K upon glutamate application. Glutamate concentration-response curves were compared between mutants and in relation to WT. It is worth noting here that in order to test the interactions of mGlu2R with different Gai mutants in later experiments (see next chapter), any endogenous Gai signaling had to be inhibited. To achieve that, experiments throughout this study, including the ones mentioned here, have been conducted in the presence of pertussis toxin subunit B (PTX), which inhibits Gi signaling (**Fig. 3.5**). Receptor was instead allowed to signal by co-expressing the PTX-insensitive Gai1 mutant C351A (or Gai1\*) (Rusinova, Mirshahi, and Logothetis 2007).

**Fig. 3.6** shows that Gi activity was completely abolished in the single mutant E758K and significantly decreased in K653E, but interestingly, partially rescued in the double mutant K653E-E758K. The efficacy of glutamate ( $E_{max}$ ) and its potency ( $pEC_{50}$ ) on different mutants are summarized in **Table 3.1**. Although the  $pEC_{50}$  in the double mutant was not different than in WT, the  $E_{max}$  remained significantly lower than that of WT. The partial, rather than complete, rescue of the  $E_{max}$  in the double mutant can be due to either reduction in surface expression level or disruption of other important interactions in the vicinity of the ionic lock.

### ***3.2.3. Single mutants of the TM6-TM7 salt bridge disrupt receptor activation but the double mutation fails to rescue receptor activation***

Although both residues in the TM6-TM7 salt bridge network showed decreased responses to glutamate upon charge substitution (partial reduction in K813E and

complete absence of responses in E758K), swapping the two charges across the pair via the double mutation failed to rescue Gi responses to glutamate (**Fig. 3.7**).

#### ***3.2.4. Role of TM3-ICL3 electrostatic interactions in receptor activation***

Our computational results predict that shifting from the receptor inactive state to the activated state changes the pattern of salt bridges formed in the TMD. Namely, the TM3-TM6 (K653E-E758K), that predominates in the inactive state, is broken and another salt bridge (TM3-ICL3) stabilizes the active state (**Fig. 3.3**). Since the residue K653 (K3.50) is involved in both salt bridges, we predicted that the major change occurring during activation is a relative movement of TM3 and ICL3 towards each other, and of TM3 and TM6 away from each other.

To test this hypothesis, we characterized the ICL3 mutant E754K that displayed an interesting phenotype; a left-ward shift in its glutamate concentration response curve compared to WT (**Fig. 3.8**). Although the E<sub>max</sub> was reduced, the significantly enhanced pEC<sub>50</sub> (**Table 3.2**) strongly suggests a role for ICL3 in receptor activation. Interestingly, the double mutant K653E-E754K rescued the Gi activation compared to K653E with a pEC<sub>50</sub> not significantly different from WT. Reestablishing the entire TM6-TM3-ICL3 salt bridge network had a similar effect. All E754K mutants (single, double, and triple) had a lower E<sub>max</sub> than glutamate despite the pEC<sub>50</sub> being either enhanced or comparable to WT. This could be due to a reduction in surface expression levels.

### 3.3. Discussion

Our interpretations of the mutation-associated shifts in the agonist concentration response curves assume changes in receptor basal activity (activity in the absence of agonist given that the ionic lock mutants are expected to destabilize an inactive receptor conformation). This could explain how the E758K mutant did not display any response to glutamate, possibly due to a high constitutive activity that does not leave a measurable range for agonist-induced current activation. On the other end of the spectrum, the ICL3 mutant E754K was associated with the highest potency for glutamate, indicating the widest range of receptor activation likely because the mutant stabilizes an active receptor conformation.

Based on these interpretations, it is fair to say that a limitation of our experiments is that they do not test the effects of the mutations on the basal activity of the receptor. A main hurdle is the large variability in basal currents of the reporter channel in TEVC. To circumvent this challenge, we have considered FRET-based approaches of assaying receptor constitutive activity (Levitz et al. 2016). We anticipate that the TM6 mutant E758K would display the highest basal activity, whereas the ICL3 mutant E754K may show no change or lower basal activity compared to control.

Another caveat is that the oocyte results do not exclude differences in surface expression to contribute to the functional changes we see in mutants. However, the changes in glutamate potency as well as the rescue effects in the double mutants suggest changes in function rather than just in expression.

Previous evidence implicated TM3 in stabilizing the receptor in the inactive state. Our work expands on the critical role of TM3 to also include a role in stabilizing the activated

state, by extending the interaction with the intracellular end of TM6 to the ICL3. These two patterns of salt bridge formation correspond to two functional states of the receptor; inactive and active.

Although the TM3-TM6 ionic lock interaction has been revealed in multiple GPCR structures (Vogel et al. 2008; Palczewski et al. 2000; Wang et al. 2018; Rasmussen et al. 2007), to our knowledge, no previous active state GPCR structures have captured the relative movement of TM3 and ICL3 towards each other with the establishment of a new salt bridge pattern for TM3 in the active state replacing the inactive state-associated ionic lock with TM6. A potential reason to explain missing this important interaction is the fact that the high flexibility and length of ICL3 preclude the formation of ordered protein crystals. Thus, in most currently available active structures ICL3 has been substituted by a fusion partner (Rasmussen et al. 2011; Huang, Manglik, et al. 2015; Kruse et al. 2013).

Other studies have also suggested a key role for ICL3 in interaction with G-protein (Francesconi and Duvoisin 1998). Our study reveals a role in GPCR activation as well. We discuss in the next chapter how same negative charge in ICL3 (E754) does not only engage in electrostatic interactions with the receptor TMD, but also with a positive charge at the opposing interface of G $\alpha$  subunit.

In summary, our results indicate that the prevailing salt bridge interaction in the inactive state is the one between TM3 and TM6, consistent with many previous studies. During activation, TM3 breaks its interaction with TM6 and engages in a different salt bridge pattern with ICL3, a region that likely also plays a role in subsequent G-protein activation and is key to understanding the structural basis of interaction between

GPCRs and intracellular partners. **Figure 3.9** illustrates conformational changes upon activation by comparing mGlu2R in unbound, Ro 64-5229-, and BINA-bound states. It can be seen that most of the changes between the simulated inactive and active states of mGlu2R appear in the intracellular loops, ICL3 and ICL2. Studying surface expression as well as basal activity of the aforementioned mutants remains of paramount importance to further test our interpretations.

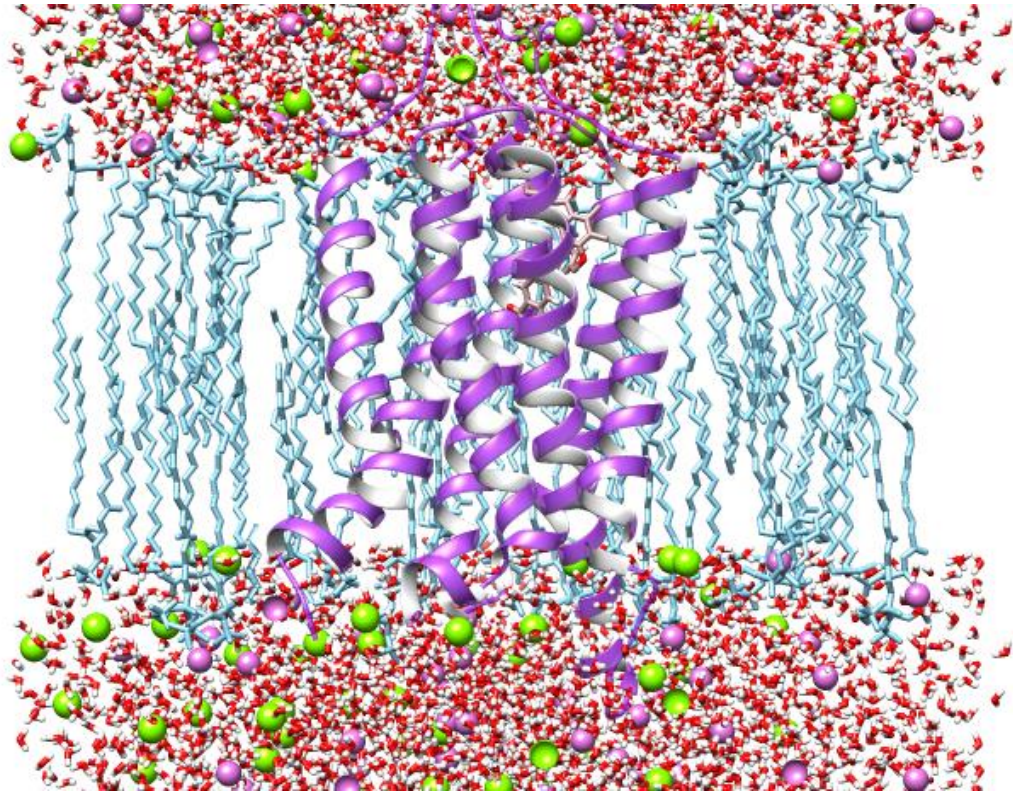


**Figure 3.1 Structural model of mGlu2R TMD.** The initial structural model of mGlu2R in truncated form during MD simulations. mGlu2R (purple ribbons) embedded in lipids (blue wires), with water molecules (red) and Na<sup>+</sup> ions (green spheres).

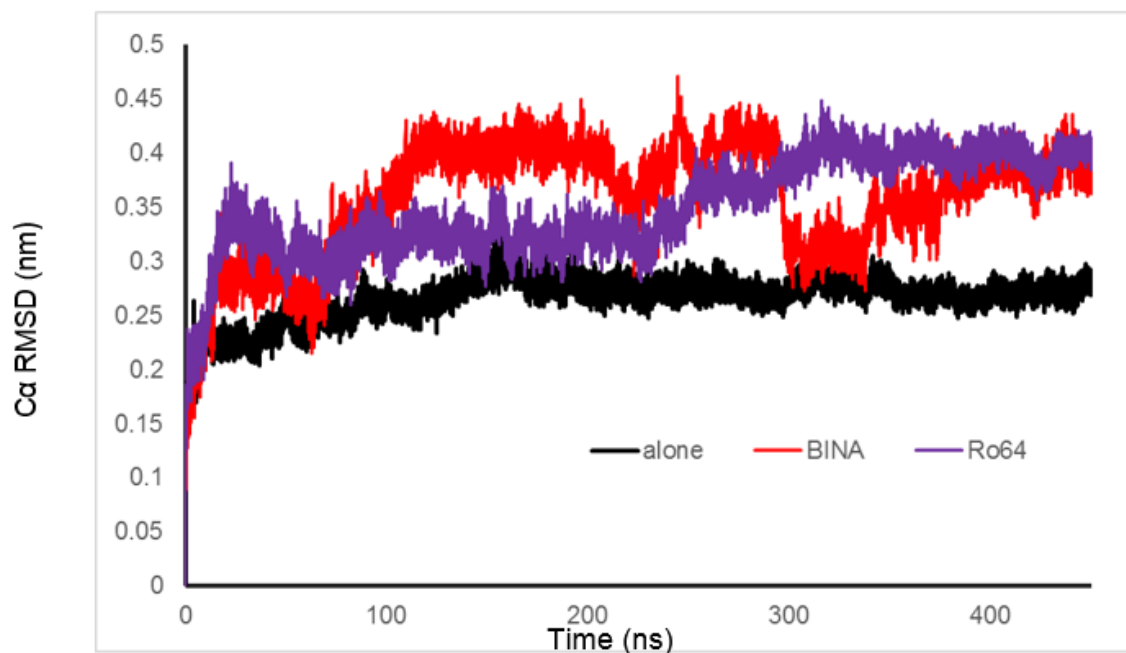


**Figure 3.2 Monitoring root-mean-square-deviation (RMSD) of the alpha carbons over a 450 nanoseconds MD run.** RMSD of  $\text{C}\alpha$  atoms during MD simulations for the truncated mGlu2R alone, with BINA, and with Ro 64-5229 binding (gray, red, and purple traces, respectively).

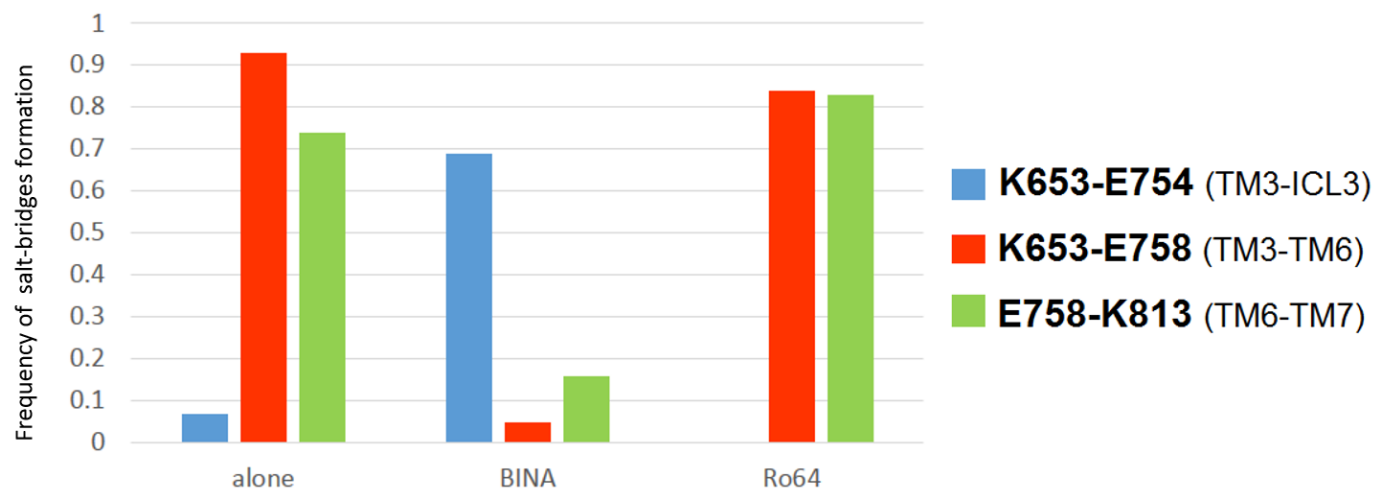


**Figure 3.3 Comparison of the patterns of salt bridges formed between 200 and 450 nanoseconds of MD runs.** Compared to the alone and the Ro 64-5229 systems, BINA causes breakage K653-E758 and E758-K813 salt bridges, and instead, an increased interaction between K653 and E754.

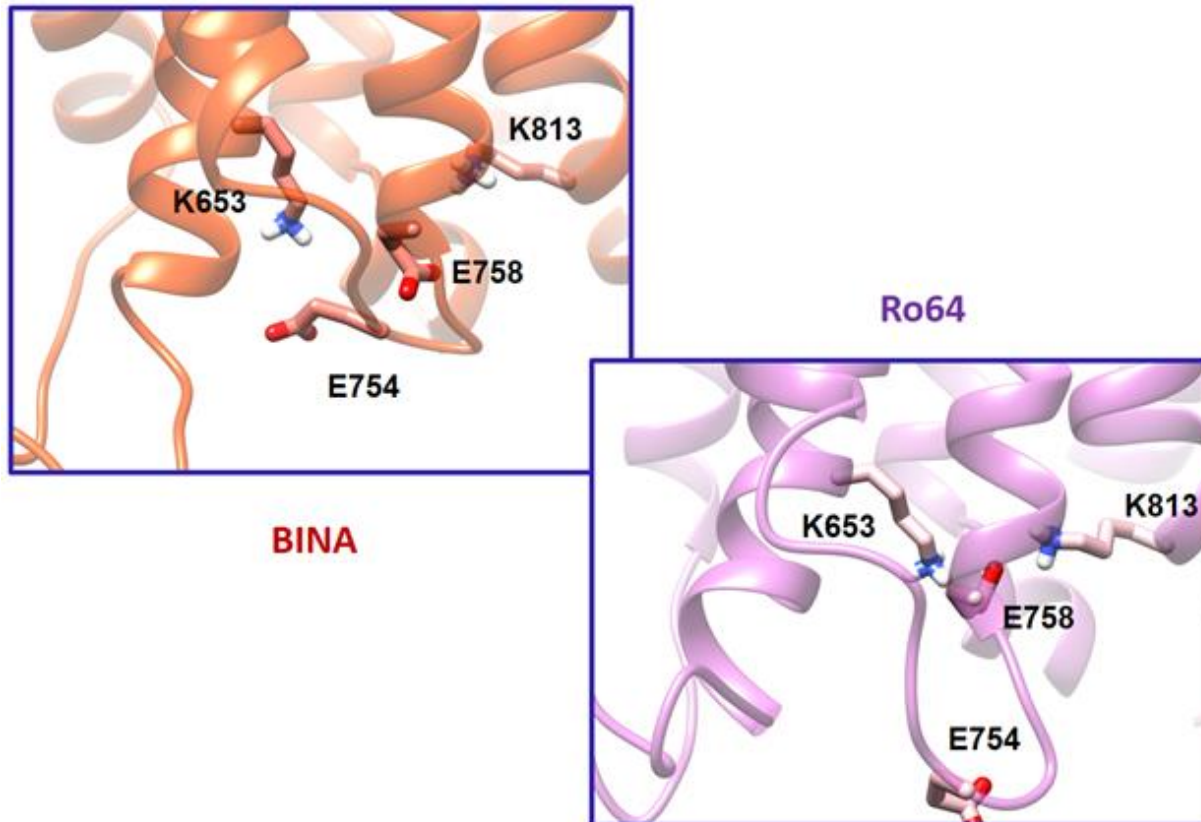


**Figure 3.4 Zoomed-in views of the intracellular side of the receptor models in the active and inactive states.** Snapshots of truncated mGlu2R in the presence of BINA (upper) or Ro 64-5229 (lower) show the competition between E758 (in TM6) and E754 (in ICL3) to interact with K653 (in TM3). Binding of BINA disrupts the ionic lock, and increase the interaction between K653 and E754.

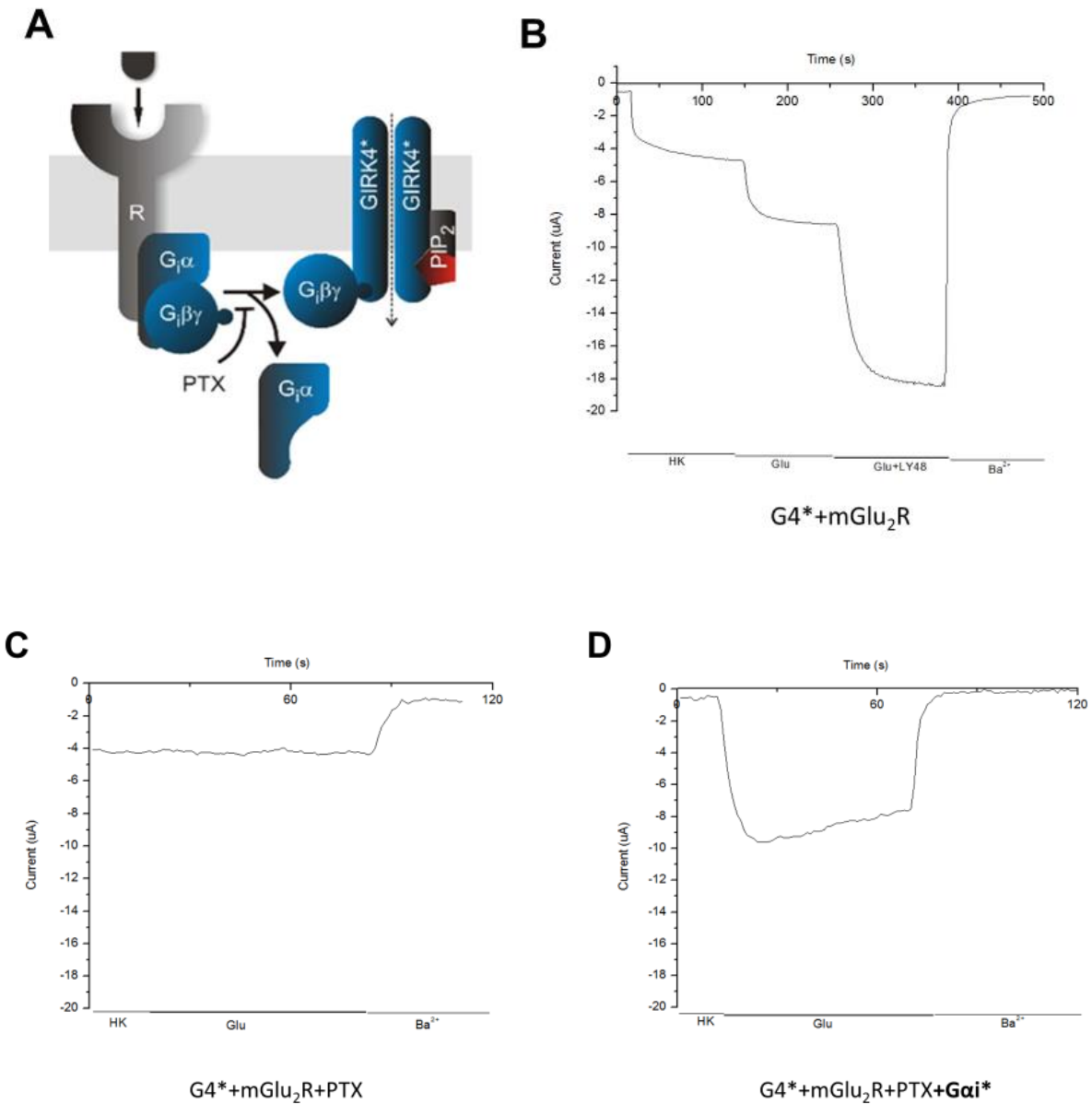


**Figure 3.5 mGlu2R functional assay in *Xenopus oocytes*.** A, Simple schematic of mGlu2R-induced Gi-dependent GIRK4\* activation assay (Fribourg et al. 2011). B, A sample recording from an oocyte injected with G4\*+mGlu2R RNA. C, A sample recording from an oocyte injected with G4\*+mGlu2R+PTX-S1 RNA. D, A sample recording from an oocyte injected with G4\*+mGlu2R+PTX+Gai1 C351A (Gai\*) RNA.

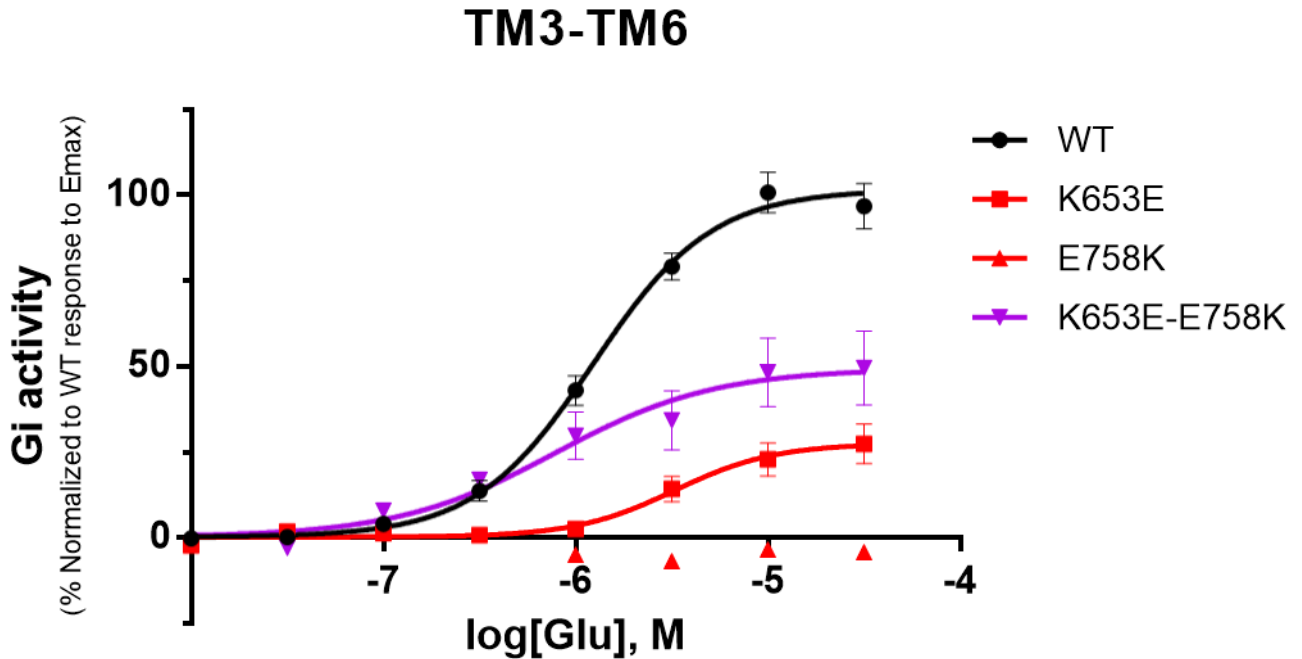


**Figure 3.6 Effect of charge reversal mutations in the K653-E758 ionic lock between TM3 and TM6.** No glutamate response was detected in the mutant E758K, and the mutant K653E exhibited a marked reduction in glutamate effect as evident by both a rightward and downward shift in glutamate concentration response curve. The effect was partially rescued when the ionic lock interaction was reestablished in the double mutant K653E-E758K ( $n \geq 6$  per condition, experiments were performed in  $\geq 2$  batches of oocytes except for E758K where  $n=4$  from one batch).

**Table 3.1. Summary of glutamate effects on the TM3-TM6 ionic lock mutants.**

|  | <b>pEC50</b>  | <b>E<sub>max</sub></b> |
|--|---------------|------------------------|
| <b>WT</b>  | 5.91 ± 0.049  | 101.50 ± 3.759         |
| <b>K653E</b>   | 5.48 ± 0.156* | 27.32 ± 4.011*         |
| <b>E758K</b>   | ND            | ND                     |
| <b>K653E-E758K</b>   | 6.10 ± 0.288† | 49.26 ± 8.669*†        |
| N.D. no response detected<br>* p-value < 0.05 when compared to WT<br>† p-value < 0.05 when compared to K653E |               |                        |

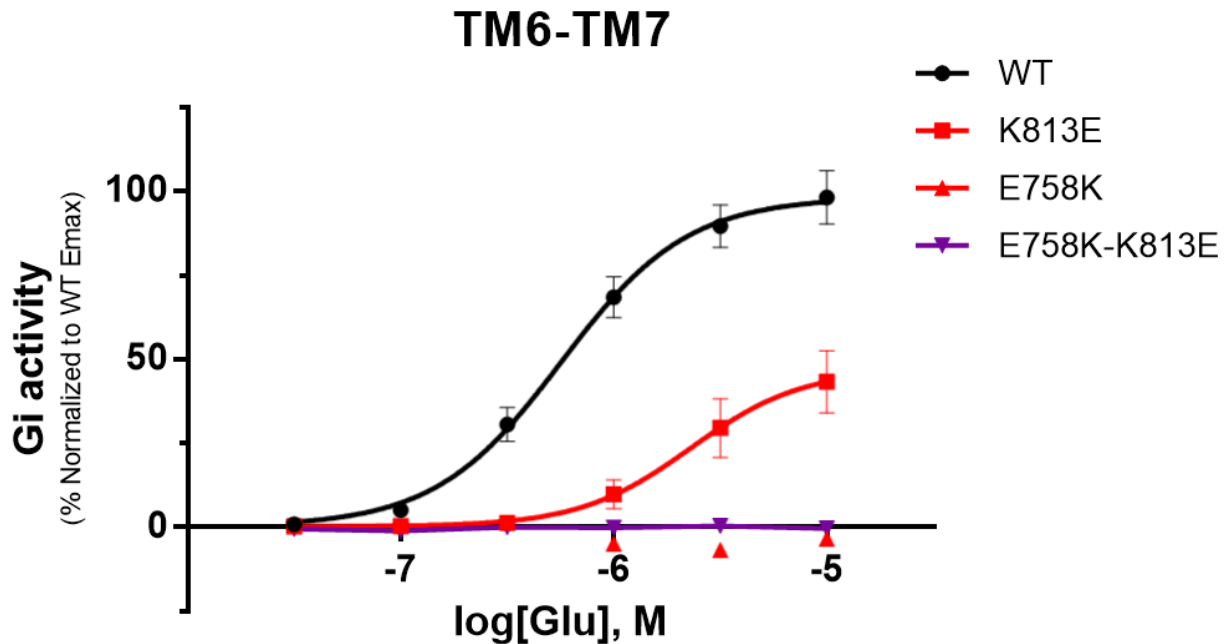


**Figure 3.7 Effect of charge reversal mutations in the E758-K813 salt bridge between TM6 and TM7.** The TM7 mutant K813E showed a rightward and downward in response to glutamate. On the other hand, no glutamate response was detected in the mutant E758K. The double mutant also did not show any response to glutamate ( $n \geq 6$  per condition, experiments were performed in  $\geq 2$  batches of oocytes except for E758K where  $n=4$  from one batch).

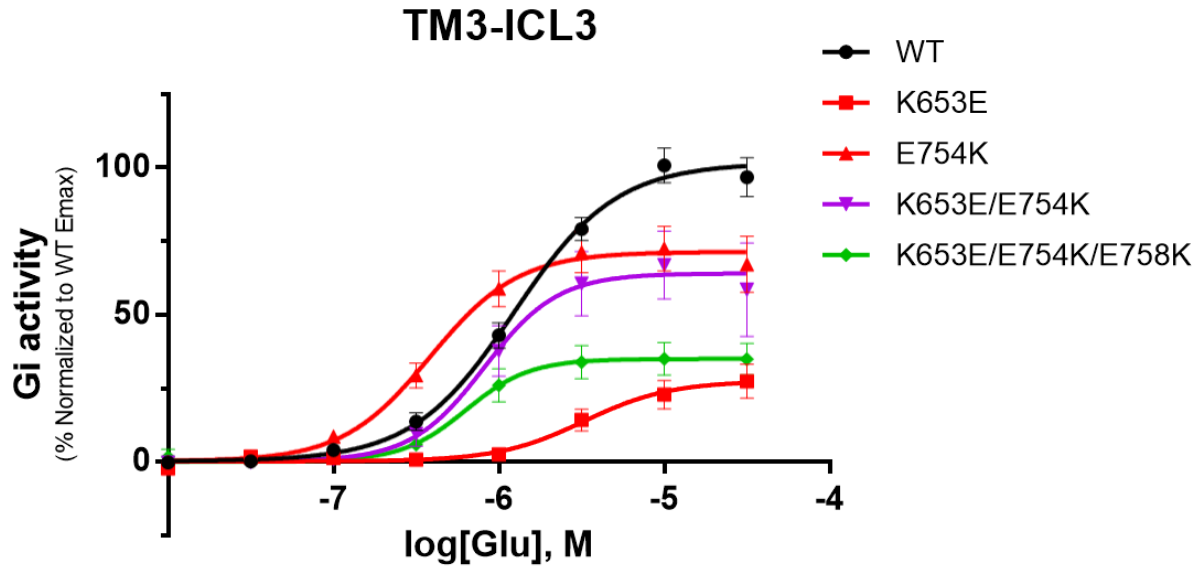


**Figure 3.8 Effect of charge reversal mutations in the TM3-ICL3 salt bridge.** The ICL3 mutant E754K displays an enhanced response to glutamate. The double mutant K653E-E754K rescues the  $G_i$  responses compared to the single mutant K653E and shows a comparable potency to that of WT. The triple mutant K653E-E754K-E758K shows similar effects to the double mutant, despite a lower  $E_{max}$  ( $n \geq 6$  per condition, experiments were performed in  $\geq 2$  batches of oocytes)

**Table 3.2. Summary of glutamate effects on the TM3-ICL3 salt bridge mutants.**

|   | <b>pEC50</b>   | <b>Emax</b>     |
|---|----------------|-----------------|
| <b>WT</b>   | 5.91 ± 0.049   | 101.50 ± 3.759  |
| <b>K653E</b>  | 5.48 ± 0.156*  | 27.32 ± 4.011*  |
| <b>E754K</b>  | 6.41 ± 0.0784* | 71.25 ± 3.645*  |
| <b>K653E-E754K</b>  | 6.09 ± 0.112†  | 63.93 ± 5.738*† |
| <b>K653E-E754K-E758K</b>  | 6.20 ± 0.098†  | 34.84 ± 2.424*  |
| * p-value < 0.05 when compared to WT<br>† p-value < 0.05 when compared to K653E |                |                 |

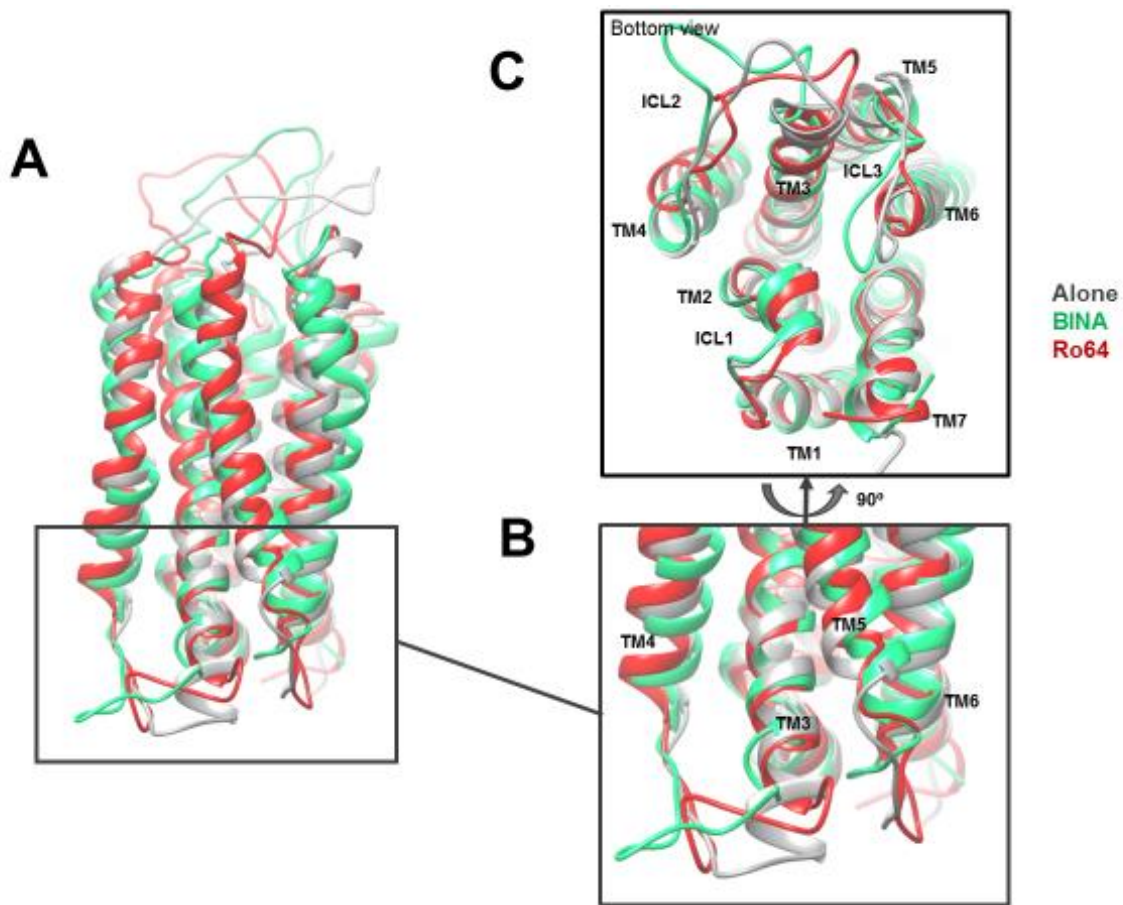


**Figure 3.9 Conformational changes of mGlu2R upon activation.** A, Superimposed truncated mGlu2R structural models in unbound (gray), NAM-bound (red), and PAM-bound (green) states. B, Zoomed in view of the intracellular end of TMD, ICL2, and ICL3. The most prominent changes are separation of TM3 and TM6, Outward movement of the intracellular end of TM6, and upward movement of ICL3 towards TM3. C, Same structures, viewed from the intracellular side.

# Chapter 4 MAPPING THE INTERMOLECULAR ELECTROSTATIC INTERACTIONS BETWEEN mGlu2R AND THE G $\alpha_i$ SUBUNIT

## 4.1 Introduction

Activation of a GPCR involves conformational changes that trigger interaction with a specific G- protein. Despite the wealth of structural information from GPCR studies, a major unsolved question is the structural basis by which a receptor catalyzes nucleotide exchange in G proteins. After we revealed a critical role for certain electrostatic interactions in receptor activation, we asked the question: are there key electrostatic interactions involved in receptor-induced G-protein activation?

The electrostatic properties of the G $\alpha$  subunits, which in some cases differ greatly not only between families but also between subfamilies suggest that electrostatic complementarity may be an important factor in receptor-G-protein coupling selectivity and/or receptor-mediated G protein activation (Baltoumas, Theodoropoulou, and Hamodrakas 2013).

In this chapter, we test for critical electrostatic interactions involved in receptor-mediated G $\alpha_i$  activation and, by revealing key intermolecular electrostatic interactions, add to the previous literature suggesting important roles for intracellular loops 2 and 3 (ICL2 and ICL3) in receptor interactions with G-protein (Ulloa-Aguirre et al. 2007; Rasmussen et al. 2011). To test computational predictions, we again employed charge reversal mutagenesis and TEVC in *Xenopus laevis* oocytes. Importantly, all G $\alpha_i$  mutations tested were introduced in the background of the PTX-insensitive G $\alpha_i$  mutant (G $\alpha_i$ 1 C351A) (Rusinova, Mirshahi, and Logothetis 2007).

## 4.2 Results

### *4.2.1 Structural modeling of mGlu2R with G $\alpha$ i*

Based on the  $\beta$ -2 adrenergic receptor—Gs protein complex (PDB:3SN6), we built the mGlu2R—Gi protein complex (**Fig. 4.1**). The truncated mGlu2R model we previously built was used to replace the  $\beta$ -2 adrenergic receptor. The G $\alpha$ s domain was also replaced by the G $\alpha$ i crystal structure with GDP bound (PDB:4N0E) (Thaker et al. 2014). 100 nanoseconds molecular dynamics (MD) simulations were performed on both unliganded-receptor and receptor bound to either BINA or Ro 64-5229. Predicted intermolecular electrostatic interactions between receptor and G-protein are summarized in **Fig. 4.2**. To test these predictions experimentally, we resorted again to TEVC experiments.

### *4.2.2 mGlu2R residues critical for the interaction with G $\alpha$ tend to be located in or adjacent to intracellular loops 2 and 3*

Our computational studies suggested that six charged residues towards the cytoplasmic side of mGlu2R form key salt bridges with G $\alpha$ . Three of those residues are located in regions that are thought to play key roles in interaction with the receptor; R670 and R672 in ICL2, and E754 in ICL3. The other 3 residues are located in TMD very close to intracellular loops; K653 and R656 in TM3, and K760 in TM6.

We proceeded to screen the effects of mutating each of these residues, apart from mutations of K653 and E754 which have already been characterized in chapter 3. **Fig. 4.3** demonstrates that all four mutants tested showed attenuated responses to glutamate-induced activation compared to WT. In order to determine which of these six

residues play critical roles in interactions with G-protein, we proceeded to test the G $\alpha$  residues predicted to form salt bridges with the aforementioned mGlu2R residues.

#### ***4.2.3 G $\alpha$ residues that seem critical for the interaction with the receptor tend to be facing intracellular loops 2 and 3 of the receptor***

According to the model, eight residues in the G $\alpha$  Ras homology domain (AHD) are engaging in intermolecular salt bridges with the previously tested six residues of mGlu2R. After screening all eight mutants (**Fig. 4.5**), three behaved significantly different from control Gai\* in response to glutamate activation. Notably, these residues are located in close proximity to the two residues of mGlu2R that the model predicts to engage in the largest number of intermolecular electrostatic interactions (**Fig. 4.6**).

Namely, Gai residue K317 is interacting with E754 in ICL3 of mGlu2R — a residue that we have shown to be key in receptor activation. Furthermore, Gai residues E33 and D193 are both competing to interact with residue R670 in ICL2 of mGlu2R.

#### ***4.2.4 mGlu2R third intracellular loop interaction with G $\alpha$ protein***

We started by mGlu2R residue E754 in ICL3, which we have shown in chapter 3 to be critical in receptor activation through its intramolecular electrostatic interactions, mainly with K653 in TM3. Our computational results predicted an interaction of mGlu2R E754 with K317 in the  $\alpha$ 4- $\beta$ 6 linker of G $\alpha$ ; an interaction that is stabilized in the active state. Thus, we wanted to test glutamate responses of cells co-expressing these two mutants together (**Fig. 4.7**).

Gai\* K317E mutant has an attenuated response to glutamate as evident by the E<sub>max</sub> being significantly lower than in control Gai\* (**Table 4.1**). Although the potency reduction was not statistically significant, co-expressing the mGlu2R mutant E754K significantly

increased the potency. Taken together, computational and experimental results support a critical role of ICL3, mediated by its negatively charged residue 754, in receptor-induced G-protein activation.

#### ***4.2.5 mGlu2R second intracellular loop interaction with G $\alpha$ protein***

According to the computational predictions, interaction of E33 with receptor ICL2 is stabilized in the active state, whereas that of D193 is stabilized in the inactive state (**Fig. 4.3A**). Experimental results supported this hypothesis (**Fig. 4.3B**) since mutating E33 interfered with mGlu2R-induced G protein activation, presumably since the mutation strengthened G $\alpha$  D193 interaction with mGlu2R R670. Mutating D193, on the other hand, enhanced activation indicating a stronger R670—E33 intermolecular active state interaction.

Residue E33 is located in the N-terminal helix- $\beta$ 1 ( $\alpha$ N- $\beta$ 1) linker while D193 is located in the  $\beta$ 2- $\beta$ 3 linker of G $\alpha$  (**Fig. 4.4**). Both residues are located in close proximity to each other and to mGlu2R R670 in ICL2.

We first wanted to answer the question if mutating the two residues, E33 and D193, simultaneously destabilizes the two salt bridges with ICL2, and thus ultimately restore the control level of receptor—G-protein signaling (**Fig. 4.8A**). Although the potency of glutamate did not significantly differ among all four G alphas, the efficacy was different with E33R showing significantly reduced responses, and the double mutant behaving in a manner comparable to control (**Fig. 4.8B**) (**Table 4.2**).

Next, we tested whether reestablishing the overall R670 (ICL2)—G $\alpha$  salt bridge network can restore receptor-mediated G-protein activation to WT levels. **Fig. 4.9** and **Table 4.3**

illustrate that when the 3 mutations are co-present, glutamate responses are mostly similar WT levels, and different from R760D(E).

To zoom in on the intermolecular electrostatic interaction between R670 and D193, we tested the effects of co-mutating both proteins at these residues. **Fig. 4.10 and Table 4.4** show that, although the potency of glutamate in the mGlu2R mutant was significantly different from control, the combined mutants did not. Moreover, the combined mutants were associated with a significantly higher  $E_{max}$  than when only mGlu2R was mutated.

Finally, we focused on the other side of the receptor ICL2— $G\alpha$  salt bridge network i.e. the electrostatic interaction between R670 and E33. **Fig. 4.11 and Table 4.5** show that, in contrary to the case with D193, co-mutating both proteins at these residues failed to rescue the responses to glutamate.

### 4.3 Discussion

In this chapter, we tested our computational predictions regarding intermolecular electrostatic interactions between mGlu2R and G $\alpha$ i. Effects of all mutations in predicted mGlu2R residues supported the model since they attenuated glutamate responses compared to in WT. Intracellular loop 3 residue E754, which we have shown in chapter 3 to be critical for agonist-induced receptor activation, seems to also be key for receptor-mediated G $\alpha$  protein activation, thus functioning as a major hub for mGlu2R intramolecular as well as intermolecular electrostatic interactions with G-protein.

Mutations in G $\alpha$ i, on the other hand, did not all alter glutamate-induced activation. This is not surprising considering that the model predicts each of the tested mGlu2R residues to engage in salt bridges with multiple G $\alpha$  residues, but those of G $\alpha$  mostly form single intermolecular salt bridges the mutation of which might not be enough to alter glutamate activation. This may also explain why single residue mutations in the G $\alpha$  C-terminus (D341R, K349E, D350K, and D350R), a region known to be physically engaged by the activated receptor, did not alter glutamate activation.

The two G $\alpha$  residues that proved to engage in key intermolecular electrostatic interactions associated with activation, E33 and K317, are located in G $\alpha$  regions known to contact the receptor;  $\alpha$ N- $\beta$ 1 loop and  $\alpha$ 4- $\beta$ 6 linker, respectively (**Fig. 4.4**).

Concomitant ICL2- and ICL3-mediated conformational changes in these linkers are likely transmitted to  $\beta$ 1- $\alpha$ 1 and  $\beta$ 6- $\alpha$ 5 loops, which coordinate the nucleotide, thus cooperatively facilitating nucleotide release.

Although previous research has shown the involvement of  $\alpha$ N- $\beta$ 1 and  $\alpha$ 2- $\alpha$ 3 linkers, which contain E33 and D193 respectively, in receptor mediated-activation of G $\alpha$

(Huang, Sun, et al. 2015; Rasmussen et al. 2011), our finding that the competition between negatively charged residues within these 2 linkers for the positively charged ICL2 to stabilize opposite states is novel. Destabilizing one interaction favors the other, and simultaneously destabilizing both restores a balanced signaling. Although charge swapping between ICL2 and D193 supports this idea, the analogous experiment for E33 failed to support this notion. Reasons that might underlie the lack of rescue for E33 could be alterations in expression levels or cumulative effects of mutations that could also be disrupting several other interactions that were not addressed.

In summary, our results add to the results from chapter 3 and indicate a key role for electrostatic interactions, especially those involving ICL2 and ICL3, in mGlu2R-mediated conformational changes in G $\alpha$  required for activation.

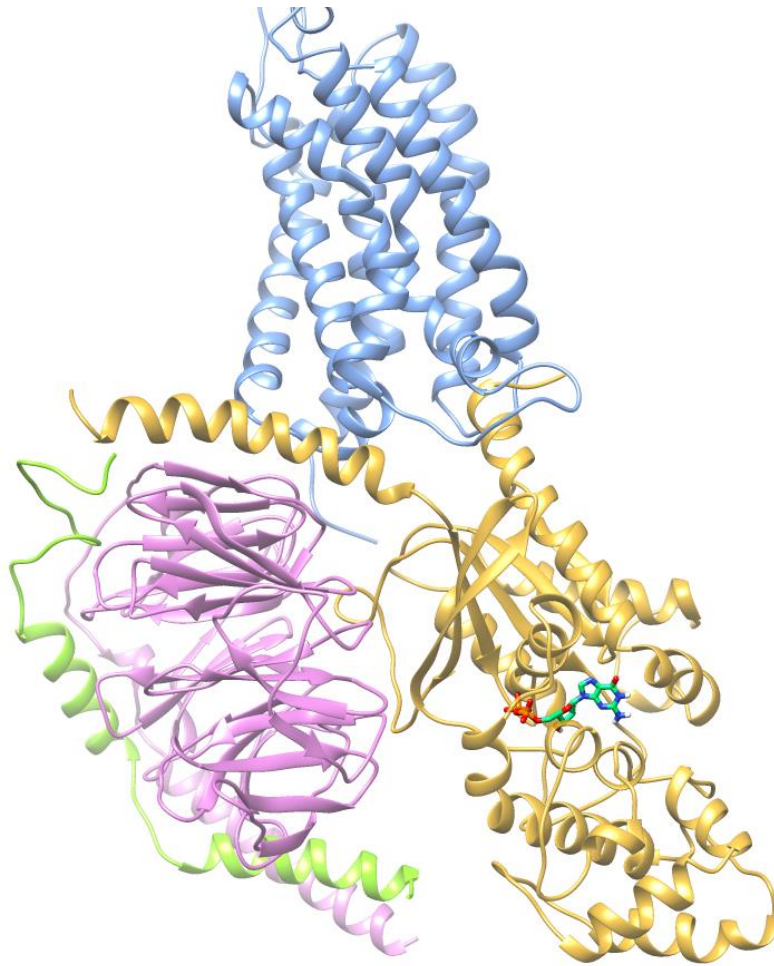


**Figure 4.1 Structural model of truncated mGlu2R — G-protein complex.** Truncated mGlu2R (blue ribbons), GDP-bound G $\alpha$  (yellow), G $\beta$  (purple), and G $\gamma$  (green).

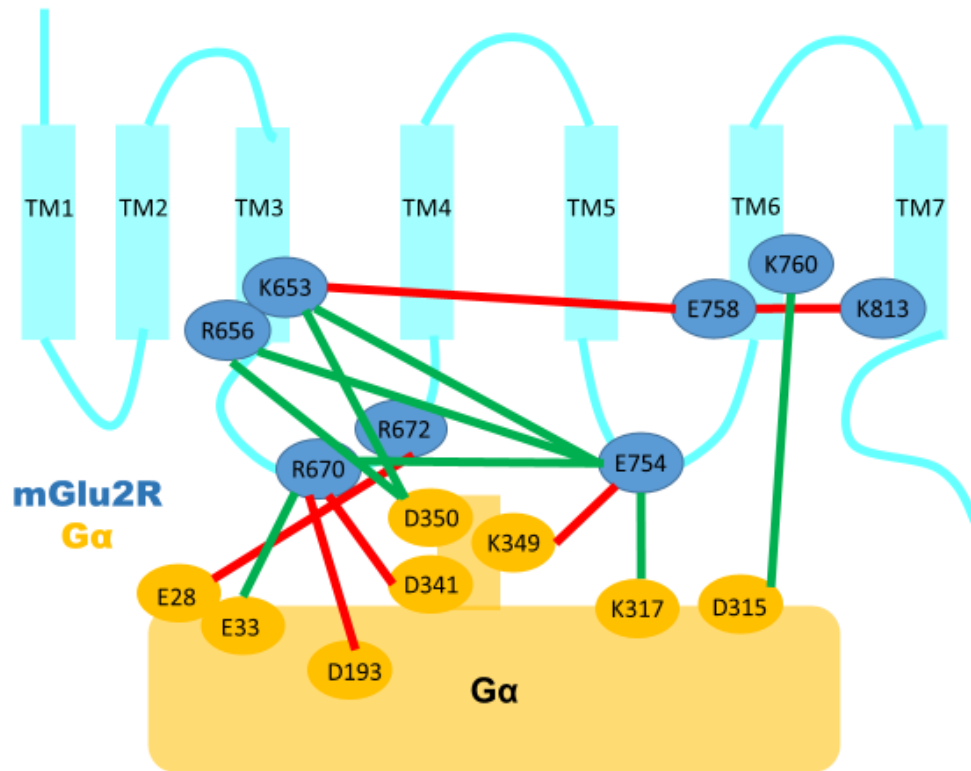


**Figure 4.2 Schematic cartoon of potential electrostatic interactions within mGlu2R — G-protein complex.** Circles represent residues predicted to form salt bridges, while the connecting lines represent potential electrostatic interactions. Red lines indicate interactions that are stabilized in the inactive state, whereas green lines are ones stabilized in the active state.

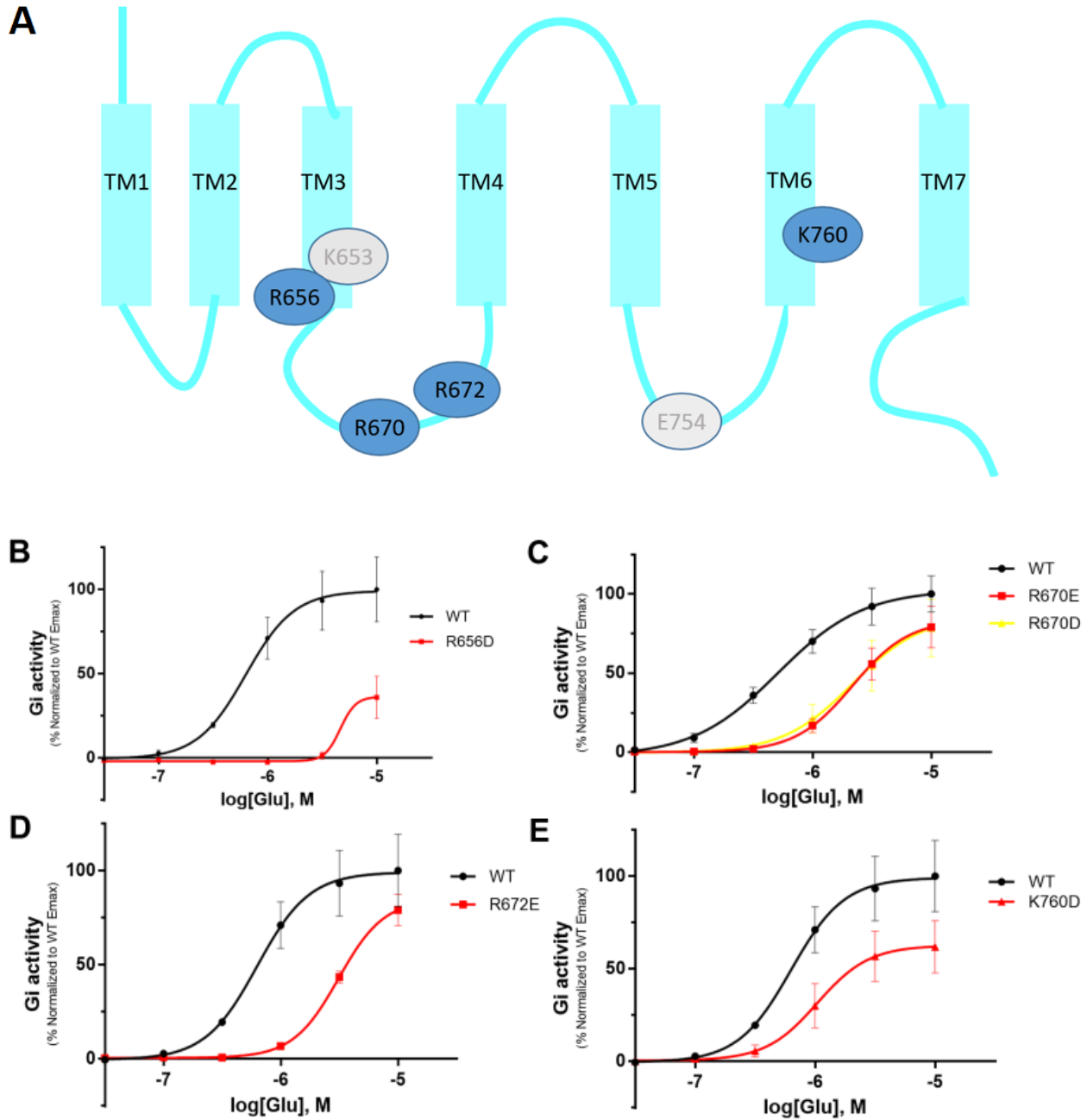


**Figure 4.3 mGlu2R residues potentially critical for the interaction with G $\alpha$  tend to be located in or adjacent to intracellular loops 2 and 3.** A, mGlu2R residues potentially critical for intermolecular interactions with G $\alpha$  are represented by circles. Residues that are also involved in intramolecular electrostatic interactions are colored gray. All other residues are colored blue. B—E, dose response curves of R656D, R670E(D), R772E, and K760D ( $n \geq 6$  per condition, experiments were performed in  $\geq 2$  batches of oocytes).

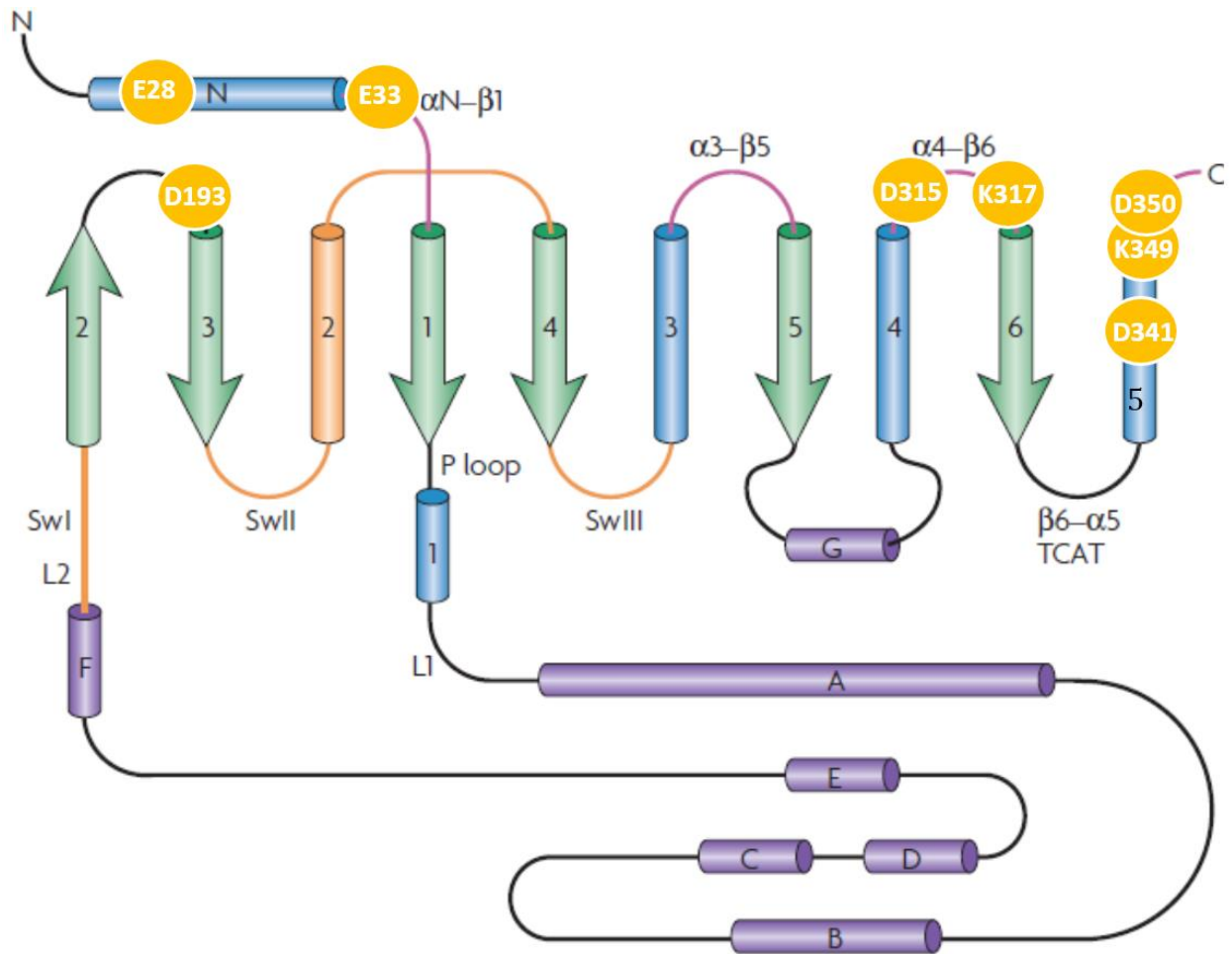


**Figure 4.4 G $\alpha$  residues predicted to engage in key electrostatic interactions with mGlu2R.** Diagram of the secondary structure of G $\alpha$  with  $\alpha$ -helices represented as cylinders and  $\beta$ -sheets as arrows. Residues predicted by computational studies to be engaging in key intermolecular electrostatic interactions with the receptor are represented by yellow circles in the Ras homology domain (RHD) (Oldham and Hamm 2008).

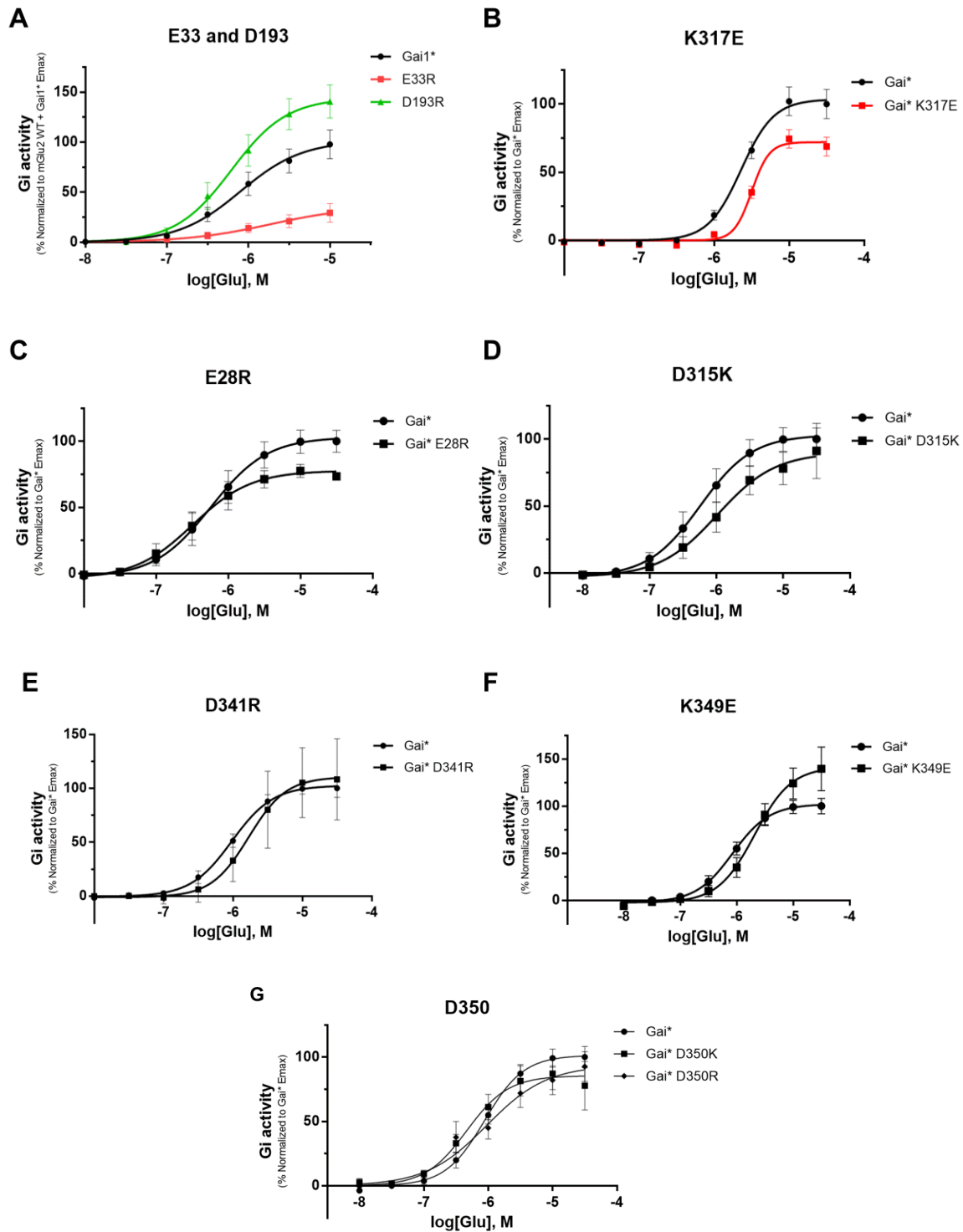
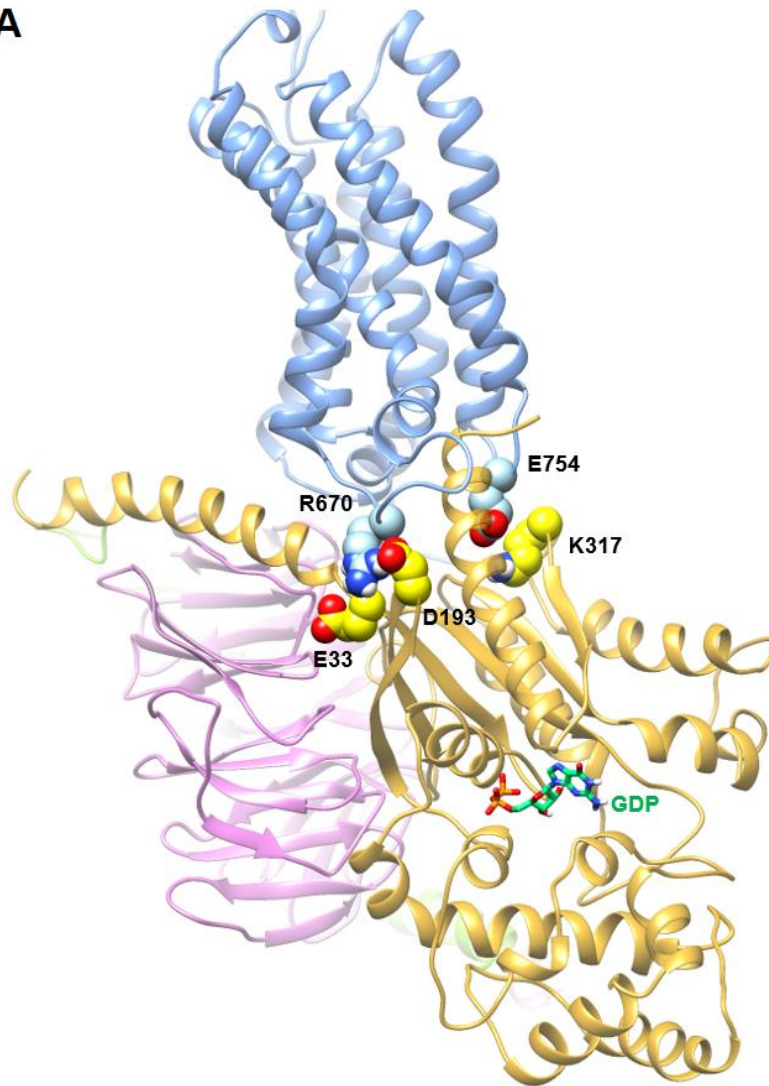
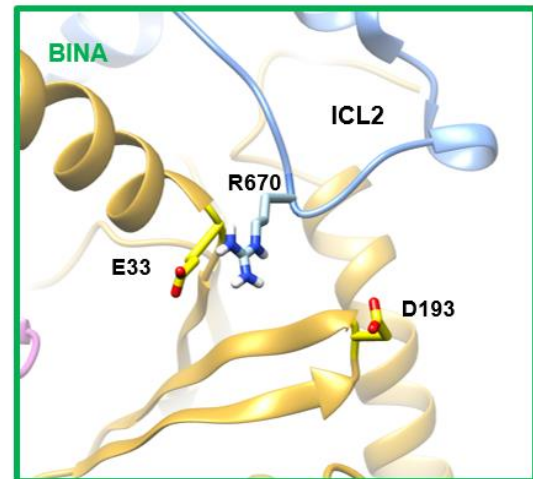
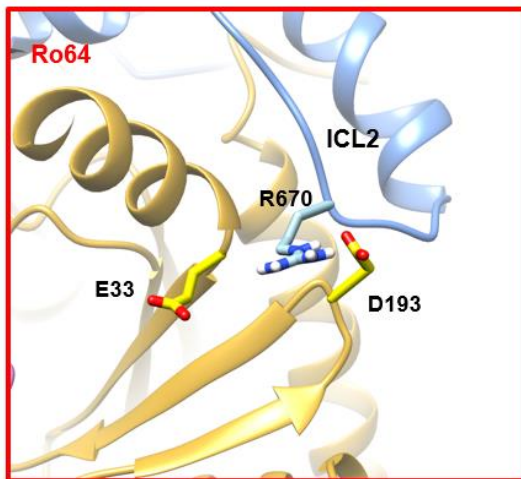


**Figure 4.5 Effects of mutations in G $\alpha$  residues proposed by computational modeling as candidates for key intermolecular electrostatic interactions. All mutations of G $\alpha$  were introduced in the background of the PTX-insensitive mutant (Gai\*) (n $\geq$ 6 per condition, experiments were performed in  $\geq$ 2 batches of oocytes). Only mutants significantly different from control (A, B) are colored.**

**A**



**B**



C

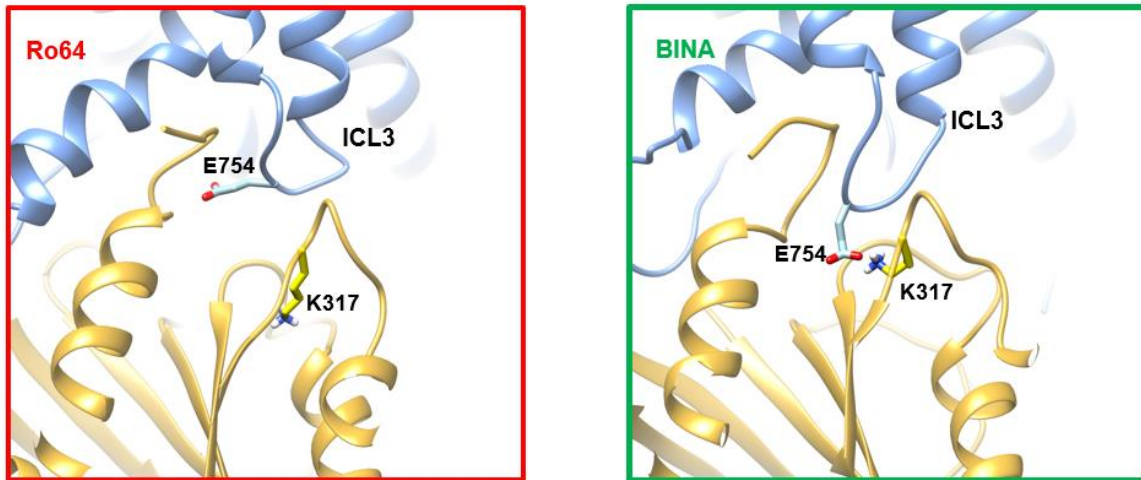


**Figure 4.6 Residues involved in intermolecular electrostatic interactions at the mGlu2R — G $\alpha$ i interface.** A, Structural model of mGlu2R—G $\alpha$ i complex with residues involved in intermolecular electrostatic interactions labeled and shown as CPK spheres. B, G $\alpha$  residues E33 and D193 are competing to interact with residue R670 in ICL2 of mGlu2R. Interaction of E33 with receptor ICL2 is stabilized in the BINA (active) state, whereas that of D193 is stabilized in the Ro64 (inactive state). C, E754 in ICL3 of mGlu2R interacts with G $\alpha$  residue K317 only in the active system.

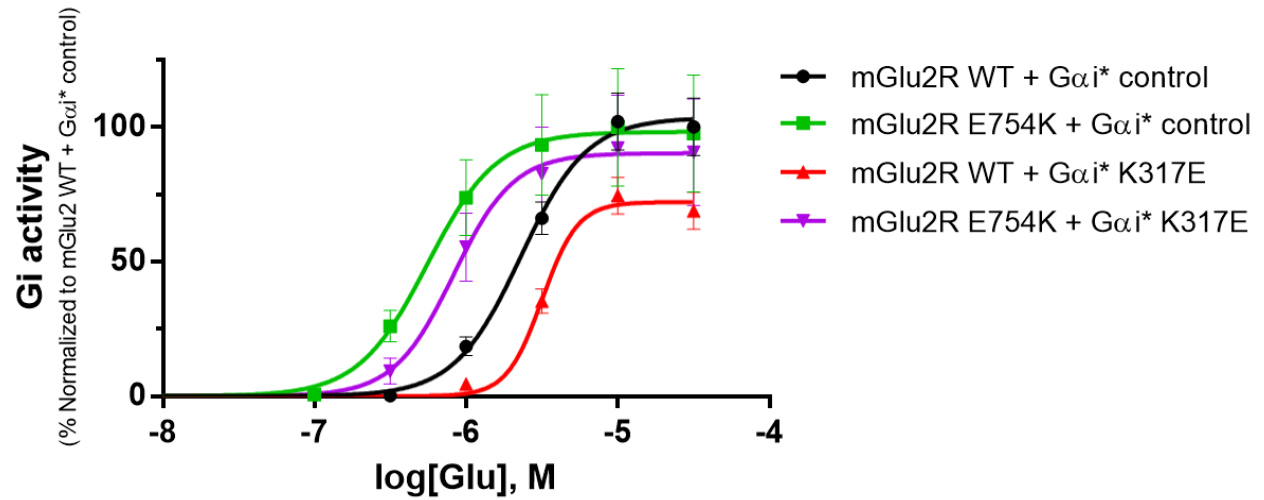


**Figure 4.7 mGlu2R intracellular loop 3 interaction with Gα K317 in α4-β6 linker.** Co-expressing mGlu2R and Gαi\* mutants E754K and K317E, respectively, rescues K317E responses to glutamate (n≥6 per condition, experiments were performed in ≥2 batches of oocytes).

**Table 4.1. Summary of the effects of mutations in mGlu2R ICL3—Gai on glutamate responses.**

|   | <b>pEC50</b>   | <b>Emax</b>    |
|---|----------------|----------------|
| <b>mGlu2R WT + Gai* control</b>   | 5.64 ± 0.054   | 103.4 ± 5.031  |
| <b>mGlu2R E754K + Gai* control</b>  | 6.26 ± 0.129*  | 98.13 ± 8.571  |
| <b>mGlu2R WT + Gai* K317E</b>   | 5.50 ± 0.027   | 72.03 ± 3.194* |
| <b>mGlu2R E754K + Gai* K317E</b>  | 6.08 ± 0.111*† | 90.21 ± 7.918  |
| * p-value < 0.05 when compared to mGlu2R WT + Gai* control,<br>† p-value < 0.05 when compared to mGlu2R WT + Gai* K317E |                |                |

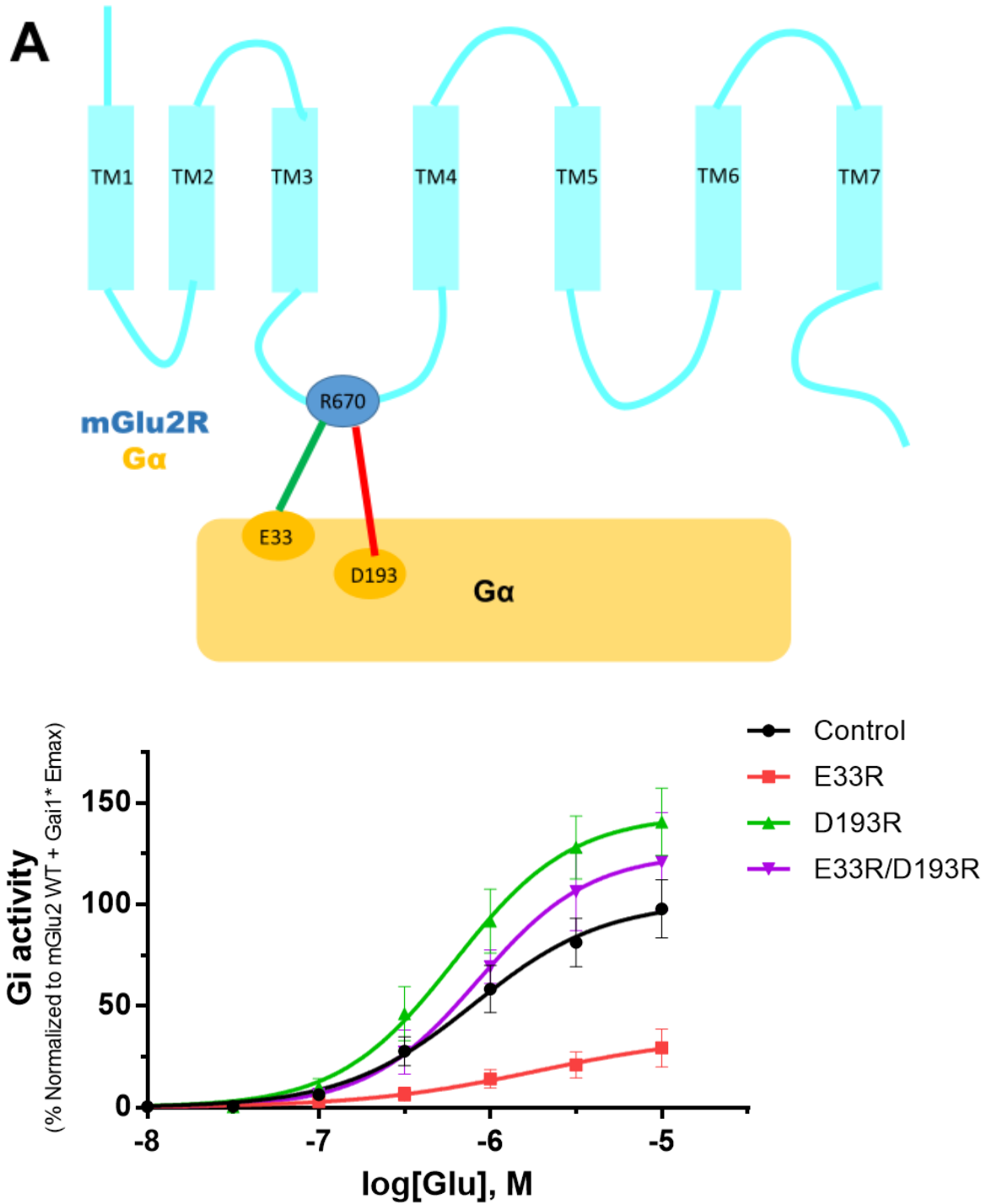


**Figure 4.8 Simultaneously destabilizing Gai E33 and D193 interactions with ICL2 restores control levels of activation.** A, a schematic cartoon of the competition between E33 and D193 of Gai to engage in salt bridges with ICL2 of mGlu2R and stabilize opposite states (red; inactive, and green; active). B, Glutamate dose response curves for single vs. double mutants ( $n \geq 6$  per condition, experiments were performed in  $\geq 2$  batches of oocytes).

**Table 4.2. Summary of glutamate responses in single and double mutants of G $\alpha$ i\* residues interacting with receptor ICL2.**

|   | <b>pEC50</b> | <b>E<sub>max</sub></b> |
|---|--------------|------------------------|
| <b>control</b>  | 5.94 ± 0.121 | 101.40 ± 13.710        |
| <b>E33R</b>   | 5.73 ± 0.701 | 35.73 ± 18.970*        |
| <b>D193R</b>  | 6.21 ± 0.129 | 143.90 ± 14.250†       |
| <b>E33R/D193R</b>   | 6.07 ± 0.167 | 125.10 ± 17.400†       |
| * p-value < 0.05 compared to control<br>† p-value < 0.05 compared to E33R |              |                        |

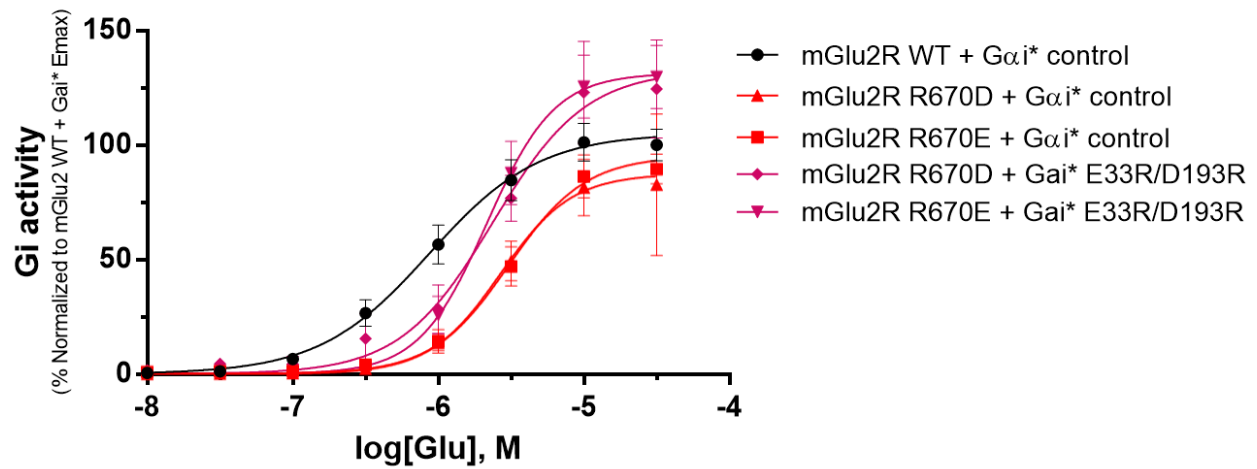


**Figure 4.9 Reestablishing the overall mGlu2R R670 — Gai1 E33/D193 Salt Bridge Network.** Co-mutating both Gα residues restores control levels of glutamate responses (n≥6 per condition, experiments were performed in ≥2 batches of oocytes).

**Table 4.3. Summary of the effect of reestablishing the salt bridge network for residue R670 in ICL2 of mGlu2R.**

|  | <b>pEC50</b>   | <b>E<sub>max</sub></b> |
|--|----------------|------------------------|
| <b>mGlu2R WT + Gai* control</b>  | 6.06 ± 0.103   | 105.20 ± 7.979         |
| <b>mGlu2R R670D + Gai* control</b>   | 5.57 ± 0.099** | 87.43 ± 9.787          |
| <b>mGlu2R R670E + Gai* control</b>   | 5.52 ± 0.077** | 95.16 ± 7.723          |
| <b>mGlu2R R670D + Gai* E33R/D193R</b>  | 5.67 ± 0.067   | 132.70 ± 15.090        |
| <b>mGlu2R R670E + Gai* E33R/D193R</b>  | 5.62 ± 0.139*  | 131.40 ± 7.682†        |
| * p-value < 0.05 when compared to mGlu2R WT + Gai* control,<br>** p-value < 0.01 when compared to mGlu2R WT + Gai* control,<br>† p-value < 0.05 when compared to mGlu2R R670E + Gai* control |                |                        |

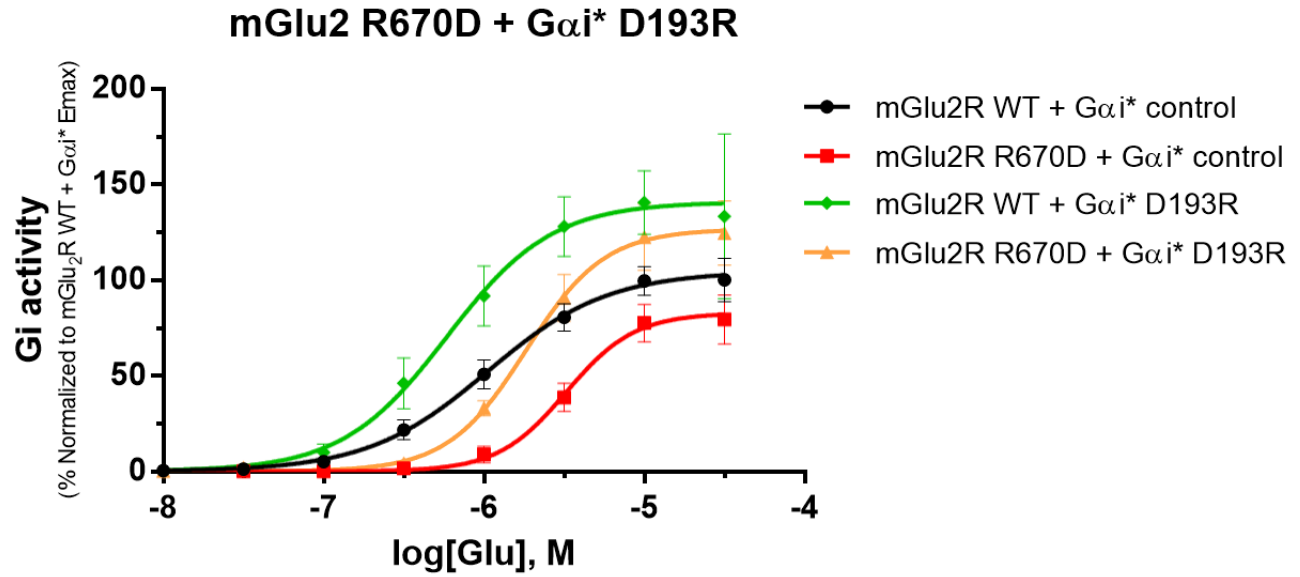


**Figure 4.10 Effects of mutations in mGlu2R ICL2—G $\alpha$ i D193 salt bridge.** Co-mutating mGlu2R ICL2 and G $\alpha$ i D193 restores control level of responses to glutamate activation ( $n \geq 6$  per condition, experiments were performed in  $\geq 2$  batches of oocytes).

**Table 4.4. Summary of the effects of mutations in mGlu2R ICL2—Gai D193 on glutamate responses.**

|  | <b>pEC50</b>  | <b>E<sub>max</sub></b> |
|--|---------------|------------------------|
| <b>mGlu2R WT + Gai* control</b>  | 5.98 ± 0.092  | 104.60 ± 7.093         |
| <b>mGlu2R R670D + Gai* control</b>   | 5.49 ± 0.072* | 82.74 ± 6.761          |
| <b>mGlu2R WT + Gai* D193R</b>  | 6.23 ± 0.122  | 140.80 ± 12.060*       |
| <b>mGlu2R R670D + Gai* D193R</b>   | 5.74 ± 0.079  | 126.60 ± 8.233†        |
| * p-value < 0.05 when compared to mGlu2R WT + Gai* control,<br>† p-value < 0.05 when compared to mGlu2R R670D + Gai* control |               |                        |

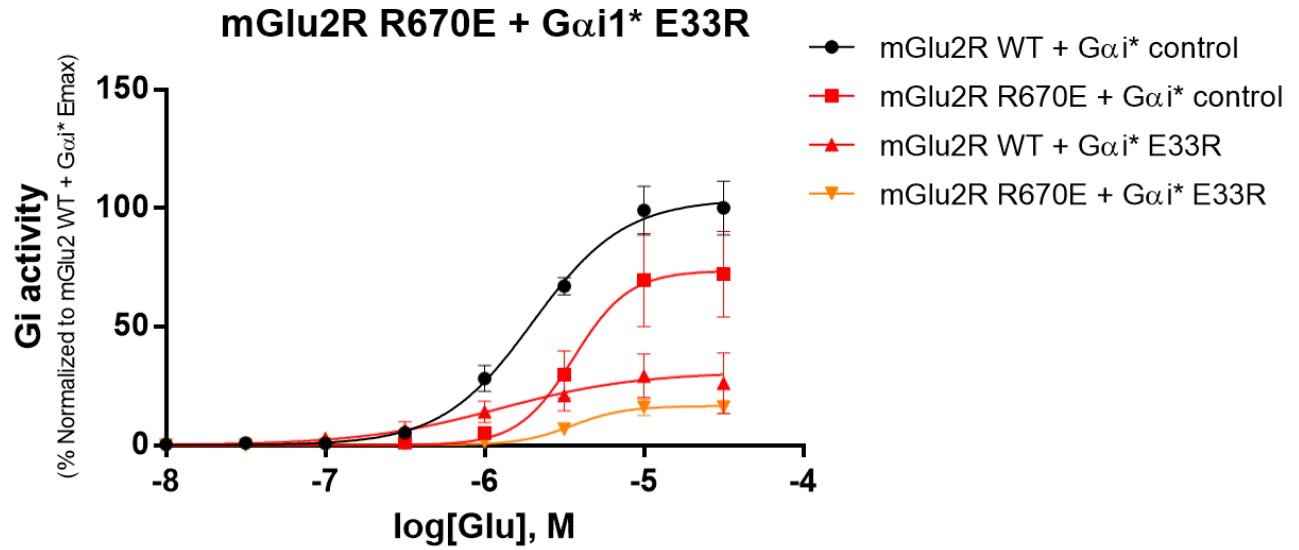


**Figure 4.11 Effects of mutations in mGlu2R ICL2—G $\alpha$ i E33 salt bridge.** Co-mutating mGlu2R ICL2 and G $\alpha$ i E33 failed to restore control level of responses to glutamate activation ( $n \geq 6$  per condition, experiments were performed in  $\geq 2$  batches of oocytes).

**Table 4.5. Summary of the effects of mutations in mGlu2R ICL2—Gai E33 on glutamate responses.**

|  | <b>pEC50</b> | <b>E<sub>max</sub></b> |
|--|--------------|------------------------|
| <b>mGlu2R WT + Gai* control</b>                            | 5.70 ± 0.069 | 103.80 ± 5.811         |
| <b>mGlu2R R670E + Gai* control</b>                         | 5.44 ± 0.119 | 73.58 ± 9.823          |
| <b>mGlu2R WT + Gai* E33R</b>                               | 5.91 ± 0.069 | 30.98 ± 9.050*         |
| <b>mGlu2R R670E + Gai* E33R</b>                            | 5.45 ± 0.082 | 16.53 ± 1.569*         |
| * p-value < 0.05 when compared to mGlu2R WT + Gai* control |              |                        |

## Chapter 5 CONCLUDING REMARKS

Three potential limitations are worth considering regarding the mGlu2R structural model used for our computational studies, which make it more similar to class A GPCRs. First, the receptor structure is truncated i.e. misses the entire N-terminal ECD that contains the glutamate binding site. Second, a PAM (BINA) structure rather than glutamate was docked into the receptor structure to study activation. Third, the structure is a monomer rather than a dimer of two mGlu2R subunits. Nevertheless, experimental data from this study supported a large number of predictions from the model, and thus, provided experimental validation for our model as a surrogate for glutamate-induced activation of the full-length dimeric receptor.

**Table 5.1.** summarizes the results of charge swapping between residues potentially engaging in key salt bridges that we tested. Briefly, we elucidated in chapter 3 the role of intermolecular electrostatic interactions in mGlu2R activation. First, we showed that similar to a large number of GPCRs, a TM3-TM6 ionic lock functions in mGlu2R to stabilize the receptor in an inactive state. We then revealed a critical role for ICL3 by which it replaces TM6 in electrostatically interacting with TM3 in order to stabilize the active state. An advantage of our theoretical computational approach is its dynamic nature, allowing us to reveal a novel role for ICL3 in intermolecular receptor activation, as opposed to the static nature of experimental structural approaches like X-ray crystallography and cryo-electron microscopy.

Full-length, glutamate-bound and/or dimeric receptor models are currently limited by technical challenges but will likely be easier to build in the future. In order for a better understanding of receptor activation, it might be important to probe any potential

intermolecular salt bridges between ICL2 and ICL3 that allows both loops to interact with each other before they both relay activation to G-protein. Whether critical mGlu2R residues such as E754 (ICL3) are conserved in distant GPCRs and play analogous roles remains to be tested.

In chapter 4, we tackled the role of intermolecular electrostatic interactions in communication of activation from the receptor to G $\alpha$ . We reveal critical roles for three charged residues, all located in regions that contact the receptor, in stabilizing different states of receptor-G-protein interactions. Two of those, E33 in the N-terminal helix- $\beta$ 1 linker and D193 in  $\beta$ 2- $\beta$ 3 linker, are competing for R670 in ICL2. The R670-D193 salt bridge stabilizes the inactive state, whereas R670-E33 stabilizes the active state. By mutating one residue, its salt bridge is destabilized allowing the competing residue's salt bridge to more strongly interact with the receptor's ICL2, favoring its inactive/active state. The third residue we identified is K317 in  $\alpha$ 4- $\beta$ 6 linker which interacts with the residue E754 in ICL3. The locations of E33 and K317 within G $\alpha$  may explain their roles in G-protein activation. Their respective and concomitant engagement by the receptor's ICL2 and ICL3 might induce structural rearrangement of the  $\beta$ 1- $\alpha$ 1 (P-) and  $\beta$ 6- $\alpha$ 5 loops, which coordinate the phosphate and the purine of the nucleotide respectively, allowing nucleotide release. This is consistent with the current notion that allosteric communication between the receptor—G-protein interface and the nucleotide binding site involves the cooperative actions of different pathways that simultaneously destabilize the phosphate and the guanine of the nucleotide ensuring efficient GDP release (Hilger, Masureel, and Kobilka 2018).

Taken together with results from chapter 3, it appears that residue E754 allows ICL3 to act as a major hub on which receptor activation converges and is relayed to G-protein.

The lack of appreciable effects of mutations of G $\alpha$  residues, also located in regions that contact the receptor, does not exclude a role these residues may play in electrostatically interacting with the receptor intracellular loops. Such roles could be revealed by testing double or triple mutants such as D341R/K349E/D350R.

Lastly, testing the effects of mutations on receptor surface expression as well as basal receptor-G-protein signaling remains an important goal for a more complete experimental characterization and understanding of the disruption and rescue of the predicted electrostatic interactions.

Our study that utilized a dynamic approach for studying mGlu2R signaling combining MD simulations with functional studies of receptor and G-protein mutants can serve as a prototype for studying the role of electrostatic interactions in other GPCRs. Additional intermolecular interactions that can be explored in the future using this approach include receptor interactions with G $\beta\gamma$  and other GPCR-interacting partners such as arrestins, G $\alpha$ —G $\beta\gamma$  interactions, and ultimately, G-protein interactions with downstream effectors.

**Table 5.1. Summary of the salt bridge interactions tested.**

| Regions Involved  | Residues Involved | Receptor State in Which the Interaction Is Stabilized | Effect of Charge Swapping on Glutamate-induced Gi Activation |
|---|-------------------|---|--|
| mGlu2R intramolecular electrostatic interactions              |                   |   |  |
| <b>TM3 — TM6</b>  | K653 — E758       | Inactive  | Rescue   |
| <b>TM6 — TM7</b>  | E758 — K813       | Inactive  | No rescue  |
| <b>TM3 — ICL3</b>   | K653 — E754       | Active  | Rescue   |
| mGlu2R — G $\alpha$ intermolecular electrostatic interactions |                   |   |  |
| <b>ICL3 — <math>\alpha</math>4-<math>\beta</math>6 linker</b> | E754 — K317       | Active  | Rescue   |
| <b>ICL2 — N-terminal helix-<math>\beta</math>1 linker</b>     | R670 — E33        | Active  | Rescue   |
| <b>ICL2 — <math>\beta</math>2-<math>\beta</math>3 linker</b>  | R670 — D193       | Inactive  | Rescue   |

## Literature cited

- Alewijnse, Astrid E, Henk Timmerman, Edwin H Jacobs, Martine J Smit, Edwin Roovers, Susanna Cotecchia, and Rob Leurs. 2000. 'The Effect of Mutations in the DRY Motif on the Constitutive Activity and Structural Instability of the Histamine H<sub>2</sub>Receptor', *Molecular pharmacology*, 57: 890-98.
- Altenbach, Christian, Ana Karin Kusnetzow, Oliver P Ernst, Klaus Peter Hofmann, and Wayne L Hubbell. 2008. 'High-resolution distance mapping in rhodopsin reveals the pattern of helix movement due to activation', *Proceedings of the National Academy of Sciences*, 105: 7439-44.
- Baki, Lia, Miguel Fribourg, Jason Younkin, Jose Miguel Eltit, Jose L Moreno, Gyu Park, Zhanna Vysotskaya, Adishesh Narahari, Stuart C Sealfon, and Javier Gonzalez-Maeso. 2016. 'Cross-signaling in metabotropic glutamate 2 and serotonin 2A receptor heteromers in mammalian cells', *Pflügers Archiv-European Journal of Physiology*, 468: 775-93.
- Ballesteros, Juan A, Anne D Jensen, George Liapakis, Søren GF Rasmussen, Lei Shi, Ulrik Gether, and Jonathan A Javitch. 2001. 'Activation of the  $\beta_2$ -adrenergic receptor involves disruption of an ionic lock between the cytoplasmic ends of transmembrane segments 3 and 6', *Journal of Biological Chemistry*, 276: 29171-77.
- Baltoumas, Fotis A, Margarita C Theodoropoulou, and Stavros J Hamodrakas. 2013. 'Interactions of the  $\alpha$ -subunits of heterotrimeric G-proteins with GPCRs, effectors and RGS proteins: a critical review and analysis of interacting surfaces, conformational shifts, structural diversity and electrostatic potentials', *Journal of structural biology*, 182: 209-18.
- Benneyworth, Michael A, Randy L Smith, and Elaine Sanders-Bush. 2008. 'Chronic phenethylamine hallucinogen treatment alters behavioral sensitivity to a metabotropic glutamate 2/3 receptor agonist', *Neuropsychopharmacology*, 33: 2206.
- Bullock, W Michael, Karen Cardon, Juan Bustillo, Rosalinda C Roberts, and Nora I Perrone-Bizzozero. 2008. 'Altered expression of genes involved in GABAergic transmission and neuromodulation of granule cell activity in the cerebellum of schizophrenia patients', *American Journal of Psychiatry*, 165: 1594-603.
- Burford, NT, JR Traynor, and A Alt. 2015. 'Positive allosteric modulators of the  $\mu$ -opioid receptor: a novel approach for future pain medications', *British Journal of Pharmacology*, 172: 277-86.
- Carlton, Susan M, Junhui Du, and Shengtai Zhou. 2009. 'Group II metabotropic glutamate receptor activation on peripheral nociceptors modulates TRPV1 function', *Brain research*, 1248: 86-95.
- Carpenter, Byron, Rony Nehmé, Tony Warne, Andrew GW Leslie, and Christopher G Tate. 2016. 'Structure of the adenosine A<sub>2A</sub> receptor bound to an engineered G protein', *Nature*, 536: 104.
- Cartmell, Jayne, James A Monn, and Darryle D Schoepp. 1999. 'The metabotropic glutamate 2/3 receptor agonists LY354740 and LY379268 selectively attenuate phencyclidine versus d-amphetamine motor behaviors in rats', *Journal of Pharmacology and Experimental Therapeutics*, 291: 161-70.
- Choe, Hui-Woog, Yong Ju Kim, Jung Hee Park, Takefumi Morizumi, Emil F Pai, Norbert Krauss, Klaus Peter Hofmann, Patrick Scheerer, and Oliver P Ernst. 2011. 'Crystal structure of metarhodopsin II', *Nature*, 471: 651.
- Christopoulos, Arthur. 2014. 'Advances in G protein-coupled receptor allostery: from function to structure', *Molecular pharmacology*, 86: 463-78.
- Christopoulos, Arthur, Jean-Pierre Changeux, William A Catterall, Dorian Fabbro, Thomas P Burris, John A Cidlowski, Richard W Olsen, John A Peters, Richard R Neubig, and Jean-Philippe Pin. 2014. 'International Union of Basic and Clinical Pharmacology. XC. Multisite pharmacology:

- recommendations for the nomenclature of receptor allosterism and allosteric ligands', *Pharmacological reviews*, 66: 918-47.
- Chung, Ka Young, Søren GF Rasmussen, Tong Liu, Sheng Li, Brian T DeVree, Pil Seok Chae, Diane Calinski, Brian K Kobilka, Virgil L Woods Jr, and Roger K Sunahara. 2011. 'Conformational changes in the G protein Gs induced by the  $\beta$  2 adrenergic receptor', *Nature*, 477: 611.
- Coleman, David E, Albert M Berghuis, Ethan Lee, Maurine E Linder, and Alfred G Gilman. 1994. 'Structures of active conformations of Gi alpha 1 and the mechanism of GTP hydrolysis', *science*, 265: 1405-12.
- Conn, P Jeffrey, Arthur Christopoulos, and Craig W Lindsley. 2009. 'Allosteric modulators of GPCRs: a novel approach for the treatment of CNS disorders', *Nature reviews Drug discovery*, 8: 41.
- Costa, Tommaso, and Albert Herz. 1989. 'Antagonists with negative intrinsic activity at delta opioid receptors coupled to GTP-binding proteins', *Proceedings of the National Academy of Sciences*, 86: 7321-25.
- De Lean, Andre, JMand Stadel, and RJ Lefkowitz. 1980. 'A ternary complex model explains the agonist-specific binding properties of the adenylate cyclase-coupled beta-adrenergic receptor', *Journal of Biological Chemistry*, 255: 7108-17.
- DeVree, Brian T, Jacob P Mahoney, Gisselle A Vélez-Ruiz, Soren GF Rasmussen, Adam J Kuszak, Elin Edwald, Juan-Jose Fung, Aashish Manglik, Matthieu Masureel, and Yang Du. 2016. 'Allosteric coupling from G protein to the agonist-binding pocket in GPCRs', *Nature*, 535: 182.
- Doré, Andrew S, Krzysztof Okrasa, Jayesh C Patel, Maria Serrano-Vega, Kirstie Bennett, Robert M Cooke, James C Errey, Ali Jazayeri, Samir Khan, and Ben Tehan. 2014. 'Structure of class C GPCR metabotropic glutamate receptor 5 transmembrane domain', *Nature*, 511: 557.
- Doumazane, Etienne, Pauline Scholler, Jurriaan M Zwier, Eric Trinquet, Philippe Rondard, and Jean-Philippe Pin. 2011. 'A new approach to analyze cell surface protein complexes reveals specific heterodimeric metabotropic glutamate receptors', *The FASEB Journal*, 25: 66-77.
- Dror, Ron O, Thomas J Mildorf, Daniel Hilger, Aashish Manglik, David W Borhani, Daniel H Arlow, Ansgar Philippsen, Nicolas Villanueva, Zhongyu Yang, and Michael T Lerch. 2015. 'Structural basis for nucleotide exchange in heterotrimeric G proteins', *science*, 348: 1361-65.
- El Moustaine, Driss, Sébastien Granier, Etienne Doumazane, Pauline Scholler, Rita Rahmeh, Patrick Bron, Bernard Mouillac, Jean-Louis Banères, Philippe Rondard, and Jean-Philippe Pin. 2012. 'Distinct roles of metabotropic glutamate receptor dimerization in agonist activation and G-protein coupling', *Proceedings of the National Academy of Sciences*, 109: 16342-47.
- Ellaithy, Amr, Jason Younkin, Javier Gonzalez-Maeso, and Diomedes E Logothetis. 2015. 'Positive allosteric modulators of metabotropic glutamate 2 receptors in schizophrenia treatment', *Trends in neurosciences*, 38: 506-16.
- Farrens, David L, Christian Altenbach, Ke Yang, Wayne L Hubbell, and H Gobind Khorana. 1996. 'Requirement of rigid-body motion of transmembrane helices for light activation of rhodopsin', *science*, 274: 768-70.
- Fell, Matthew J, Jeffrey M Witkin, Julie F Falcone, Jason S Katner, Kenneth W Perry, John Hart, Linda Rorick-Kehn, Carl D Overshiner, Kurt Rasmussen, and Stephen F Chaney. 2011. 'N-(4-((2-(trifluoromethyl)-3-hydroxy-4-(isobutyryl) phenoxy) methyl) benzyl)-1-methyl-1H-imidazole-4-carboxamide (THIIC), a novel metabotropic glutamate 2 potentiator with potential anxiolytic/antidepressant properties: in vivo profiling suggests a link between behavioral and central nervous system neurochemical changes', *Journal of Pharmacology and Experimental Therapeutics*, 336: 165-77.
- Francesconi, Anna, and Robert M Duvoisin. 1998. 'Role of the second and third intracellular loops of metabotropic glutamate receptors in mediating dual signal transduction activation', *Journal of Biological Chemistry*, 273: 5615-24.

- Fribourg, Miguel, José L Moreno, Terrell Holloway, Davide Provasi, Lia Baki, Rahul Mahajan, Gyu Park, Scott K Adney, Candice Hatcher, and José M Eltit. 2011. 'Decoding the signaling of a GPCR heteromeric complex reveals a unifying mechanism of action of antipsychotic drugs', *Cell*, 147: 1011-23.
- Ghanouni, Pejman, Zygmunt Gryczynski, Jacqueline J Steenhuis, Tae Weon Lee, David L Farrens, Joseph R Lakowicz, and Brian K Kobilka. 2001. 'Functionally Different Agonists Induce Distinct Conformations in the G Protein Coupling Domain of the  $\beta$ 2Adrenergic Receptor', *Journal of Biological Chemistry*, 276: 24433-36.
- Ghose, Subroto, Jeremy M Crook, Cynthia L Bartus, Thomas G Sherman, Mary M Herman, Thomas M Hyde, Joel E Kleinman, and Mayada Akil. 2008. 'Metabotropic glutamate receptor 2 and 3 gene expression in the human prefrontal cortex and mesencephalon in schizophrenia', *International Journal of Neuroscience*, 118: 1609-27.
- Ghose, Subroto, Kelly A Gleason, Bryan W Potts, Kelly Lewis-Amezcuca, and Carol A Tamminga. 2009. 'Differential expression of metabotropic glutamate receptors 2 and 3 in schizophrenia: a mechanism for antipsychotic drug action?', *American Journal of Psychiatry*, 166: 812-20.
- González-Maeso, Javier, Rosalind L Ang, Tony Yuen, Pokman Chan, Noelia V Weisstaub, Juan F López-Giménez, Mingming Zhou, Yuuya Okawa, Luis F Callado, and Graeme Milligan. 2008. 'Identification of a serotonin/glutamate receptor complex implicated in psychosis', *Nature*, 452: 93.
- Griebel, Guy, Philippe Pichat, Denis Boulay, Vanessa Naimoli, Lisa Potestio, Robert Featherstone, Sukhveen Sahni, Henry Defex, Christophe Desvignes, and Franck Slowinski. 2016. 'The mGluR2 positive allosteric modulator, SAR218645, improves memory and attention deficits in translational models of cognitive symptoms associated with schizophrenia', *Scientific reports*, 6: 35320.
- Gupta, Daya S, Robert E McCullumsmith, Monica Beneyto, Vahram Haroutunian, Kenneth L Davis, and James H Meador-Woodruff. 2005. 'Metabotropic glutamate receptor protein expression in the prefrontal cortex and striatum in schizophrenia', *Synapse*, 57: 123-31.
- Gurevich, Vsevolod V, and Eugenia V Gurevich. 2017. 'Molecular Mechanisms of GPCR Signaling: A Structural Perspective', *International journal of molecular sciences*, 18: 2519.
- Hatcher-Solis, Candice, Miguel Fribourg, Katerina Spyridaki, Jason Younkin, Amr Ellaithy, Guoqing Xiang, George Liapakis, Javier Gonzalez-Maeso, Hailin Zhang, and Meng Cui. 2014. 'G protein-coupled receptor signaling to Kir channels in *Xenopus* oocytes', *Current pharmaceutical biotechnology*, 15: 987-95.
- Hermans, Emmanuel. 2003. 'Biochemical and pharmacological control of the multiplicity of coupling at G-protein-coupled receptors', *Pharmacology & Therapeutics*, 99: 25-44.
- Hilger, Daniel, Matthieu Masureel, and Brian K Kobilka. 2018. 'Structure and dynamics of GPCR signaling complexes', *Nature structural & molecular biology*, 25: 4.
- Hopkins, Corey R. 2013. "Is there a path forward for mGlu2 positive allosteric modulators for the treatment of schizophrenia?" In.: ACS Publications.
- Huang, Jianyun, Yutong Sun, J Jillian Zhang, and Xin-Yun Huang. 2015. 'Pivotal Role of Extended Linker 2 in the Activation of  $G\alpha$  by G Protein-coupled Receptor', *Journal of Biological Chemistry*, 290: 272-83.
- Huang, Weijiao, Aashish Manglik, AJ Venkatakrishnan, Toon Laeremans, Evan N Feinberg, Adrian L Sanborn, Hideaki E Kato, Kathryn E Livingston, Thor S Thorsen, and Ralf C Kling. 2015. 'Structural insights into  $\mu$ -opioid receptor activation', *Nature*, 524: 315.
- Isogai, Shin, Xavier Deupi, Christian Opitz, Franziska M Heydenreich, Ching-Ju Tsai, Florian Brueckner, Gebhard FX Schertler, Dmitry B Veprintsev, and Stephan Grzesiek. 2016. 'Backbone NMR reveals allosteric signal transduction networks in the  $\beta$  1-adrenergic receptor', *Nature*, 530: 237.

- Jazayeri, Ali, Mathieu Rappas, Alastair JH Brown, James Kean, James C Errey, Nathan J Robertson, Cédric Fiez-Vandal, Stephen P Andrews, Miles Congreve, and Andrea Bortolato. 2017. 'Crystal structure of the GLP-1 receptor bound to a peptide agonist', *Nature*, 546: 254.
- Johnson, Kari A, and David M Lovinger. 2015. 'Metabotropic Glutamate Receptor 2 Positive Allosteric Modulators: Closing the Gate on Drug Abuse?', *Biological psychiatry*, 78: 436-38.
- Jones, Carrie K, Elizabeth Lutz Eberle, Stephen C Peters, James A Monn, and Harlan E Shannon. 2005. 'Analgesic effects of the selective group II (mGlu2/3) metabotropic glutamate receptor agonists LY379268 and LY389795 in persistent and inflammatory pain models after acute and repeated dosing', *Neuropharmacology*, 49: 206-18.
- Kammermeier, Paul J, and June Yun. 2005. 'Activation of metabotropic glutamate receptor 1 dimers requires glutamate binding in both subunits', *Journal of Pharmacology and Experimental Therapeutics*, 312: 502-08.
- Kenny, Paul J, Fabrizio Gasparini, and Athina Markou. 2003. 'Group II metabotropic and  $\alpha$ -amino-3-hydroxy-5-methyl-4-isoxazole propionate (AMPA)/kainate glutamate receptors regulate the deficit in brain reward function associated with nicotine withdrawal in rats', *Journal of Pharmacology and Experimental Therapeutics*, 306: 1068-76.
- Kim, Soong Ho, Paul E Fraser, David Westaway, Peter H St George-Hyslop, Michelle E Ehrlich, and Sam Gandy. 2010. 'Group II metabotropic glutamate receptor stimulation triggers production and release of Alzheimer's amyloid  $\beta$ 42 from isolated intact nerve terminals', *Journal of Neuroscience*, 30: 3870-75.
- Kinon, Bruce J, Brian A Millen, Lu Zhang, and David L McKinzie. 2015. 'Exploratory analysis for a targeted patient population responsive to the metabotropic glutamate 2/3 receptor agonist pomaglumetad methionil in schizophrenia', *Biological psychiatry*, 78: 754-62.
- Kinon, Bruce J, Lu Zhang, Brian A Millen, Olawale O Osuntokun, Judy E Williams, Sara Kollack-Walker, Kimberley Jackson, Ludmila Kryzhanovskaya, Natalia Jarkova, and HBBI Study Group. 2011. 'A multicenter, inpatient, phase 2, double-blind, placebo-controlled dose-ranging study of LY2140023 monohydrate in patients with DSM-IV schizophrenia', *Journal of clinical psychopharmacology*, 31: 349-55.
- Kniazeff, Julie, Anne-Sophie Bessis, Damien Maurel, Hervé Ansanay, Laurent Prézeau, and Jean-Philippe Pin. 2004. 'Closed state of both binding domains of homodimeric mGlu receptors is required for full activity', *Nature Structural and Molecular Biology*, 11: 706.
- Kniazeff, Julie, Laurent Prézeau, Philippe Rondard, Jean-Philippe Pin, and Cyril Goudet. 2011. 'Dimers and beyond: The functional puzzles of class C GPCRs', *Pharmacology & Therapeutics*, 130: 9-25.
- Kobilka, Brian K, and Xavier Deupi. 2007. 'Conformational complexity of G-protein-coupled receptors', *Trends in pharmacological sciences*, 28: 397-406.
- Kordi-Tamandani, Dor Mohammad, Nahid Dahmardeh, and Adam Torkamanzehi. 2013. 'Evaluation of hypermethylation and expression pattern of GMR2, GMR5, GMR8, and GRIA3 in patients with schizophrenia', *Gene*, 515: 163-66.
- Kruse, Andrew C, Aaron M Ring, Aashish Manglik, Jianxin Hu, Kelly Hu, Katrin Eitel, Harald Hübner, Els Pardon, Celine Valant, and Patrick M Sexton. 2013. 'Activation and allosteric modulation of a muscarinic acetylcholine receptor', *Nature*, 504: 101.
- Kunishima, Naoki, Yoshimi Shimada, Yuji Tsuji, Toshihiro Sato, Masaki Yamamoto, Takashi Kumasaka, Shigetada Nakanishi, Hisato Jingami, and Kosuke Morikawa. 2000. 'Structural basis of glutamate recognition by a dimeric metabotropic glutamate receptor', *Nature*, 407: 971.
- Kurita, Mitsumasa, Terrell Holloway, Aintzane García-Bea, Alexey Kozlenkov, Allyson K Friedman, José L Moreno, Mitra Heshmati, Sam A Golden, Pamela J Kennedy, and Nagahide Takahashi. 2012. 'HDAC2 regulates atypical antipsychotic responses through the modulation of mGlu2 promoter activity', *Nature neuroscience*, 15: 1245.

- Lambright, David G, Joseph P Noel, Heidi E Hamm, and Paul B Sigler. 1994. 'Structural determinants for activation of the  $\alpha$ -subunit of a heterotrimeric G protein', *Nature*, 369: 621.
- Lambright, David G, John Sondek, Andrew Bohm, Nikolai P Skiba, Heidi E Hamm, and Paul B Sigler. 1996. 'The 2.0 Å crystal structure of a heterotrimeric G protein', *Nature*, 379: 311.
- Latorraca, Naomi R, AJ Venkatakrishnan, and Ron O Dror. 2016. 'GPCR dynamics: structures in motion', *Chemical reviews*, 117: 139-55.
- Lefkowitz, R. J. 2007. 'Seven transmembrane receptors: a brief personal retrospective', *Biochim Biophys Acta*, 1768: 748-55.
- Levitz, Joshua, Chris Habrian, Shashank Bharill, Zhu Fu, Reza Vafabakhsh, and Ehud Y Isacoff. 2016. 'Mechanism of assembly and cooperativity of homomeric and heteromeric metabotropic glutamate receptors', *Neuron*, 92: 143-59.
- Liang, Yi-Lynn, Maryam Khoshouei, Mazdak Radjainia, Yan Zhang, Alisa Glukhova, Jeffrey Tarrasch, David M Thal, Sebastian GB Furness, George Christopoulos, and Thomas Coudrat. 2017. 'Phase-plate cryo-EM structure of a class B GPCR–G-protein complex', *Nature*, 546: 118.
- Litman, Robert E, Mark A Smith, James J Doherty, Alan Cross, Shane Raines, Lev Gertsik, and Stephen R Zukin. 2016. 'AZD8529, a positive allosteric modulator at the mGluR2 receptor, does not improve symptoms in schizophrenia: A proof of principle study', *Schizophrenia research*, 172: 152-57.
- Logothetis, Diomedes E, Shahla Movahedi, Carol Satler, Klaus Lindpaintner, and Bernardo Nadal-Ginard. 1992. 'Incremental reductions of positive charge within the S4 region of a voltage-gated K<sup>+</sup> channel result in corresponding decreases in gating charge', *Neuron*, 8: 531-40.
- Mahajan, Rahul, Junghoon Ha, Miao Zhang, Takeharu Kawano, Tohru Kozasa, and Diomedes E Logothetis. 2013. 'A computational model predicts that G $\beta\gamma$  acts at a cleft between channel subunits to activate GIRK1 channels', *Sci. Signal.*, 6: ra69-ra69.
- Mahoney, Jacob P, and Roger K Sunahara. 2016. 'Mechanistic insights into GPCR–G protein interactions', *Current opinion in structural biology*, 41: 247-54.
- Manglik, Aashish, Tae Hun Kim, Matthieu Masureel, Christian Altenbach, Zhongyu Yang, Daniel Hilger, Michael T Lerch, Tong Sun Kobilka, Foon Sun Thian, and Wayne L Hubbell. 2015. 'Structural insights into the dynamic process of  $\beta$ 2-adrenergic receptor signaling', *Cell*, 161: 1101-11.
- Manglik, Aashish, and Andrew C Kruse. 2017. 'Structural basis for G protein-coupled receptor activation', *Biochemistry*, 56: 5628-34.
- Marek, Gerard J. 2010. 'Metabotropic glutamate2/3 (mGlu2/3) receptors, schizophrenia and cognition', *European journal of pharmacology*, 639: 81-90.
- Mastroiacovo, Federica, Slaviana Moyanova, Milena Cannella, Anderson Gaglione, Remy Verhaeghe, Giovanna Bozza, Michele Madonna, Marta Motolese, Anna Traficante, and Barbara Riozzi. 2017. 'Genetic deletion of mGlu2 metabotropic glutamate receptors improves the short-term outcome of cerebral transient focal ischemia', *Molecular brain*, 10: 39.
- Matrisciano, F, A Caruso, R Orlando, M Marchiafava, V Bruno, G Battaglia, SHM Gruber, D Melchiorri, R Tatarelli, and P Girardi. 2008. 'Defective group-II metabotropic glutamate receptors in the hippocampus of spontaneously depressed rats', *Neuropharmacology*, 55: 525-31.
- Metcalfe, Cameron S, Brian D Klein, Misty D Smith, Tim Pruess, Marc Ceusters, Hilde Lavreysen, Stefan Pype, Nancy Van Osselaer, Roy Twyman, and H Steve White. 2017. 'Efficacy of mGlu2-positive allosteric modulators alone and in combination with levetiracetam in the mouse 6 Hz model of psychomotor seizures', *Epilepsia*, 58: 484-93.
- Milligan, G., and E. Kostenis. 2006. 'Heterotrimeric G-proteins: a short history', *British Journal of Pharmacology*, 147: S46-S55.

- Mixon, Mark B, Ethan Lee, David E Coleman, Albert M Berghuis, Alfred G Gilman, and Stephen R Sprang. 1995. 'Tertiary and quaternary structural changes in  $G\alpha 1$  induced by GTP hydrolysis', *science*, 270: 954-60.
- Moghaddam, Bitá, and Barbara W Adams. 1998. 'Reversal of phencyclidine effects by a group II metabotropic glutamate receptor agonist in rats', *science*, 281: 1349-52.
- Moreno, José L, Terrell Holloway, Laura Albizu, Stuart C Sealton, and Javier González-Maeso. 2011. 'Metabotropic glutamate mGlu2 receptor is necessary for the pharmacological and behavioral effects induced by hallucinogenic 5-HT2A receptor agonists', *Neuroscience letters*, 493: 76-79.
- Moreno, José L, Terrell Holloway, Vinayak Rayannavar, Stuart C Sealton, and Javier González-Maeso. 2013. 'Chronic treatment with LY341495 decreases 5-HT2A receptor binding and hallucinogenic effects of LSD in mice', *Neuroscience letters*, 536: 69-73.
- Moreno, José L, Carolina Muguruza, Adrienne Umali, Steven Mortillo, Terrell Holloway, Fuencisla Pilar-Cuéllar, Giuseppe Mocci, Jeremy Seto, Luis F Callado, and Rachael L Neve. 2012. 'Identification of three residues essential for 5-hydroxytryptamine 2A-metabotropic glutamate 2 (5-HT2A· mGlu2) receptor heteromerization and its psychoactive behavioral function', *Journal of Biological Chemistry*, 287: 44301-19.
- Motolese, Marta, Federica Mastroiacovo, Milena Cannella, Domenico Bucci, Anderson Gaglione, Barbara Riozzi, Robert Lütjens, Sonia M Poli, Sylvain Celanire, and Valeria Bruno. 2015. 'Targeting type-2 metabotropic glutamate receptors to protect vulnerable hippocampal neurons against ischemic damage', *Molecular brain*, 8: 66.
- Muguruza, Carolina, J Javier Meana, and Luis F Callado. 2016. 'Group II metabotropic glutamate receptors as targets for novel antipsychotic drugs', *Frontiers in pharmacology*, 7: 130.
- Nakanishi, Shigetada. 1992. 'Molecular diversity of glutamate receptors and implications for brain function', *science*, 258: 597-603.
- Noel, Joseph P, Heidi E Hamm, and Paul B Sigler. 1993. 'The 2.2 Å crystal structure of transducin- $\alpha$  complexed with GTP $\gamma$ S', *Nature*, 366: 654.
- Nygaard, Rie, Yaozhong Zou, Ron O Dror, Thomas J Mildorf, Daniel H Arlow, Aashish Manglik, Albert C Pan, Corey W Liu, Juan José Fung, and Michael P Bokoch. 2013. 'The dynamic process of  $\beta 2$ -adrenergic receptor activation', *Cell*, 152: 532-42.
- Oldham, William M, and Heidi E Hamm. 2008. 'Heterotrimeric G protein activation by G-protein-coupled receptors', *Nature reviews Molecular cell biology*, 9: 60.
- Palczewski, Krzysztof, Takashi Kumasaka, Tetsuya Hori, Craig A Behnke, Hiroyuki Motoshima, Brian A Fox, Isolde Le Trong, David C Teller, Tetsuji Okada, and Ronald E Stenkamp. 2000. 'Crystal structure of rhodopsin: AG protein-coupled receptor', *science*, 289: 739-45.
- Patil, Sandeep T, Lu Zhang, Ferenc Martenyi, Stephen L Lowe, Kimberley A Jackson, Boris V Andreev, Alla S Avedisova, Leonid M Bardenstein, Issak Y Gurovich, and Margarita A Morozova. 2007. 'Activation of mGlu2/3 receptors as a new approach to treat schizophrenia: a randomized Phase 2 clinical trial', *Nature medicine*, 13: 1102.
- Rasmussen, S. G., H. J. Choi, D. M. Rosenbaum, T. S. Kobilka, F. S. Thian, P. C. Edwards, M. Burghammer, V. R. Ratnala, R. Sanishvili, R. F. Fischetti, G. F. Schertler, W. I. Weis, and B. K. Kobilka. 2007. 'Crystal structure of the human beta2 adrenergic G-protein-coupled receptor', *Nature*, 450: 383-7.
- Rasmussen, Søren GF, Hee-Jung Choi, Juan Jose Fung, Els Pardon, Paola Casarosa, Pil Seok Chae, Brian T DeVree, Daniel M Rosenbaum, Foon Sun Thian, and Tong Sun Kobilka. 2011. 'Structure of a nanobody-stabilized active state of the  $\beta 2$  adrenoceptor', *Nature*, 469: 175.
- Rasmussen, Søren GF, Brian T DeVree, Yaozhong Zou, Andrew C Kruse, Ka Young Chung, Tong Sun Kobilka, Foon Sun Thian, Pil Seok Chae, Els Pardon, and Diane Calinski. 2011. 'Crystal structure of the  $\beta 2$  adrenergic receptor-Gs protein complex', *Nature*, 477: 549.

- Rasmussen, Søren GF, Anne D Jensen, George Liapakis, Pejman Ghanouni, Jonathan A Javitch, and Ulrik Gether. 1999. 'Mutation of a highly conserved aspartic acid in the  $\beta$ 2 adrenergic receptor: constitutive activation, structural instability, and conformational rearrangement of transmembrane segment 6', *Molecular pharmacology*, 56: 175-84.
- Ray, Kausik, and Benjamin C Hauschild. 2000. 'Cys-140 is critical for metabotropic glutamate receptor-1 dimerization', *Journal of Biological Chemistry*, 275: 34245-51.
- Reiner, Andreas, Joshua Levitz, and Ehud Y Isacoff. 2015. 'Controlling ionotropic and metabotropic glutamate receptors with light: principles and potential', *Current opinion in pharmacology*, 20: 135-43.
- Richards, Grayson, Jürg Messer, Richard LM Faull, Heinz Stadler, Jürgen Wichmann, Philipp Huguenin, Bernd Bohrmann, and Vincent Mutel. 2010. 'Altered distribution of mGlu2 receptors in  $\beta$ -amyloid-affected brain regions of Alzheimer cases and aged PS2APP mice', *Brain research*, 1363: 180-90.
- Romano, Carmelo, Wan-Lin Yang, and Karen L O'Malley. 1996. 'Metabotropic glutamate receptor 5 is a disulfide-linked dimer', *Journal of Biological Chemistry*, 271: 28612-16.
- Rondard, Philippe, and Jean-Philippe Pin. 2015. 'Dynamics and modulation of metabotropic glutamate receptors', *Current opinion in pharmacology*, 20: 95-101.
- Rusinova, Radda, Tooraj Mirshahi, and Diomedes E Logothetis. 2007. 'Specificity of G $\beta\gamma$  signaling to Kir3 channels depends on the helical domain of pertussis toxin-sensitive G $\alpha$  subunits', *Journal of Biological Chemistry*, 282: 34019-30.
- Samama, Pa, S Cotecchia, T Costa, and RJ Lefkowitz. 1993. 'A mutation-induced activated state of the beta 2-adrenergic receptor. Extending the ternary complex model', *Journal of Biological Chemistry*, 268: 4625-36.
- Sanacora, Gerard, Carlos A Zarate, John H Krystal, and Husseini K Manji. 2008. 'Targeting the glutamatergic system to develop novel, improved therapeutics for mood disorders', *Nature reviews Drug discovery*, 7: 426.
- Scheer, A, F Fanelli, T Costa, PG De Benedetti, and S Cotecchia. 1996. 'Constitutively active mutants of the alpha 1B-adrenergic receptor: role of highly conserved polar amino acids in receptor activation', *The EMBO Journal*, 15: 3566-78.
- Scheer, Alexander, Francesca Fanelli, Tommaso Costa, Pier G De Benedetti, and Susanna Cotecchia. 1997. 'The activation process of the  $\alpha$ 1B-adrenergic receptor: potential role of protonation and hydrophobicity of a highly conserved aspartate', *Proceedings of the National Academy of Sciences*, 94: 808-13.
- Scheerer, Patrick, Jung Hee Park, Peter W Hildebrand, Yong Ju Kim, Norbert Krauß, Hui-Woog Choe, Klaus Peter Hofmann, and Oliver P Ernst. 2008. 'Crystal structure of opsin in its G-protein-interacting conformation', *Nature*, 455: 497.
- Schoepp, Darryle D. 2001. 'Unveiling the functions of presynaptic metabotropic glutamate receptors in the central nervous system', *Journal of Pharmacology and Experimental Therapeutics*, 299: 12-20.
- Schwartz, Thomas L, Shilpa Sachdeva, and Stephen M Stahl. 2012. 'Glutamate neurocircuitry: theoretical underpinnings in schizophrenia', *Frontiers in pharmacology*, 3: 195.
- Seifert, Roland, and Katharina Wenzel-Seifert. 2002. 'Constitutive activity of G-protein-coupled receptors: cause of disease and common property of wild-type receptors', *Naunyn-Schmiedeberg's archives of pharmacology*, 366: 381-416.
- Shapiro, David A, Kurt Kristiansen, David M Weiner, Wesley K Kroeze, and Bryan L Roth. 2002. 'Evidence for a model of agonist-induced activation of 5-hydroxytryptamine 2A serotonin receptors that involves the disruption of a strong ionic interaction between helices 3 and 6', *Journal of Biological Chemistry*, 277: 11441-49.

- Sondek, John, David G Lambright, Joseph P Noel, Heidi E Hamm, and Paul B Sigler. 1994. 'GTPase mechanism of Gproteins from the 1.7-Å crystal structure of transducin  $\alpha$ -GDP AIF- 4', *Nature*, 372: 276.
- Sounier, Rémy, Camille Mas, Jan Steyaert, Toon Laeremans, Aashish Manglik, Weijiao Huang, Brian K Kobilka, H el ene D em en e, and S ebastien Granier. 2015. 'Propagation of conformational changes during  $\mu$ -opioid receptor activation', *Nature*, 524: 375.
- Sprang, Stephen R. 2016. 'Invited review: Activation of G proteins by GTP and the mechanism of  $\alpha$ -catalyzed GTP hydrolysis', *Biopolymers*, 105: 449-62.
- Standfuss, J org, Patricia C Edwards, Aaron D'Antona, Maikel Fransen, Guifu Xie, Daniel D Oprian, and Gebhard FX Schertler. 2011. 'The structural basis of agonist-induced activation in constitutively active rhodopsin', *Nature*, 471: 656.
- Stewart, Gregory, Julie Kniazeff, Laurent Pr ezeau, Philippe Rondard, Jean-Philippe Pin, and Cyril Goudet. 2012. 'Metabotropic Receptors for Glutamate and GABA.' in, *Pharmacology (InTech)*.
- Strader, Catherine D, Irving S Sigal, and RA Dixon. 1989. 'Structural basis of beta-adrenergic receptor function', *The FASEB Journal*, 3: 1825-32.
- Sunahara, Roger K, John JG Tesmer, Alfred G Gilman, and Stephen R Sprang. 1997. 'Crystal structure of the adenylyl cyclase activator  $G_{\alpha s}$ ', *science*, 278: 1943-47.
- Thaker, Tarjani M, Maruf Sarwar, Anita M Preininger, Heidi E Hamm, and TM Iverson. 2014. 'A transient interaction between the phosphate binding loop and switch I contributes to the allosteric network between receptor and nucleotide in  $G_{\alpha i1}$ ', *Journal of Biological Chemistry*, 289: 11331-41.
- Therapeutics, Addex. 2012. "Addex Reports Top-line Data from a Successful Phase 2a Clinical Study with ADX71149 in Schizophrenia Patients." In.: Addex Therapeutics Press Release.
- Tizzano, Joseph P, Kelly I Griffey, and Darryle D Schoepp. 2002. 'The anxiolytic action of mGlu2/3 receptor agonist, LY354740, in the fear-potentiated startle model in rats is mechanistically distinct from diazepam', *Pharmacology Biochemistry and Behavior*, 73: 367-74.
- Ulloa-Aguirre, Alfredo, A ıda Uribe, Teresa Zari an, Ismael Bustos-Jaimes, Marco A P erez-Solis, and James A Dias. 2007. 'Role of the intracellular domains of the human FSH receptor in  $G_{\alpha s}$  protein coupling and receptor expression', *Molecular and cellular endocrinology*, 260: 153-62.
- Urban, Jonathan D, William P Clarke, Mark Von Zastrow, David E Nichols, Brian Kobilka, Harel Weinstein, Jonathan A Javitch, Bryan L Roth, Arthur Christopoulos, and Patrick M Sexton. 2007. 'Functional selectivity and classical concepts of quantitative pharmacology', *Journal of Pharmacology and Experimental Therapeutics*, 320: 1-13.
- Vauquelin, Georges, and Bengt Von Mentzer. 2008. *G protein-coupled receptors: Molecular pharmacology* (John Wiley & Sons).
- Vogel, Reiner, Mohana Mahalingam, Steffen L udeke, Thomas Huber, Friedrich Siebert, and Thomas P Sakmar. 2008. 'Functional role of the "ionic lock"—an interhelical hydrogen-bond network in family A heptahelical receptors', *Journal of molecular biology*, 380: 648-55.
- Wacker, D., R. C. Stevens, and B. L. Roth. 2017. 'How Ligands Illuminate GPCR Molecular Pharmacology', *Cell*, 170: 414-27.
- Wang, Sheng, Tao Che, Anat Levit, Brian K Shoichet, Daniel Wacker, and Bryan L Roth. 2018. 'Structure of the D 2 dopamine receptor bound to the atypical antipsychotic drug risperidone', *Nature*.
- Witkin, JM, JA Monn, DD Schoepp, X Li, C Overshiner, SN Mitchell, G Carter, B Johnson, K Rasmussen, and LM Rorick-Kehn. 2016. 'The rapidly acting antidepressant ketamine and the mGlu2/3 receptor antagonist LY341495 rapidly engage dopaminergic mood circuits', *Journal of Pharmacology and Experimental Therapeutics*, 358: 71-82.

- Wu, Huixian, Chong Wang, Karen J Gregory, Gye Won Han, Hyekyung P Cho, Yan Xia, Colleen M Niswender, Vsevolod Katritch, Jens Meiler, and Vadim Cherezov. 2014. 'Structure of a class C GPCR metabotropic glutamate receptor 1 bound to an allosteric modulator', *science*, 344: 58-64.
- Yang, Hong-Ju, Hai-Ying Zhang, Guo-Hua Bi, Yi He, Jun-Tao Gao, and Zheng-Xiong Xi. 2017. 'Deletion of Type 2 Metabotropic Glutamate Receptor Decreases Sensitivity to Cocaine Reward in Rats', *Cell reports*, 20: 319-32.
- Yao, Xiao Jie, Gisselle Vélez Ruiz, Matthew R Whorton, Søren GF Rasmussen, Brian T DeVree, Xavier Deupi, Roger K Sunahara, and Brian Kobilka. 2009. 'The effect of ligand efficacy on the formation and stability of a GPCR-G protein complex', *Proceedings of the National Academy of Sciences*, 106: 9501-06.
- Zhang, Yan, Bingfa Sun, Dan Feng, Hongli Hu, Matthew Chu, Qianhui Qu, Jeffrey T Tarrasch, Shane Li, Tong Sun Kobilka, and Brian K Kobilka. 2017. 'Cryo-EM structure of the activated GLP-1 receptor in complex with a G protein', *Nature*, 546: 248.

## Vita

**Birthdate:** July 1, 1989

**Birthplace:** Dakahliya, Egypt

**Citizenship:** Egypt

### Education

- 2018 Ph.D. Neuroscience, Virginia Commonwealth University School of Medicine, Richmond, VA
- 2013 MB BCh Mansoura Manchester Programme for Medical Education, Mansoura University, Egypt

### Awards and Honors

- May 2016 **Robert W. Ramsey Award**, VCU  
**Phi Kappa Phi honor society award**  
**Charles C. Clayton award**
- May 2014 **VCU Global Education Office Travel Award** to participate in the Erice course on Biophysics of channels and transporters. International School of Biophysics, Erice, Sicily, Italy.
- June 2012 **Mansoura University Travel Grant** to present a poster at the 19th International Student Congress of Medical Sciences (ISCOMS). University Medical Center Groningen (UMCG), Groningen, Netherlands.  
**Best poster presentation in Neurology**, 19<sup>th</sup> ISCOMS  
**ISCOMS Research Fellowship**
- May 2012 **World Hellenic Biomedical Association (WHBA) Scholarship**
- 2007-2012 **Mansoura University Dean's list**

### Publications

1. Younkin J\*, Gaitonde SA\*, **Ellaithy A\***, Vekariya R, Baki L, Moreno JL, Shah S, Hideshima KS, Eltit JM, González-Maeso, J Logothetis DE, Dukat M, Glennon RA. Reformulating a Pharmacophore for 5-HT<sub>2A</sub> Serotonin Receptor Antagonists. *ACS Chem Neurosci*. 2016;7(9):1292-9.

\* *Co-First/Equal authorship*

2. **Ellaithy A**, Younkin J, Gonzalez-Maeso J, Logothetis DE. Positive allosteric modulators of metabotropic glutamate 2 receptors in schizophrenia treatment. *Trends Neurosci*. 2015; 38:506-16.
3. Hatcher-Solis C, Fribourg M, Spyridaki K, Younkin J, **Ellaithy A**, Xiang G, Liapakis G, Gonzalez-Maeso J, Zhang H, Cui M, Logothetis DE. G protein-coupled receptor signaling to kir channels in *Xenopus* oocytes. *Curr Pharm Biotechnol*. 2014;15:987-95.
4. Salama M, Helmy B, El-Gamal M, Reda A, **Ellaithy A**, Tantawy D, Mohamed M, El-Gamal A, Sheashaa H, Sobh M. Role of L-thyroxine in counteracting rotenone induced neurotoxicity in rats. *Environ Toxicol Pharmacol*. 2013;35:270-7.
5. Salama M, **Ellaithy A**, Helmy B, El-Gamal M, Tantawy D, Mohamed M, Sheashaa H, Sobh M, Arias-Carrión O. Colchicine Protects Dopaminergic Neurons in a Rat Model of Parkinson's Disease. *CNS Neurol Disord Drug Targets*. 2012;11:836-43.

### **Abstracts**

1. **Ellaithy A**, Xu Y, Kawano T, Gonzalez-Maeso J, Logothetis D. Ionic Lock: Functional Role in Activation of Metabotropic Glutamate Receptor 2. Poster presentation at Chemistry and Pharmacology of Drug Abuse (CPDA) conference, Boston, MA, August 2017.
2. Xu Y, **Ellaithy A**, Kawano T, Gonzalez-Maeso J, Logothetis D. Ionic Lock: Functional Role in Activation of Metabotropic Glutamate Receptor 2. *Biophysical Journal*. 2017;112(3):530a. Poster presentation at Biophysical Society meeting, New Orleans, LA, February 2017.
3. **Ellaithy A**, Younkin J, Baki L, Logothetis DE. A positive allosteric modulator of metabotropic glutamate 2 receptor alters 5-HT<sub>2A</sub> receptor signaling in a heteromeric complex. Poster presentation at Biophysical Society meeting, Baltimore, MD, February 2015.
4. **Ellaithy A**, Helmy B, Salama M. Does Colchicine possess a neuroprotective effect in Parkinson's disease? Poster presentation at University Medical Center Groningen ISCOMS, June 2012, Netherlands.